THE EFFECTS OF BURIED IONIZABLE AMINO ACIDS ON THE STABILITY OF RIBONUCLEASE SA

A Dissertation

by

ANTHANY LAURENCE EVERETT

Submitted to the Office of Graduate and Professional Studies of
Texas A&M University
in partial fulfillment of the requirements for the degree of

DOCTOR OF PHILOSOPHY

Chair of Committee,	J. Martin Scholtz
Co-Chair of Committee,	C. Nick Pace
Committee Members,	Sarah Bondos
	Paul Straight
Head of Department,	Gregory D. Reinhart

December 2014

Major Subject: Biochemistry

ABSTRACT

The aim of this study was to investigate the stability contribution of buried ionizable amino acids in proteins. To study the stability contribution of a naturally occurring buried aspartic acid, two stabilized forms of RNase Sa designated 7S and 8S were used. In 7S, aspartic acid 79 has an elevated pK of 7.4 due to its location in the hydrophobic protein core. The stability contribution of this buried anion was calculated by comparing the $\Delta(\Delta G)$ of 7S at pH 6, 7, and 9 with that of 8S. The stability contribution of ionized Asp79 in RNase Sa 7S is estimated to be -1.8 kcal/mol.

To investigate the stability contribution of non-native buried ionizable groups, we introduce aspartic acid, lysine, and alanine residues at positions 70, 71, and 92 in 7S and 8S, and measure the change in stability, $\Delta(\Delta G)$. Positions 70 and 92 are in close proximity to Asp 79, whereas position 71 is further away and partially shielded by a β-sheet. All mutants were less stable than the parental protein, and the magnitude of the stability change is dependent on the specific location in the protein.

Since structural changes can account for differences in the environment of buried charges, it is important to determine whether buried charge mutations alter the structure of our mutant proteins. To date, the structures of the 7S I71A and 8S I71D variants have been resolved by X-ray crystallography. Using software to align crystal structures based on geometries of the residue side-chains, we find that 7S I71A and 8S I71D are comparable in structure to both RNase Sa WT and to each other. Crystal structure

analysis indicates that the ionizable groups of the mutant residues are isolated from aqueous solvent.

The differences in stabilities of variants were measured in 7S and 8S over a pH range to determine pK values of the mutant ionizable residues. In instances where the pK of buried ionizable mutant side chains are shifted, there is an apparent positive correlation between the magnitude of the pK shift and the magnitude of the change in stability. Thus, the buried ionizable mutants that are the least likely to be charged at physiological pH were observed to have the largest stability contribution. The calculated pK values were then used to assign charge values to the ionizable groups. Once charge values were assigned, the stability contribution of electrostatic interactions was calculated using Coulomb's law. We calculated the difference in stabilities due to electrostatic effects in the presence or absence of Asp79 in 7S and 8S, respectively. Coulombic interactions were estimated in a range between -0.9 – 1.8 kcal/mol. Lastly, we investigate the localized effect of buried ionizable mutants on the dielectric constant. We find that introducing buried Asp mutants in 7S increases the dielectric constant, whereas making buried Lys mutations decreases the dielectric constant at each location.

DEDICATION

To my family, friends, and colleagues

Your love, support, and advice are immeasurable and invaluable by any standard.

ACKNOWLEDGEMENTS

I thank my committee members, Dr. Marty Scholtz, Dr. Nick Pace, Dr. Sarah Bondos, and Dr. Paul Straight, for their input and advice. I would especially like to thank Dr. Marty Scholtz and Dr. Nick Pace for allowing me an opportunity to do research in their lab and under their academic tutelage. I cannot stress enough how helpful Dr. Gerald Grimsley was by acting as both a sounding board for ideas and for ordering anything I needed or wanted to get my projects done. Thanks go to everyone involved in my growth as a scientist including, but not limited to, Drs. Karen and Herman Scholthof. Mass spectrometry analysis of all mutants in this work was performed by Dr. Larry Dangott in the Protein Chemistry Laboratory in the department of Biochemistry and Biophysics and would not have been otherwise possible. I extend a heart-felt *Thank You* to Dr. Dangott and appreciate all his hard work and advice. I also want to thank and acknowledge Kazufumi Takano (Graduate School of Life and Environmental Sciences, Kyoto Prefectural University, Kyoto, Japan) for crystallization, X-ray crystallography, and structure determinations of my proteins. Lastly, I want to thank Dr. Gabriel F. K. Everett for being my best friend, critic, and "advisor." Her input and support have been irreplaceable. I also thank Dr. Everett for her love and vast amounts of patience during this process.

TABLE OF CONTENTS

Page

Page

LIST OF FIGURES

LIST OF TABLES

CHAPTER I

INTRODUCTION

In an aqueous environment, most proteins assume a higher-order three dimensional shape that is more structured than the molten-globule structure of the denatured state.[1] The formation of the final structural state, known as the folded state, depends on the amino acid sequence of the protein and the interaction of the amino acids with the protein's environment. When globular proteins unfold, the interior of the protein is more exposed to solvent and we define this state as the unfolded state. The denatured state has been shown to retain residual structure and it may resemble a molten globule more than an extended and fully solvated peptide.[2, 3] Generally, there exists an equilibrium in protein structure that can readily transition between the folded and unfolded states, and the relative population of each state is dependent on solvent conditions. If no apparent intermediate thermodynamic states exist, this equilibrium closely approaches a two-state mechanism that adheres to LeChatlier's classical chemical principle of solute equilibrium and can be defined by the equation:

$$\textbf{Folded} \rightleftharpoons \textbf{Unfolded} \qquad (1)$$

Equation 1 describes a chemical equilibrium in which: the folded state and unfolded states exist as separate populations, the combined population of states is finite, the only

source of one state is the other state, and that at some point, the populations (concentrations) of the states will be equal. Willard Gibbs famously described this relationship in thermodynamic terms when the temperature and pressure were known and derived an equation for the free energy required to move between states:

$$\Delta G = G_U - G_F = -RT\ln K_{eq} \quad (2)$$

$$K_{eq} = [U]/[F] \quad (3)$$

From equations 2 and 3, ΔG will be negative when conditions favor the unfolded states. Conversely, ΔG will be positive when the folded state is favored. When the equilibrium constant (K_{eq}) is 1, or [U] = [F], and $\Delta G = 0$. Of note is that ΔG is dependent on temperature. Rearrangement of the derivation gives the Gibbs-Helmholtz equation and shows the temperature dependence of ΔG. Equation 4 introduces the change in enthalpy (ΔH) and heat capacity (ΔCp).

$$\Delta G = \Delta H_{TM}(1 - T/T_M) - \Delta Cp[(T_M - T) + T \ln(T/T_M)] \quad (4)$$

When $T = T_M$, $\Delta G = 0$ and the temperature is known as the melting temperature (T_M). Setting equations 2 and 4 equal to zero shows that T_M is the temperature where [U] = [F], by equation 3. Conformational stability is defined as the free energy required to transition from the folded state to the unfolded state. Since energy is conserved, the

transition in the opposite direction has the same magnitude, but opposite sign. Therefore, protein stability can be viewed as an intrinsic characteristic that depends on the amino acid sequence and its interaction with the environment.

Typically, proteins are only marginally stable (5-10 kcal/mol) under physiological conditions, and the native stability is the additive contribution of all forces acting to stabilize and destabilize both the folded and unfolded state.[2, 4-11] For example, ionizable amino acids in soluble globular proteins are favorably located on the solvent-exposed protein surface, whereas non-polar amino acids are typically found in the solvent-inaccessible protein interior. One would expect an increase in stability as proteins get larger, as more hydrophobic residues are removed from solvent. Generally, the marginality of stability has been determined to be independent of size, as it appears that some larger proteins bury more destabilizing ionizable residues to compensate for the increased stability.[10, 12-14]

The current hypothesis is that the small difference in energy required to transition between states is to allow for efficient protein turnover or optimal catalysis/function.[15-18] Function is lost if the protein is unfolded, but activity is also diminished if the protein becomes too stable.[19] Trevino *et al*. show that stabilized variants of RNase Sa have reduced substrate binding, but increases in catalytic efficiency, suggesting that minimal stability might optimize efficient substrate docking.[20] Additional evidence suggests that under physiological conditions, many proteins are maintained in a more unfolded-like state until functionally required, further supporting the importance of maintaining marginal stability.[21-23] That is not to say that the contributing forces are marginal or

miniscule, *per se*, as many of them can be quite large collectively, but that opposing forces are additive and their sum is small under biologically relevant conditions.[4, 9, 24-26] Forces that contribute to maintaining the folded state include the hydrophobic effect, disulfide bond formation, ionic interactions, hydrogen bonds, and van der Waal interactions.[2, 4, 7, 8, 24, 27-39] The latter includes dipole-dipole interactions, induced dipole interactions, and London dispersion forces. The largest contributing force favoring the unfolded state is conformational entropy.[4, 5, 7, 8, 17, 18, 24, 37, 40-44] All of the contributing forces except disulfide bonds are non-covalent weak atomic forces. It should be stressed that the "weak" designation should not diminish the view of the collective contribution of those forces to protein stability. A brief description of each follows.

The hydrophobic effect

As eloquently stated by John Bernal, "… a force of association is provided which is not so much that of attraction between hydrophobe groups, which is always weak, but that of repulsion of the groups out of the water medium."[45, 46] The magnitude of the repulsion would not be widely accepted until after Walter Kauzmann's seminal paper on the subject of the hydrophobicity of amino acids.[47] The tendency of water to drive hydrophobic non-polar side-chains to the interior of proteins is a major force driving the final structure of globular proteins with each buried aliphatic carbon contributing approximately 1.1 kcal/mol to protein stability.[47-52] The process of "water hating" residue sequestration by aqueous solvent is an example of the hydrophobic effect and the

residues are called hydrophobic resides.[45] There are other forces that contribute to maintaining the structure of proteins that are widely known that will be discussed below.

The hydrophobic amino acids (Ala, Val, Ile, Leu, Met, Phe, Trp, and Pro) are those that are uncharged and non-polar.[47-49, 53-57] Phenylalanine and tryptophan have aromatic side-chains, containing carbon-rich rings, and Met is the only sulfur containing non-polar residue.[47, 48, 53, 55, 56] The rest of the hydrophobic residues have carbon-rich side-chains with different carbon content and configuration. On average, 80% of non-polar residues are buried. The protein core more resembles a solid than a liquid and tight packing results in optimized van der Waal's interactions between residue side-chains.[58] Van der Waal's interactions are further discussed below. The propensity for residues to be buried was determined by phase partition experiments into organic solvents/vapor or amphipathic detergent micelles to create hydrophobicity scales.[48, 53, 56-58] These scales have been used extensively to estimate the level of polar group burial. In addition, the hydrophobicity of the residues has been combined with other physical properties, such as surface area, to give a more detailed picture of residue interactions and solvation.[7-9, 51, 52, 57, 59-61] Multiple laboratories, including our own, have used hydrophobic residue substitutions in proteins to determine their contribution to protein stability. The stability calculations are comparable, with each additional -CH_2- group observed to contribute 1.1 kcal/mol to the stability.[49-51, 62, 63] In RNase Sa, the hydrophobic effect was estimated to contribute 110 kcal/mol to protein stability.[2]

Disulfide bonds

Intramolecular disulfide bonds in proteins are formed from the sulfur (thiol) groups of cysteine side chains. The disulfide bond in peptides is formed spontaneously, though inefficiently.[64, 65] John Beckwith's lab showed that formation of the bond *in vivo* requires an oxidative environment and in *E. coli* is facilitated by the now well-known Dsb pathway. Thus, cytosolic proteins in *E. coli* do not typically form permanent disulfide bonds in the more reducing environment of the cytosol.

The formation of a disulfide bond "locks" two cysteine side chains together, generally shifting the structure to a more folded state-like conformation.[9, 28, 66-68] Contrarily, disulfide bonds can also contribute to the adoption of the unfolded state by introducing strain into the protein backbone, thereby shifting the structure away from the folded state.[24, 69] Typically, the structural cost to the unfolded state is higher than the cost to the folded state, resulting in a net stabilizing contribution, and the magnitude of the stability change upon forming the bond is related to the size of the loop of peptides between the cysteines involved.[9, 28] In some cases, like RNase A, disulfides are necessary to maintain the folded state.[8, 9] In other proteins, the magnitude of the contribution to stability from a single disulfide bond can vary when multiple disulfide bonds are present. For instance, stability was calculated for disulfide bonds in RNase T1 and was estimated to be 3.4 kcal/mol up to as high as 7 kcal/mol.[24, 28]

Engineering disulfides into proteins for the purpose of increasing stability is attractive and some success was seen in T4 lysozyme.[70] However, attempts in subtilisin proved to be problematic and only slightly increased stability.[8, 9, 70-73] The slight increase

in stability is likely a result of using candidate positions with a backbone topology and geometry that had already been evolutionarily optimized without the need for a disulfide.

Ionic interactions

An ionic interaction is a non-covalent interaction between charged species. The type of species, the polarity of their environment, and the distance between them directly affect the strength of the interaction. The resultant free energy based on those interactions is described by Coulomb's Law (equation 5):

$$\Delta G = \sum_j \frac{q_i q_j}{D r_{ij}} \quad (5)$$

where ΔG is the free energy of the interaction as it relates to fixed species j and i, q_n are the interacting charges of the species, D is the dielectric constant, a metric describing the ability of the medium to transfer charge, and r_{ij} is the distance between the charges. When a point charge is positive, q = 1, and when a point charge is negative, q = -1. Based on Coulomb's equation, the free energy of interaction between two charged species at some distance "r" in a medium with dielectric constant of "D" will be positive and unfavorable for ions of the same charge and negative and favorable for ions of opposite charge. Thus, electrostatic interactions in unfolded proteins are diminished as charged groups are farther apart and in the highly polar environment of aqueous solvent with a dielectric constant near 80.[39]

In proteins, charged species result from the ionizable amino acids Tyr, Cys, His, Arg, Lys, Asp, Glu and from the N- and C-termini. These groups are labeled polar-uncharged or polar-charged based on whether they are ionized at physiological pH. The polar-uncharged groups are Tyr, Cys, and His, as they have a predominantly neutral charge at pH = 7.4. The polar-charged amino acids are Arg, Lys, Asp, Glu and the termini. Arg and Lys are positively charged at pH = 7.4 and are called "basic residues." Asp and Glu are negatively charged at pH 7.4 and are called "acidic residues." The ionization state can be defined mathematically based on the proton concentration by using the Henderson-Hasselbalch equation, equation 6:

$$\mathbf{pK = pH - \log_{10}([B]/[A])} \quad (6)$$

where $pH = -\log_{10}[H^+]$, $[H^+]$ is the proton concentration, [B] is the concentration of the deprotonated conjugate base species, and [A] is the concentration of the protonated conjugate acid species. The pK of any ionizable group is the pH at which half the species in solution are ionized, [B] = [A]. The groups are protonated below the pK and deprotonated above the pK. Model compound pK values for the ionizable amino acids are shown in Table 1.[48, 74, 75] Since ionizable amino acids in proteins are surrounded by other amino acids, pK values were measured in pentapeptides with the form Ala-Ala-X-Ala-Ala. This is a better model for these groups in a protein than free amino acids in solution.[13, 76] The pentapeptide pK values are termed intrinsic pK values and are reported in Table 1 along with the pK values for the N- and C- termini. Table 1 also

includes the classical values reported for ionizable residues in order to illustrate how values deviate between the two.

The pK of ionizable amino acids that are located in the hydrophobic interior of proteins is typically shifted to neutralize the charge of the side chain as it is energetically unfavorable to transfer a charged group from a polar environment to the non-polar environment of the protein core.[10, 13] His and Cys are the most abundant buried polar groups found in proteins, as their pK values are closest to pH 7.[10] Buried Asp and Glu residues will have pKs that are typically elevated so that the carboxyl groups stay protonated and the pKs of the side groups of Lys and Arg are depressed to keep them deprotonated. For instance, the pK of the native buried and unpaired Asp 79 in RNase Sa has one of the highest pKs for an Asp measured to date at 7.37.[20] In contrast, recent studies in Staphylococcal Nuclease (SNase) have shown that Arg pKs are unaltered regardless of whether they are found on the protein surface or in the protein interior.[77] This phenomenon may be anomalous due to the penetration of water into the protein interior of SNase (discussed below), or the physical properties of the Arg side group, like the delocalized charge on the guandino group.[78]

Calculations of the electrostatic contribution to stability using Coulomb's Law are difficult for two reasons. First, the ionizable functional group of Asp, Glu, Arg, Lys, His, and the protein termini are resonant and do not act as simple point charges. In these cases, the groups have charges that spread out over multiple atoms. A common approach is to use the N- group for Lys, His, Arg, and the N-terminus, and the carboxy-carbon of Asp, Glu, and C-termins for the distance measurement of "r".[79]

Table 1. Model compound and intrinsic pK values for ionizable amino acids.

Group	pK_{NT}[a]	pK[b]
	Termini	
Carboxyl	3.8	3.7
Amino	7.5	9.1
	Polar-Uncharged	
Cys	9.5	8.6
His	6.3	6.5
Tyr	9.6	9.8
	Acidic	
Asp	4.0	3.9
Glu	4.4	4.3
	Basic	
Arg	12.5[c]	-
Lys	10.4	10.4

[a]From Nozaki *et al*. (1967).[74]
[b]From Grimsley *et al*. (2009).[13]
[c]From Dawson *et al*. (1959).[75]

The second reason lies in the value of the dielectric constant "D." More polar environments have higher dielectric constants. The dielectric constants of a pure vacuum, hexane, octanol, ethanol, and water have been measured as 1, 4, 10, 25, and 80, respectively.[80-83] The dielectric constant in proteins is surely not a constant and estimates must be used.[83] As the dielectric can change based on interactions within its environment, any estimation of the value of the dielectric constant must be a function of the boundaries between non-polar and polar environments. The change is non-linear and

is affected by cavitation, solvation of the non-smooth molecular surface of the protein, and the ordering and distance between polar and non-polar species.[78, 80-85] Warshel points out that the term dielectric "constant" is typically a misnomer and that the true value of "D" is dependent on the model being used to determine the value.[82] Thus, the value of D can be an issue of contention between laboratories using different models. The dielectric constant calculated for the interior of folded proteins has been empirically determined over a wide range from 6 – 45.[79, 80, 85, 86] In previous studies, our lab has found good agreement in electrostatic calculations when using a value of D = 45 for RNase Sa WT and an RNase Sa mutant with multiple lysine substitutions on the surface of the protein.[79]

The estimated value of the dielectric constant is important when calculating the magnitude of electrostatic interactions. For example, recent techniques using a probabilistic approach (Gaussian) have been used to decrease the Root Mean Square Deviation (RMSD) of dielectric constant values in a set of 91 proteins that were less than 70% similar.[85] Simply, the protein interior was treated as a collection of separate smooth boundaries with different dielectric densities between them (termed Epsilon) instead of the traditional approach of layering two large, smooth non-polar and polar rigid surfaces.[79] In doing this, the dynamic nature of proteins upon ionization of individual groups is accounted for. Of note is that the authors found that in using D = 10 for the interior SNase instead of the widely used D = 20, that pK calculations for buried ionizable amino acids were more accurate (RMSD = 1.77 vs. RMSD = 2.44).[85] The lower and more accurate estimations are seemingly contradictory to other research

suggesting that the protein interior of SNase is cavitated and transiently accessible to bulk water, which would raise the dielectric constant.[78] Taken together, these results suggest that the interpretation of data collected from studies using SNase as a model remains challenging.

Intuitively, the magnitude of the energy of electrostatic interactions is greater in the more compact folded state versus the unfolded state as: 1) the distance between ionic groups is decreased, and 2) the hydrophobic environment of the protein core has a smaller dielectric constant.[82, 83]

Ion pairs and salt bridges are distinct types of electrostatic interactions that contribute to protein stability.[5, 9, 81, 87-92] Both are a result of the non-covalent interaction of charged ions. The first type, ion pairing, occurs when the two oppositely charged ions are less than 5 Å apart and can be stabilizing or destabilizing to proteins depending on their location and the context of their interaction.[10, 87, 91] For instance, an attractive interaction can be favorable for holding a protein in a more native-like structure or can introduce unfavorable strain, which holds the protein in a more unfolded state. On average, a 100 residue protein will have one repulsive ion pair for every 4 attractive ion pairs.[93] Ion pairs in the protein interior have been shown to contribute between 2-6 kcal/mol to stability.[61] Salt bridges in proteins are typically formed between the hydrogen group of positively charged nitrogens or basic residues and a negatively charged carboxylate.[88, 94] They have been experimentally determined to contribute between 3 – 5 kcal/mol to protein stability in the protein interior, and less on the solvent exposed protein surface.[10, 61, 92, 94-96] Studies suggest that the formation of ion pairs and

salt bridges in the non-polar environment of the protein interior would mitigate the desolvation penalty of removing charged residues from water and provide an attractive approach for increasing stability. In one case, hydrophobic substitutions for any one, two, or all three residues of a buried charge triad were found to increase stability in the Arc repressor of bacteriophage P22.[89] In the thermophile *Thermococcus celer* L30e protein, the magnitude of the stability contribution of charge-to-alanine mutations was shown to be dependent on the location of the mutation.[97] That is not to say that salt bridges cannot be stabilizing.

In RNase Sa, buried Asp33 forms 3 hydrogen bonds and when removed by mutation to Ala, decreases stability of RNase Sa by an estimated 6 kcal/mol.[79, 98] Additionally, hydrogen bonding can affect the pK of ionizable groups. For example, Asp70 in T4 lysozyme and Asp76 in RNase T1 have three and four hydrogen bonds, respectively, and both have a pK near 0.5![99] Statistical analysis of proteins reveals most native buried ionizable groups are involved in forming either ion pairs or salt bridges, but only one in five ion pairs is buried.[58, 100, 101] In all, experiments testing the response of protein stability to changes in pH show that electrostatic interactions collectively contribute up to 10 kcal/mol, about 1/10 that of either the hydrophobic effect or van der Waal's interactions.[2, 10, 24, 39, 51, 102, 103]

Hydrogen bonds

A hydrogen atom has a single proton in the nucleus and a single electron. During the formation of a covalent bond with another atom, the electron is shared. The

electronic sharing induces a duality in the electromagnetic field of the hydrogen atom, making the hydrogen atom a partial dipole. By taking on a positive charge character on the non-bonded side of the atom, the hydrogen becomes attracted to other electronegative atoms. In proteins, hydrogen bonds are formed between hydrogen atoms and the lone electron pairs of nitrogen, oxygen, and sulfur. The strength of hydrogen bonds depends on both the geometry of the interacting groups and the polarizability of the local environment in which the bond is formed.[104] For instance, Gao *et al*. show that hydrogen bonds are ≈1 kcal/mol stronger in a non-polar environment than a polar environment.[105] Multiple hydrogen bonds are formed between the peptide backbone amides and carboxyl oxygen groups to shape and maintain the major secondary structural elements of proteins such as α-helices and β-sheets which determine the overall tertiary structure.[47, 106] Approximately 70% of all hydrogen bonds in proteins are formed between groups of the peptide backbone.[101] Of note is that hydrogen bonds are formed in almost every case in which conditions are favorable for their formation.[101, 107-110]

The magnitude of the contribution of hydrogen bonds in protein stability and folding has classically been an area of contention. The debate will not be covered here for the sake of brevity. Pace has provided a good primer on the subject.[101, 111] Additionally, a recent study by Pace *et al*. concludes that the contribution of hydrogen bonds on protein stability is: 1) favorable, 2) context dependent, 3) similar for side chain and peptide groups, and 4) similar in small and large proteins.[101]

The importance of hydrogen bonds is emphasized by studies that show that 90% of all polar residues in proteins are hydrogen bonded.[110] In some cases, the pK of polar groups will be shifted in order to optimize favorable hydrogen bonding interactions.[101] Though hydrogen bonds are considered "weak" electrostatic interactions, their collective contribution to protein stability is second only to the hydrophobic effect (see above).[111] Although hydrogen bonding can induce steric strain, they are generally stabilizing, as decreases in conformational stability are larger when removing groups that are hydrogen bonded versus those that are not.[101] Some of the first experimental evidence for the favorable contribution of hydrogen bonds concluded that that each hydrogen bond contributes ≈1 kcal/mol to protein stability.[112] That value is in good agreement with later studies.[2, 24, 52, 101, 102, 111, 113-115] The average number of hydrogen bonds is ≈1 hydrogen bond/residue. The free energy of a hydrogen bond depends on their environment and is near 1 kcal/mol per residue but in individual cases has been estimated as high as 5 kcal/mol.[58, 59, 101] Thus, the average free energy contribution to stability from hydrogen bonds for a 100 residue protein would be ≈100 kcal/mol.[111] For example, RNase Sa has 96 residues, and hydrogen bonds contribute approximately 90 kcal/mol to the conformational stability of the protein.[39]

Van der Waal interactions

The non-covalent electrostatic interactions between permanent and induced dipoles are called van der Waals interactions. When a dipole comes into proximity of another molecule, it induces a dipole in the second molecule. London dispersion forces

result from an induced dipole-induced dipole interaction between non-polar molecules. For instance, the hydrogen atoms that are connected to carbons in nonpolar residue side-chains only have one electron to share. In doing so, they can produce to a dipole moment. The dipole moment subsequently induces a dipole in neighboring non-polar molecules. Though weak in comparison to hydrogen bonds or ionic bonds, van der Waal interactions may play a major role in protein stability and structure due to the packing density of residues in the folded state.[9, 116] For example, in T4 lysozyme, mutations that remove -CH_2- groups and introduce cavities in the protein show that larger cavities result in larger changes in conformational stability due to loss of favorable van der Waal interactions.[117] This result suggests that van der Waal interactions may even make larger stability contributions than non-polar surface burial.[39, 118]

Lennard-Jones estimated the energy of van der Waal interactions. The magnitude of the energy is based on the distance, r, between atoms. The distance giving this minimum magnitude of the energy is called the van der Waal radius. Mathematically, the energy of the interaction can be defined by equation 7:

$$\mathbf{E} = \frac{\mathbf{B}}{\mathbf{r^{12}}} - \frac{\mathbf{A}}{\mathbf{r^{6}}} \tag{7}$$

where E is the energy of the interaction, the B term describes the physical interaction of the atom electron clouds (steric effects), and A describes the electrostatic interactions between the atoms (polarizability).

The generally compact form of the native state of globular proteins brings the atoms of the amino acids in close proximity. Consequently, van der Waal interactions undoubtedly contribute to the stability of a protein, possibly on the scale of the hydrophobic effect.[88, 116, 119]

Conformational entropy

The largest force contributing to the unfolded state of proteins is conformational entropy.[9] The force arises from the rotational degrees of freedom that exist around every covalent bond in the protein. The degrees of freedom are reduced as a protein folds. The confinement of residues decreases the entropy of the unfolded state ensemble and is experienced both by the protein backbone and separately by the amino acid side chains.[36, 47, 120-123] Furthermore, the reason disulfide bonds are stabilizing is that they decrease the degrees of freedom of the backbone, thereby decreasing the conformational entropy of the denatured state.[28, 71] It is estimated that conformational entropy contributes ≈2 kcal/mol per residue to the stability of the native state.[39, 124]

Division of amino acid populations in proteins

The 20 amino acids that are used by living organisms to build proteins can be divided into three distinct chemical groups.[47-49, 53, 55, 56] The first group is the non-polar amino acids that are typically located in the interior of soluble proteins with minimal contact with aqueous solvent. The second group is the polar-uncharged group, whose side chains readily interact with water, and are believed to play largely a structural role

through hydrogen bonding and van der Waal's interactions.[59, 63] The last group is the polar-charged residues that are typically charged at physiological pH and are generally found on the protein surface where they are solvated. The latter group includes the basic residues, Lysine and Arginine, that are positively charged and the acidic residues, Glutamic and Aspartic acid, that are negatively charged at pH 7, respectively. Taken together, these three groups establish a useful foundation for this work and provide a simple way to think about how single amino acid residues contribute to protein stability and structure.

Though descriptions of the forces that contribute to protein stability in the previous sections provide a primer on the energetics of maintaining the folded state, it must be noted that the locations of amino acids in proteins is diverse. In 1959, Kauzmann called proteins, "…oil droplets wearing a polar coat." Since then, multiple investigations have shown there to be exceptions to our basic rules of thumb.[5, 24, 45] For instance, the occasional polar residue gets buried in the protein core and non-polar residues can be solvent exposed. A brief summary of the population diversity is below.

Non-polar residues

The hydrophobic effect describes the result of an interaction between non-polar residues and polar water.[47] Non-polar residues cannot form hydrogen bonds with water. Consequently, in an attempt to maximize its own hydrogen bonding requirements, water forces non-polar residues out of solution.[47, 125] When more than one non-polar species is present, water will tend to group the species together to decrease the accessible surface

area of contact.[47, 125, 126] It makes sense then, that the majority of non-polar residues are found in the interior of soluble globular proteins away from aqueous solvent.

Using a non-redundant database of 106,000 proteins, the total proportion of each type of residue (non-polar, polar-uncharged, polar-charged) has been estimated.[127] The values reported are more stringent than previous studies using far fewer proteins.[5, 128] Hydrophobic residues make up ≈48% of proteins. The average solvent accessible surface area of hydrophobic groups was estimated to ≈14%.[57] Taken together, an estimated 40% of residues are buried and hydrophobic and 8% are solvent exposed hydrophobic residues. Previous research indicates that surface hydrophobic residues can increase overall oligomer stability by increasing subunit affinity or by increasing the binding affinity of the hydrophobic face of substrates.[129-131] Values are summarized for all group types in Table 2.

Polar-uncharged residues

The polar-uncharged residues are those that contain an oxygen and/or nitrogen or sulfur in the side-group, but are generally uncharged near pH 7. Members of this group serve diverse functions. For instance, Cys can form disulfides to increase stability and the near physiological pK of 6.5 for His allow it to act as both a nucleophile and electrophile during catalysis in the active site of many enzymes, including RNase Sa.[133-136] Additionally, and depending on their protonation state, members of the group can form hydrogen bonds and salt bridges to increase stability.[101, 111] Blaber *et al*. show that the loss of hydrogen bonds between residues was observed to be destabilizing in T4 lysozyme.[137] Takano *et al*. concluded that forming hydrogen bonds was not the only

role of the polar-uncharged groups when studying Thr to Val mutants in RNase Sa.[59] Thus, the local environment of these groups dictates whether or not they require hydrogen bonds. Additionally, the incorporation of polar-uncharged groups has been implicated in the optimization of packing during protein folding.[55, 116, 138-141] In all, this group has a diverse role in protein folding, stability, and function.

Table 2. Proportion of residue types found in the protein interior and surface.

Residue type	Total in proteins[a]	Surface[b]	Buried[c]
Nonpolar[e]	48%	8%	40%
Polar-uncharged[e]	30%	18%	12%
Polar Charged[e]	22%[d]	15%	7%

[a]Values from Trinqier and Sanejouand (1998).[127]
[b]Values are the proportion of each residue type as determined by Trinqier and Sanjouand (1998) multiplied by the average accessible surface area calculated by Lesser and Rose (1990).[57, 127]
[c]Values are calculated by multiplying the total proportion of each residue type as determined by Trinqier and Sanejouand (1998) by the average solvent accessible surface area determined by Lesser and Rose (1990) and subtracting from the total.[57, 127]
[d]Kim *et al*. report that the proportion of buried polar groups increases with increased protein size.[132]
[e]Non-polar groups include Gly, Ala, Val, Leu, Ile, Met, Pro, Phe, and Trp. Polar-uncharged groups include Ser, Tyr, Thr, Gln, Asn, His, and Cys. Polar charged groups include Arg, Lys, Glu, and Asp.

The polar-uncharged residues have been estimated to make up 30% of the residues in a large group of proteins in a non-redundant database.[127] On average, ≈60% of all the polar-uncharged amino acids found in proteins will have solvent exposed surface area.[57] Taken together, 12% of the residues in the hydrophobic core are polar-

uncharged, whereas 18% are solvent exposed. Values are summarized for all group types in Table 2.

Polar-charged residues

The polar-charged residues include Arg, Lys, Asp, and Glu. At pH near 7, the side chains of this group are charged. The basic residues, Arg and Lys, are positively charged below their pK's of 12.5 and 10.4, respectively.[75, 76] The acidic residues, Asp and Glu, are negatively charged above their pK's of 3.7 and 4.3, respectively.[76] Other than Arg, these values are the empirically determined dissociation constants in a pentapeptide with the Ala-Ala-X-Ala-Ala motif.[76] Since these residues are charged, they are readily solvated in aqueous solution.[48, 49, 53, 57] The polarity of these groups explains why they are typically found on the protein exterior of soluble globular proteins. Additionally, solvent-exposed charged residues have been shown to be important in modulating the solubility of proteins.[10, 103, 142] Of course, not all polar-charged groups are exposed. In fact, not only are some charged groups buried, the number of buried charge-groups buried may increase with protein size.[132] Kim *et al*. estimated 1 of every 50 polar-charged groups is buried in proteins of approximately 100 residues, and that number increases to about 1 in every 25 for a protein of about 300 residues.[132] In agreement, Kajander *et al*. find that 65% more polar groups are buried in a 700 residue protein versus a protein of 100 residues.[19] Multiple studies conclude that an increase in the number of buried charged-groups may allow for proteins to maintain marginal

stability, and this is supported, by studies that show that the removal of buried charged groups can increase protein stability.[10, 19, 20, 58, 143]

The polar-charged residues are estimated to comprise approximately 22% of the residues in proteins.[127] Of those, the average solvent accessible surface area for the groups is 68%.[57] Taken together, polar residues make up ≈7% of the residues in the hydrophobic protein interior and ≈15% of the residues on the solvent exposed protein surface. In general, the magnitude of the contribution of polar-charged residues to protein stability is dependent on their environment. That is, whether the groups are solvent exposed, non-covalently interacting by being part of an ion pair or salt bridge, involved in other electrostatic interactions, or a combination of these factors. The contribution to stability of each of the non-covalent electrostatic interactions between these groups is described above. Values for the proportion of groups buried are summarized for all group types in Table 2.

Surface charged groups have been shown to increase stability by forming ion pairs and salt bridges. Akke and Forsén measured the free energy of unfolding for acidic residue amide analog mutants (Glu → Gln; Asp→Asn) on the surface of a Bovine calbindin D derivative.[144] They found that acidic charged groups contributed 1-3 kcal/mol to stability compared to their polar-uncharged analogs. However, the contribution to stability of surface charge groups has been shown to be context dependent, as acidic to basic substitutions at surface positions can be stabilizing or destabilizing.[34]

The free energy cost to fully bury polar-charged groups in the interior of a protein has been calculated to be 19 kcal/mol, which is almost 4 fold higher than the gain from burying a hydrophobic group.[4, 145-147] Therefore, burying a charged group is more destabilizing than burying a hydrophobic group is stabilizing. The desolvation penalty is typically mitigated by electrostatic interactions, including: ion pairing, salt bridge formation, and/or pK shift to deionize the side chain.[8, 13, 34, 59, 79, 81, 88, 100, 132, 147] Honig *et al*. estimated the cost of burying an ion pair to be 7 kcal/mol and a salt bridge to be 6-10 kcal/mol when transferred to media of low dielectric constant of 2.4.[145-147]

The pK of many buried ionizable groups on polar-charged amino acids will often be shifted in the hydrophobic interior of a protein so that the group either becomes neutral or stays charged in order to fulfill a biological or structural role.[10, 13] In some cases, the shift can be substantial and is context dependent.[10, 98, 148, 149] For instance, the carboxyl of Asp79 in RNase Sa forms no apparent hydrogen bonds and has a pK = 7.4, whereas Asp76 in RNase T1 forms three hydrogen bonds and has a pK = 0.5.[20, 98] The differences in pK values of 3.7 and -3.2 relative to values measured in model pentapeptide studies respectively represent two of the largest pK shifts for buried ionizable groups reported to date.[10, 98] In recent studies of SNase, buried ionizable group contributions to stability were measured by making substitutions at different positions in the protein.[150-152] The authors found that: the pK of Glu residues were generally

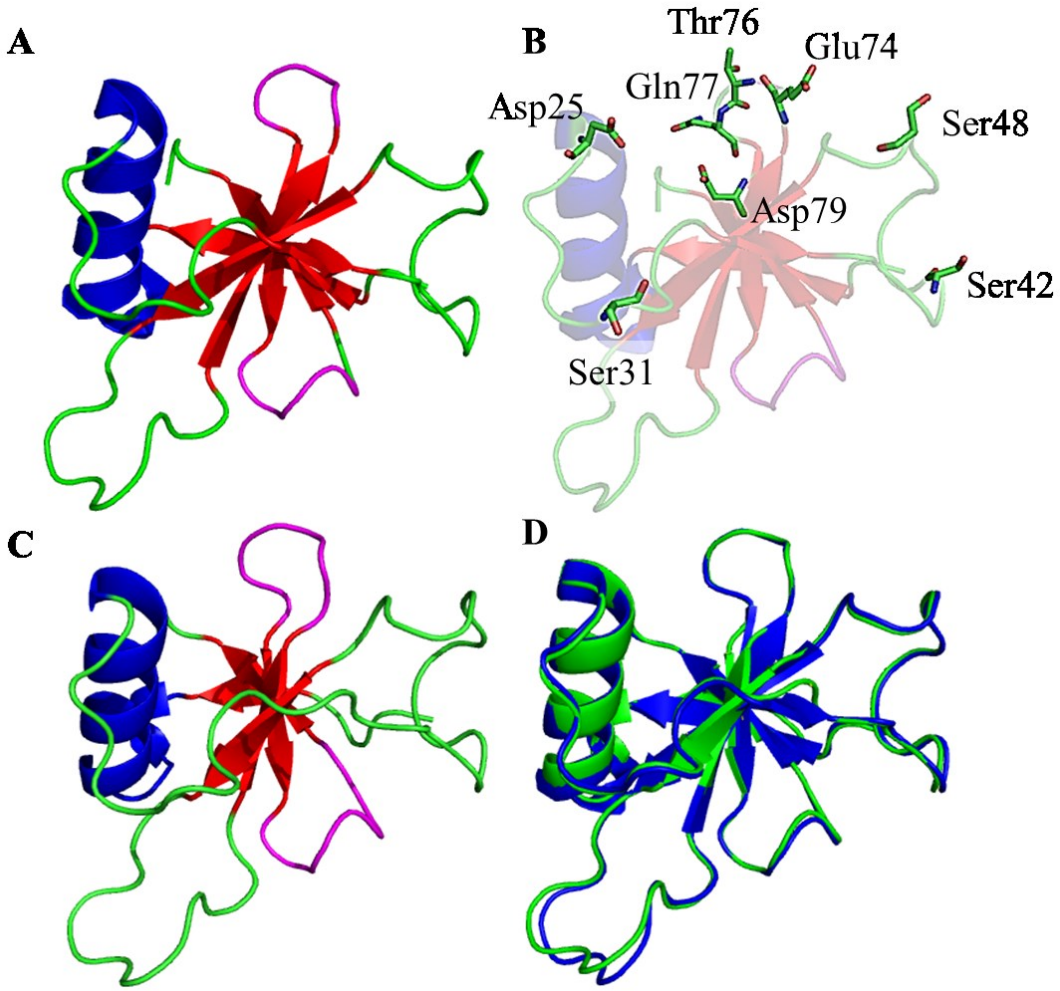

Figure 1. Ribbon diagrams of RNase and 7S. Secondary structures are colored to differentiate between helices (blue), β-strands (red), β-turns (magenta), and random coil (green). A) RNase Sa, from 1rgg.pdb.[153] B) RNase Sa with 7 positions in turns and loops highlighted that form 7S after mutations: D25K, S31P, S42G, S48P, E74K, T76P, and Q77G.[36] Mutation of Asp79 to Phe in addition to the other residues forms 8S.[20, 44] The contribution to stability of the mutations is detailed in Table 3. C) 7S, modified from the crystal structure of 7SI71A mutant determined in the laboratory of Kazufumi Takano, Kyoto, Japan. Reversion of Ala71 to the native Ile was perfomed *in silico* using the program PyMol.[154] The side-change conformer of highest probability was chosen for determination of the final structure after mutation. D) Structural alignment of (A) RNase Sa WT (blue) and (C) 7S (green). Alignments are based on the peptide bond geometry of conserved residues between models. Backbone topology for all diagrams is calculated using the program PyMol.[154]

increased to ≈7, Lys residues could be shifted to as low as ≈6, and Arg residues exhibited no change in pK.[77, 150, 151] The contribution to stability of the ionization of buried Glu was determined to be between 3-7 kcal/mol.[151] The contribution of ionization of buried Lys to the stability of SNase was estimated to be between 2-7 kcal/mol.[150] Lastly, the contribution to stability of buried and charged Arg was reported to be between 2-10 kcal/mol.[77] These results may need to be approached with caution as, 1) the authors defined "buried" groups "...as those in which the Cα–Cβ vector of a side chain points toward the protein interior," instead of on solvent accessible surface area of the side chain, 2) SNase has a protein interior that appears to be accessible to bulk water , 3) the protein interior of both SNase and the stabilized mutant used in their studies appear to have a high dielectric constant, and 4) packing density within the protein core of SNase has been shown to be dynamic upon buried group ionization.[78, 149, 152, 155, 156]. Additionally, Uversky *et al*. report that SNase has been shown to form folding intermediates at different salt concentrations, in the presence of anions at low pH, and when self-associating.[157, 158] Thus, the wide range of free energy values calculated for contributions to stability in SNase ionizable group mutants may be a consequence of inadvertently measuring the stability contribution of an intermediate state induced by the presence of a buried ion mutant.

RNase Sa stabilized mutants as a model system

The model systems used in this work are stabilized variants of the eponymous enzyme Ribonuclease Sa (RNase Sa) from *Streptomyces aureofaciens* (Figure 1A).[159]

RNase Sa is a 96-amino acid secreted endoribonuclease that preferentially cleaves RNA by hydrolyzing the 3',5'-phosphodiester linkage of guanylic acid via a 2'-3' cyclic intermediate.[135, 160, 161] The active site residues responsible for catalysis are His53 and Glu54.[135, 162] The protein contains one disulfide bond between Cys 7 and Cys 96. RNase Sa is a good model system as it contains all the most commonly represented protein secondary structures: a single α-helix, a 6-strand β-sheet, β-turns between the strands, and random coil (Figure 1A). Furthermore, RNase is highly soluble (≈2 mg/ml) and expression in *E. coli* yields 50-100 mg dry weight of protein per liter of bacterial culture.[2, 163]

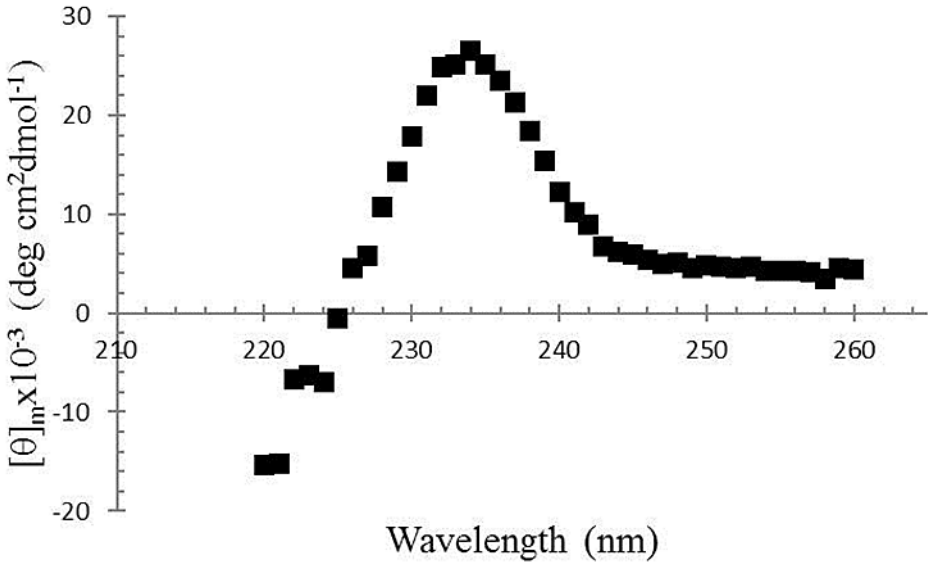

Figure 2. Circular dichroism spectra of RNase Sa wild-type obtained between 260-220 nm wavelengths. RNase Sa exhibits a unique CD absorbance peak at 234 nm.

As described in previous sections, the desolvation penalty for burying ionizable groups in the hydrophobic interior of a protein is high. Consequently, stabilized variants of RNase Sa were used to study the effects of burying ionizable groups (Figure 1C). Highly destabilizing mutations would cause the wild-type (WT) protein to be too unstable, and thus unfolded, at the all conditions under which protein stability could be studied. To circumvent that possibility, two stabilized variants of RNase Sa were used. RNase Sa 7S (7S) and RNase Sa 8S (8S) were previously made and are named based on the 7 or 8 stabilizing mutations they contain, respectively (Table 3, Figure 1B,C).[20, 36, 44, 164] RNase Sa 7S was constructed by: 1) improving protein-solvent interactions by making two acidic to Lys mutations on the protein surface (D25K, E74K) and 2) improving β-turn dynamics and structure by introducing Gly mutations (S42G, Q77G) to reduce strain and Pro mutations to decrease the entropy of unfolding (S31P, S48P, and S76P).[164] The latter approach reduces the conformational entropy of the unfolded state to collectively increase stability by 4.4 kcal/mol (Figure 1C).[36, 44] Taken together, 7S is 5.8 kcal/mol more stable than WT RNase Sa (Table 3).[44] Structural alignments of RNase Sa WT and 7S show comparable backbone topology (Figure 1D). Additionally, 7S contains two buried aspartic acids at position 33 and 79.[10, 13, 20, 79, 101] The side chain of Asp33 is 100% buried, makes three hydrogen bonds, and has a depressed pK of 2.4.[79, 101] The side chain of Asp79 is 89% buried, makes no hydrogen bonds, and has an elevated pK of 7.2.[20, 79] The lack of hydrogen bonds with Asp79 made it attractive for stability studies.

Table 3. Stability contribution of individual mutations in RNase Sa 7S and 8S.

Mutation Type	Mutation[a]	Δ(ΔG) (kcal/mol)[b]
Surface Charge	D25K	0.9
	E74K	1.1
β-Turn	S31P	0.7
	S42G	0.7
	S48P	1.3
	S76P	1.0
	Q77G	0.8
7S Total		5.8
Buried Charge	D79F	2.6[d]
8S[b] Total		8.2

[a]From Fu *et al*. (2009) and Fu *et al*. (2010)[36, 44]
[b]Adapted from Fu *et al*. (2009) and Fu *et al*. (2010).[36, 44]
[c]The value for 8S Total was determined in Fu *et al*. (2010), independently of the individual contribution of D79F in wild-type RNase Sa from Trevino *et al*. (2005).[20, 44]
[d]From Trevino *et al*. (2005).

The 8S variant is derived from 7S by making a D79F substitution in 7S.[44] The D79F variant was estimated to be the most stabilizing mutation in a study where the native buried Asp79 of WT RNase Sa was replaced with 14 other amino acids.[20, 44] Stability was increased by 3 kcal/mol over WT RNase Sa and 2.6 kcal/mol over 7S when making the D79F mutation in each background, respectively (Table 3).[44] In addition to the stabilizing mutations, both 7S and 8S contain an inactivating H85Q mutation that prevents endonuclease activity. The inactive mutation was made to prevent non-specific ribonuclease activity *in vivo* during protein expression and purification. The H85Q mutation makes no appreciable change in protein stability.[162]

The folded state of RNase Sa is studied by following a unique ellipticity absorbance peak at 234 nm wavelength using circular dichroism spectroscopy (CD) (Figure 2).[165] This unique peak is thought to result from the absorbance of buried Tyr residues and the electronic interactions of the aromatic rings of the side chains with their environment.[165] As RNase Sa unfolds, the Tyr residues become unstacked, exposed to solvent, and the strength of the optical signal decreases. The change in the magnitude of CD absorbance between the folded and unfolded conformations of RNase Sa provides a useful method to follow RNase unfolding under changing conditions.[9]

Research objectives

The aim of this study is to investigate the contribution to stability that buried ionizable groups have on the stabilized variants, 7S and 8S, of RNase Sa. Stability is defined as the free energy of unfolding of buried ionizable group mutants. A group is defined as buried if the side chain of the native group being replaced has a 0% solvent accessible surface area as determined by the in-house program *pfis* (see Materials and Methods).[114] As seen in Table 2, approximately 59% of the surface area of all residues is buried. With such a large proportion of residues on the interior of the protein, it is important to understand the contribution to stability different types of groups have on the free energy of unfolding. Consequently, these measurements contribute to the overall stability requirements of proteins as they obtain their folded structure. Specifically, ionizable amino acids make up 7% on average of buried residues. Furthermore, polar-uncharged groups have been suggested to contribute more to stability than buried

hydrophobic residues.[138] For these reasons, we investigate the small, but important, group of buried polar-charged amino acids and their contribution to protein stability. Here, we measure the contribution to stability of buried ionizable group mutants at solvent inaccessible positions by following the unfolding reaction during thermal denaturation, as monitored by circular dichroism spectrometry.

The objectives of this work are to: 1) determine the contribution to stability of ionization of the native and buried Asp79 in 7S by comparing the stability of 7S and 8S over a pH range in which ionization occurs 2) determine the change in stability for substituting an ionizable group at 3 buried positions whose native residue is the hydrophobic residue Ile, 3) determine the pK of buried ionizable group mutants, 4) calculate the electrostatic contribution between buried acidic and basic ionizable group mutants and the native buried Asp79, and 5) determine if buried ionizable group mutants alter protein structure or allow water access to the protein core by analyzing crystal structures of the variants resolved by Kazufumi Takano, Graduate School of Life and Environmental Sciences, Kyoto Prefectural University, Kyoto, Japan.

CHAPTER II

MATERIALS AND METHODS

Reagents

All reagents were molecular biology grade or higher and were purchased from Fisher Scientific (Pittsburg, PA) or Sigma-Aldrich (St. Lois, MO). All buffers were filter sterilized and made in filtered autoclaved ddH_2O. Water used for large batch buffers, such as succinate buffers used in protein purification, was filtered using autoclaved Whatman #3 filters before use to remove any particulates.

RNase Sa 7S and 8S plasmids

The RNase Sa 7S and 8S genes are in the pHFSa plasmid, which is a pETDuet derivative containing two multiple cloning sites under the control of a T7 promoter.[36, 44] The sequence encoding barstar, an RNase Sa activity inhibitor, is in the upstream multiple cloning site. The down-stream multiple cloning site encodes RNase Sa 7S or 8S with the additional 25 residue N-terminal phoA cleavable signal sequence. The phoA tag directs protein secretion into the periplasmic space of *E. coli*, and is cleaved off by signal peptidase I, releasing full length RNase Sa into the periplasmic space for later osmotic shock purification (see below). The pHFSa plasmid was constructed by Hailong Fu as previously described.[36]

Picking buried positions using PDB_File Information Software (*pfis*)

The solvent accessible surface area of the amino acid side chains in the crystal structure of RNase Sa (rgg_h.pdb) were calculated computationally by the *pfis* program.[114] The program exposes the protein surface to a sphere approximately the size of a water molecule and determines the percent of side chain accessible surface area that comes in contact with the sphere as proposed by Lee and Richards.[126] There are 10 residues in 7S that are ≈100% buried excluding glycine: Ala15, Asp33, Leu44, Thr56/82, Val 57, Ile70/71/92, and Phe89. The 3 isoleucine residues are chosen as substitution candidates based on the following reasons: the side chains of were 100% buried in RNase Sa, and isoleucine had the highest population of a single type of residue (n=3). Position 70 and 71 are adjacent, but face in opposite directions on the third β-strand. Position 92 is 5Å away from, and on the same side of the β-sheet as Ile70, but on β-strand five. Both Ile70 and Ile92 are within direct contact distance (6 Å) of the native, 85% buried Asp79 side chain, allowing us to test electrostatic effects with Asp79. In contrast, Ile71 is 11Å from Asp79 and lies out of direct contact with Asp79. Additionally, the side chain of Ile71 is separated from Asp79 by other residues in the core of the protein, whereas Ile70 and Ile92 are not. The dichotomy of the local environments and distances between Ile70 and Ile92, Ile71, and Asp79 provide a convenient system for testing the effects of the native Asp79 on other ionizable group mutants.

Mutagenesis

All RNase Sa mutants were made by nicked single-strand DNA amplification PCR using the QuikChange™ mutagenesis kit from Agilent Technologies (Santa Clara, CA). Cloning and mutagenesis primers were ordered from and created by IDT (Integrated DNA Technologies, Corallville, IA). Lyophilized primers were reconstituted in ddH_2O to a working concentration of 100 μmol/μL. Final concentrations in reaction tubes were between 5-25 pmol/μL. Mutagenesis primers and thermocycler parameters were designed according to the QuikChange kit protocol. Briefly, all mutagenesis primers were designed to have a melting temperature (T_M) near 60 °C, annealing temperatures were 4-5 degrees below the T_M, and the extension temperature was 68 °C. Annealing temperatures were adjusted as needed and usually were dropped or raised by 1-2 degrees depending on a lack of mutation or non-specific binding, respectively. After DpnI incubation, plasmids were transformed into *E. coli* strain XL-1 Blue using standard protocols.[166] Plasmids were isolated using a Qiagen Mini-prep kit (Valencia, CA). Standard DNA sequencing was performed by Eton Bioscience (San Diego, CA) and the sequences checked for the correct mutation.

Protein expression and purification

RNase Sa and mutant proteins were purified as previously described.[163] Briefly, pHFSa plasmid containing a mutant RNase Sa gene was transformed into *E. coli* BL21 C43 (DE3) cells and grown overnight with moderate shaking (180 RPM) at 37 °C. Protein was harvested from the periplasmic space by osmotic shock. The cells were

removed from culture media by centrifugation at 3000xG for 20 min and equilibrated in 180 ml of 20% Sucrose –15 mM Tris buffer for 10 min. The cells were once again pelleted for 20 min at 8000xG and the supernatant put aside. Pellets were resuspended in ice-cold non-sucrose 15 mM Tris buffer, shaken on ice for 45 min at 180RPM, and centrifuged for 30 min at 8000xg. Supernatants were combined and unwanted proteins precipitated by adding enough succininc acid to bring the final concentration to 50 mM succinic acid and the pH adjusted to 3.25 with 1 M HCl. The acid precipitation was allowed to reach room temperature before precipitants were removed by a 45 min centrifugation at 3000xg. The supernatant was decanted and loaded onto a 4 x10cm chromatography column containing cation exchange resin equilibrated in loading buffer (50 mM succinic acid, pH 3.25) overnight. RNase Sa and its mutants were purified by cation exchange on SP Sephadex C25 by fractionation. A pH gradient maker holding 500 ml each of 50 mM succinic acid buffer at pH 3.25 and 20 mM succininc acid + 100 mM NaCl at pH 10 was used to release protein from the resin since RNase Sa and mutants have a pI between 3.8 and 4.1. Fractions containing protein, as determined by absorbance of light at $\lambda = 280$, were flash frozen by putting the flask containing pooled fractions in dry ice and 100% ethanol and then lyophilized. The lyophilized protein was desalted over a 4 x100 cm Sephadex G50 column. Lyophilized protein was resolubilized in 15 mL of degassed ABC buffer (4 g ammonium biocarbonate/L H_2O) and allowed to fully enter the resin by gravity before eluting with 4 L degassed ABC buffer. Fractions were collected in 12 mL aliquots after approximately 700 mL of

buffer had passed through the resin. The elutate containing protein, as determined by the absorbance at $\lambda = 280$, was frozen, lyophilized, and stored at -20 °C until needed.

SDS-PAGE/MALDI protein identification and confirmation

RNase Sa identification was confirmed by SDS-PAGE. Briefly, 10 μg of protein (dry wt.) was boiled in 30 μL Laemmli sample loading buffer for 10 minutes before being loaded into precast 16% acrylamide SDS-PAGE gels from BioRad (Hercules, CA).[166] Proteins were separated for 1 hr at 120 mAmps. RNase Sa and mutants have an approximate molecular weight of 10 kDa and were visualized in the gels by exposure to Coomassie Stain for 4 hours followed by destaining in 10% glacial acetic acid + 40% methanol (vol/vol). Additionally, all samples that were positive for protein presence as determined by SDS-PAGE were sent for mutant identification by mass spectrometry. Matrix-assisted laser desorption ionization- time of flight (MALDI-TOF) mass spectrometry was performed on each purified RNase Sa mutant in the Protein Chemistry Lab of Texas A&M University. The mass of RNase Sa 7S is 10.492 kDa and was used as a control for all MALDI-TOF mass determinations.

Circular dichroism wavelength scan and thermal denaturation

All RNase Sa variant solutions for experimentation were made in 30 mM MOPS buffer that was subsequently filter sterilized and degassed before use. All CD experiments were conducted using an Aviv 202:CD spectrometer (Aviv Biomedical, Inc., Lakewood Township, NJ).[37] The spectra of RNase Sa has a unique positive

absorbance peak at 231 nm when measured by circular dichroism spectrometry (CD) and exhibits unfolding consistent with a two-state unfolding mechanism (Figure 2, 3).[165] The unique peak decreases when Tyr residues in the protein are exposed to solvent.[165] Consequently, CD spectra were obtained from 220-240 nm for each protein (10 sec averaging time per 1 nm wavelength step) before every thermal denaturation experiment to ensure that proteins are both folded and at a concentration that produces minimal background noise (0.05 – 0.2 mg/ml: dry wt/vol).

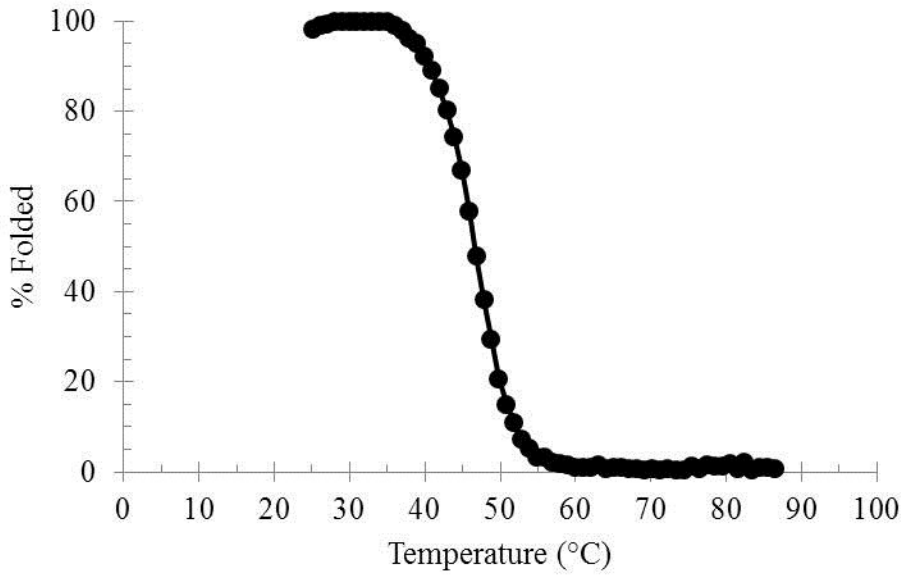

Figure 3. Thermal denaturation of RNase Sa wild-type. At temperatures below 40 °C or above 55 °C, RNase Sa WT is either 100% in the folded or unfolded state, respectively. The midpoint of the transition state is at 48 °C, and is the point the fractional population of each state is 50% and is called the melting temperature (T_M). RNase Sa has one transition and is deemed "two-state." The line is added to guide the eye.

Thermal denaturation curves of each protein are followed at 234 nm where the difference in the maximum and minimum absorbance is greatest between the obtained spectra for the folded and unfolded states (Figure 3). The experimental parameters for thermal denaturation at $\lambda = 234$ nm are as follows: 0.1 mg/ml protein in a 1 cm quartz cuvette, temperature range: 5 – 95 °C, 3 min. equilibration time per 1 °C temperature step, and a 30 sec. averaging time per wavelength. A reverse scan from 95 – 5 °C follows every

run to determine if the protein reversibly folds. In instances where the thermal stability of mutants was very low, the starting temperature was lowered to -5 °C in order to acquire sufficient data points in the pre-transition region.

All melting temperatures (T_M) were determined and calculated from a minimum of four independent replicates at pH = 7 except in the case of determining the contribution to stability at different pH (described below). The T_M is the temperature at which the fraction of folded to unfolded protein is equal and is visualized on thermal denaturation curves as the mid-point of the transition region (Figure 3). A shift to higher transition or melting temperature indicates increased stability and vice versa. The T_M is calculated as previously described in detail and in "Free energy calculations" below.[37]

Free energy calculations

All T_M, ΔG, and ΔH values were determined and calculated from four independent replicates of thermal denaturation curves as previously described.[37, 167]

To calculate the T_M, the data obtained from thermal denaturation monitored by CD at 234 nm were fit to equation 8:

$$\mathbf{y} = \frac{(\mathbf{y_F}+\mathbf{T_{MF}})+(\mathbf{y_U}+\mathbf{T_{MU}})\cdot\mathbf{e}^{(-\Delta\mathbf{H_{TM}}\cdot\frac{\frac{\mathbf{1}}{\mathbf{T+273.15}}-\frac{\mathbf{1}}{\mathbf{TM+273.15}}}{\mathbf{R}})}}{\mathbf{1}+\mathbf{e}^{(-\Delta\mathbf{H_{TM}}\cdot\frac{\frac{\mathbf{1}}{\mathbf{T+273.15}}-\frac{\mathbf{1}}{\mathbf{TM+273.15}}}{\mathbf{R}})}} \quad (8)$$

where y is the ellipticity measured at temperature (T), y_N is the y-intercept of the linear extrapolation of the pre-transition (folded state) region baseline with slope m_F, y_U is the y-intercept of the linear extrapolation of the post-transition (unfolded state) region baseline with slope m_U, T_M is the mid-point of the transition region (melting temperature), R is the gas constant, and ΔH_{TM} is the van't Hoff enthalpy of unfolding at the melting temperature. Fits were performed in the Origin Lab 6.1 program (Origin Lab Corp., Northampton, MA) using consecutive iterations of the Levenberg-Marquardt non-linear least squares regression until obtaining a X^2-minima (minimum error deviation from the fit).

Obtained values for T_M and ΔH_{TM} were used to calculate the free energy of unfolding using the heat capacity change (ΔCp) calculated by Fu *et al*. for 7S or 8S, respectively, using equation 4 which has been previously described in detail.[36, 44, 167]

pK shift calculations

Samples prepared in buffers at different pH values were made as previously described using the following filtered and degassed buffers: ddH_2O at pH 1 and 1.5, 30 mM glycine at pH 2 and 3, 30 mM sodium acetate at pH 4 and 5, 30 mM MES at pH 6, 30 mM MOPS at pH 7, 30 mM diglycine at pH 8 and 9, and 30 mM glycine at pH.[167] Using the difference in the calculated free energy (see Calculations) between the wild-type and the mutant thermal denaturation curves at each pH, the pK of the mutant substitutions was indirectly determined as previously described.[76] Briefly, the pK is determined by fitting the difference in free energy between a variant and parental protein at each pH to equation 9:

$$\Delta G_{H^+} = \Delta G_{H^+ \to \infty} + RT\left(\ln \sum_{i=1}^{n} \frac{1+\frac{K_{iF}}{[H^+]}}{1+\frac{K_{iU}}{[H^+]}}\right) \quad (9)$$

where ΔG_{H}^{+} is the free energy of unfolding, $\Delta G_{H+ \to \infty}$ is the free energy change when all ionizable groups are protonated, R is the gas constant, T is the temperature in °K, K_{iF} is the dissociation constant for group "*i*" in the folded state, and K_{iU} is the dissociation constant of the group in the unfolded state. The values for K_{iF} have been determined for all ionizable groups in RNase Sa and are reported in Table 4. The latter, K_{iU}, is based on the experimental pentapeptide values reported by Grimsley *et al*. and in Table 1.[13] The reagents chosen for use in each buffer is based on the low heat of ionization for the reagent at the indicated pH value.

Table 4. Ionizable group pKs in RNase Sa.

Position	Residue	pK[a]
1	Asp	3.4
14	Glu	5.0
17	Asp	3.7
25	Lys	10.4
33	Asp	2.4
40	Arg	12.5
41	Glu	4.1
53	His	8.7
54	Glu	3.4
63	Arg	12.5
65	Arg	12.5
68	Arg	12.5
69	Arg	12.5
74	Lys	10.4
78	Glu	3.1
79	Asp	7.3
84	Asp	3.0
93	Asp	3.1

[a]Measured values are previously reported.

Electrostatic interaction calculations

The electrostatic contribution of interacting ionized groups with buried native Asp79 in 7S can be calculated using a variant of equation 5, equation 10:

$$\Delta G_e = \sum_j \frac{q_{D79} q_j}{Dr_{D79:j}} \quad (10)$$

where ΔG_e is the free energy contribution of the electrostatic interaction, q_{D79} is the partial charge of ionized Asp79 (-0.5), q_j is the charge on interacting ion j, D is the

dielectric constant, and $r_{D79\text{-}j}$ is the Euclidian distance between the γ-carbon of Asp79 and the interacting species determined. When a point charge is positive, q = 1, and when a point charge is negative, q = -1. Based on Coulomb's equation (equation 10), the free energy to keep two charged species at some distance "r" in a medium with dielectric constant of "D" will be positive for ions of the same charge (repulsive) and negative for ions of opposite charge (attractive). Electronic resonance can shift the position of electrons in ionizable groups (e.g. carboxylic acid) and thus shift the location of the charge. Thus, the nearest carbon atom is used as the point of reference for distance measurements and the group is given a ½ charge value of -0.5 or +0.5 for resonant anions or cations, respectively. Values for the Cartesian position of each atom were modeled from the structure file of 7S I71A and used to calculate r using equation 11:

$$\mathbf{r} = \sqrt{(\mathbf{x_j} - \mathbf{x_{D79}})^2 + (\mathbf{y_j} - \mathbf{y_{D79}})^2 + (\mathbf{z_j} - \mathbf{z_{D79}})^2} \qquad (11)$$

where x_j, y_j, and z_j are the coordinates of the ion groups and x_{D79}, y_{D79}, and z_{D79} are the coordinates of the Asp79 carboxyl. The structure file for 7S was obtained by reversion of 7SI71A to 7S by *in silico* mutagenesis using the PyMol program.[154] The rotamer of highest probability for Ile71 was used for backbone topology calculations in PyMol. The structure file for 7S I71A was obtained from Kazafumi Takano, Graduate School of

Life and Environmental Sciences, Kyoto Prefectural University, Kyoto, Japan. It must be pointed out that the distance between charges may be different between the crystal and the protein in solution at a different pH values.[168]

Free energy of unfolding for buried ionizable groups in RNase Sa 7S

The total free energy of unfolding in buried ionizable variants of RNase Sa 7S and 8S includes the contribution from burying the group and from electrostatic interactions with that group. Buried ionizable group variants of 7S will have the additional contribution of electrostatic interactions conferred by Asp79 compared to 8S, which contains the D79F mutation. To isolate the contribution of a burying an ionizable group in the protein interior, the free energy contribution from electrostatic interactions was subtracted from the total free energy of unfolding as described above using equation 12:

$$\mathbf{\Delta G_j = \Delta G_T - \Delta G_e} \qquad (12)$$

where ΔG_j is the free energy contribution of the mutant buried ionizable group, ΔG_T is the free energy of unfolding for an RNase Sa 7S or 8S variant, and ΔG_e is the calculated electrostatic interactions. The ΔG_e values resulting from and interaction between buried ionizable groups and Asp79 were estimated by subtracting the free energy of unfolding for 7S from 8S variants, as an electrostatic interaction between Asp79 and the mutants will be absent in 8S.

X-ray crystallography

X-ray crystallography and structural determination was performed in the Kazufumi Takano Lab at the Graduate School of Life and Environmental Sciences, Kyoto Prefectural University, Kyoto, Japan. Briefly, crystals were grown in CombiClover Junior plates by the sitting drop vapor diffusion method. A description for the parameters for each mutant was provided by Kazufumi Takano (personal correspondence) and follows.

7S I71A

A 10 mg/mL stock protein solution was made in 0.1 M citric acid and 0.2 M phosphoric acid at pH 5. A 200 µL reservoir solution stock was made consisting of 2 M ammonium sulfate and 0.1 M citric acid at pH 5.5. Protein drops are made by adding 2 µL of the protein stock solution to 2 µL of the reservoir stock solution and stored at 20 °C until crystal formation occurred.

8S I71D

A 10 mg/mL stock protein solution was made in 0.2 M sodium phosphate at pH 7. A 200 µL reservoir solution stock was made consisting of 1.6 M ammonium sulfate, 10% vol/vol 1,4-dioxane, and 0.1 M citric acid at pH 6.5. Protein drops are made by adding 2 µL of the protein stock solution to 2 µL of the reservoir stock solution and stored at 20 °C until crystal formation occurred.

CHAPTER III

CONTRIBUTION OF ASPARTIC ACID 79 TO THE STABILITY OF RNASE SA 7S

Introduction

Ionizable groups on the side chains of amino acids are crucial for protein activity, solubility, and stability. Polar-charged groups are typically found on the protein surface where they readily interact with the polar environment of aqueous solvent; though, not all polar-charged groups are solvent exposed.[47-49, 53, 57] Approximately 14% of polar-charged groups are buried into the non-polar environment of the protein interior during folding, >90% of which are the carboxyl groups of glutamic and aspartic acid.[57, 127] Buried ionizable groups likely aid in protein turnover or increase flexibility to optimize enzyme activity.[15-18]

To mitigate the large desolvation penalty of burying charged groups in the non-polar protein core, proteins use multiple strategies including forming ion pairs, hydrogen bonding, and shifting the pK of the side group to a neutral charge state.[4, 9, 17, 24] In doing so, proteins can not only neutralize the destabilizing effects of buried carboxyl groups, but in many instances carboxyl groups can be stabilizing. For instance, the buried Asp70 of T4 lysozyme forms a salt bridge with His31 that contributes 3-5 kcal/mol to stability.[95] The side chain of RNase T1 Asp76 is 99% buried, forms three intramolecular hydrogen bonds and one intermolecular hydrogen to water, and to date has one of the lowest recorded pKs measured at pK = 0.5.[10, 13, 76, 98, 101] This suggests that the charge is required for the stabilizing property of the buried carboxyl. In support of this, when Asp

is mutated to Asn, the stability of RNase T1 decreases by 3.1 kcal/mol. Similarly, RNase Sa Asp33 is 100% buried, forms three hydrogen bonds, and has a pK of 2.4.[10, 13, 79] The pK of Asp33 increases when hydrogen bonding partners are removed by mutation. In agreement with this, Anderson *et al*. state, "The unfolded state is stabilized only if acidic groups in the folded state have lower pK values than in the unfolded state."[95] When Asp33 is mutated to Ala, the conformational stability decreases by 6 kcal/mol.[98] In contrast, RNase Sa Asp79 is 89% buried, forms no hydrogen bonds, and has an elevated pK of 7.4.[10, 13, 20, 76, 101] When Asp79 is mutated to an Ala, the stability increases by 3.3 kcal/mol.[20] Therefore, the stability change due to burying an Asp carboxyl can vary by ≈9 kcal/mol! The decrease in stability measured for Asp79 results from the unfavorable Born self-energy of burying an unpartnered charge in the non-polar interior of RNase Sa. Basically, the Born energy is the difference in energy to move a charged sphere of some radius between a vacuum and a medium with a non-zero dielectric constant. Trevino *et al*. suggest replacing buried charges as a means to increase protein stability.[20] Of interest is the stability contribution of an isolated buried charge in the protein interior. The focus of this study is to measure the stability contribution of a buried charge by measuring the contribution of the ionized aspartic acid carboxyl of Asp79 in RNase Sa 7S, a stabilized variant tolerates destabilizing substitutions.

Stability is the additive contribution of all forces acting to fold or unfold a protein.[4, 7, 9, 17, 24, 58] Therefore, stability is an intrinsic property of proteins based on their amino acid sequence and environment. The typical approach to determining the

contribution to stability of buried ionizable groups is to use mutagenesis to replace the group and measure the resultant change in free energy.[20, 77, 90, 97, 99, 112, 143, 150-152] Interpretation of the results from these studies can be difficult, as packing and cavitation are important to protein stability.[50, 55, 116, 169-172]

Another approach is to test the contribution of ionizable groups in their ionized and non-ionized states. A complication to taking this approach is that the pK of buried ionizable side chains can be shifted towards or near physiological pH when put in the hydrophobic environment of the protein interior.[10, 13, 76] Consequently, the isolation of the contribution to stability of the group of interest is difficult to separate from the contribution from His and Cys. To circumvent this, we use a stabilized variant, 7S, of the 96 amino acid endonuclease RNase Sa, that has a single native buried group (aspartic acid) containing a carboxyl side-group that ionizes in the pH range of 6-9. The pK values of ionizable groups in RNase Sa WT are reported in Table 4.

RNase Sa 7S is a variant of RNase Sa WT with 7 stabilizing mutations. 7S contains the native buried aspartic acid at position 79 (Asp79). The pK of Asp79 is 7.2. Thus, at physiological pH of 7.4, 7S Asp79 is half ionized. The pK values of every ionizable group in RNase Sa have been previously determined, and there are no other ionizable groups in 7S that ionize within 1 pK unit of 7.4 (Figure 4). By calculating the difference in free energy of unfolding below and above the pK of Asp79 (at pH = 6 or 9), the magnitude of the contribution to stability of a single buried anion can be measured. In order to minimize background contributions to stability from the ionization of the carboxyl of Asp79 in calculations, the results are compared to

experiments in a 7S variant in which Asp79 is mutated to a Phe residue (8S). Taken together, an isolated buried anion is measured to contribute 1.8 kcal/mol to the stability of RNase Sa 7S.

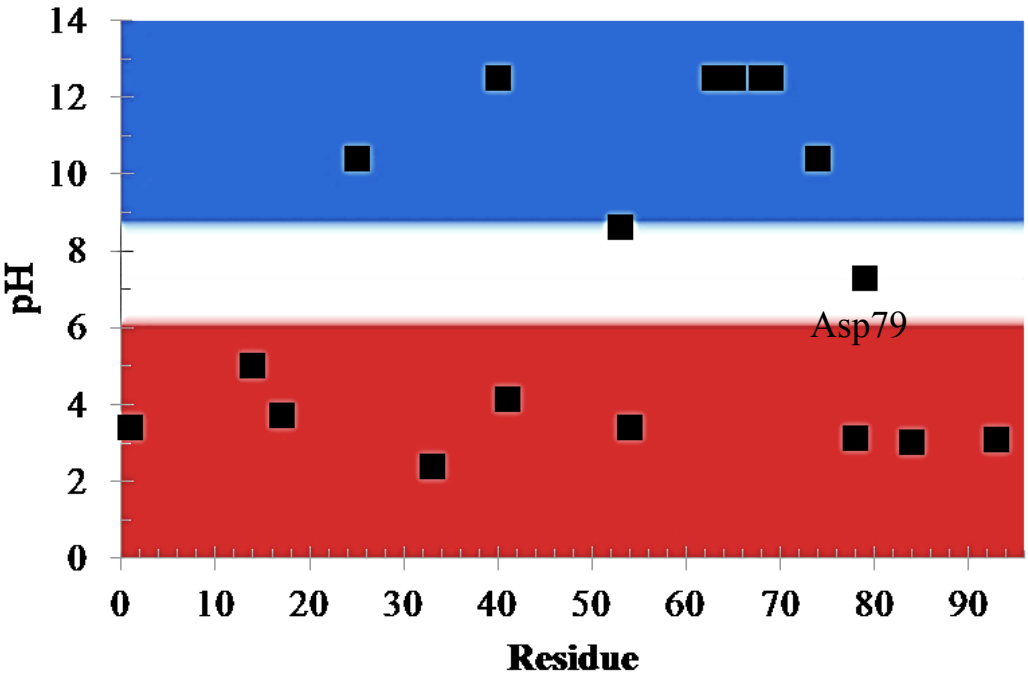

Figure 4. pK values of ionizable groups in RNase Sa. The pK values (squares) of ionizable groups in RNase Sa have been previously determined and are reported in Table 4. Acidic residues are negatively charged at pH values above their pK (red area). Basic residues are positively charged at pH values below their pK (blue area). The pK of Asp79 is 7.2 (white line) and the gradient demarks the pH range 6-9. Asp79 is completely protonated and uncharged below a pH = 6 and completely ionized (anionic) above pH = 9.

Results

CD spectra of RNase Sa 7S and 8S

To test that 7S and 8S have the indicative absorbance peak described above (see Materials and methods), CD spectra were obtained for both proteins over a range of 222-240 nm (Figure 5). Both 7S and 8S exhibit the unique peak and were analyzed by CD to obtain the free energy of unfolding as determined by thermal denaturation. CD spectra were also obtained for 7S and 8S at pH 6, 7, and 9 to ensure that the proteins are folded. The fully folded state is further indicated by UV-Vis spectrometry analysis of the samples, as a blue shift that results from unfolding was not observed in the absorbance peak at 280 nm in 7S and 8S (data not shown).

Thermal denaturation of 7S and 8S at pH 6, 7, 9.

To compare the stability contributions in the presence and absence of Asp79, thermal denaturation curves of 7S and 8S at pH 6, 7, and 9 were followed by measuring the CD at 234 nm over a temperature range of 5 – 95°C (Figure 6). Four independent replicate curves (n=4) were obtained for pH 6 and 9. For pH 7, 12 independent replicates were obtained (n=12). The data were analyzed as previously described (see also Materials and methods).[37] Using the linear extrapolation method and the equations 13 and 14 to determine the fraction folded (f_F) and unfolded (f_U)[7]:

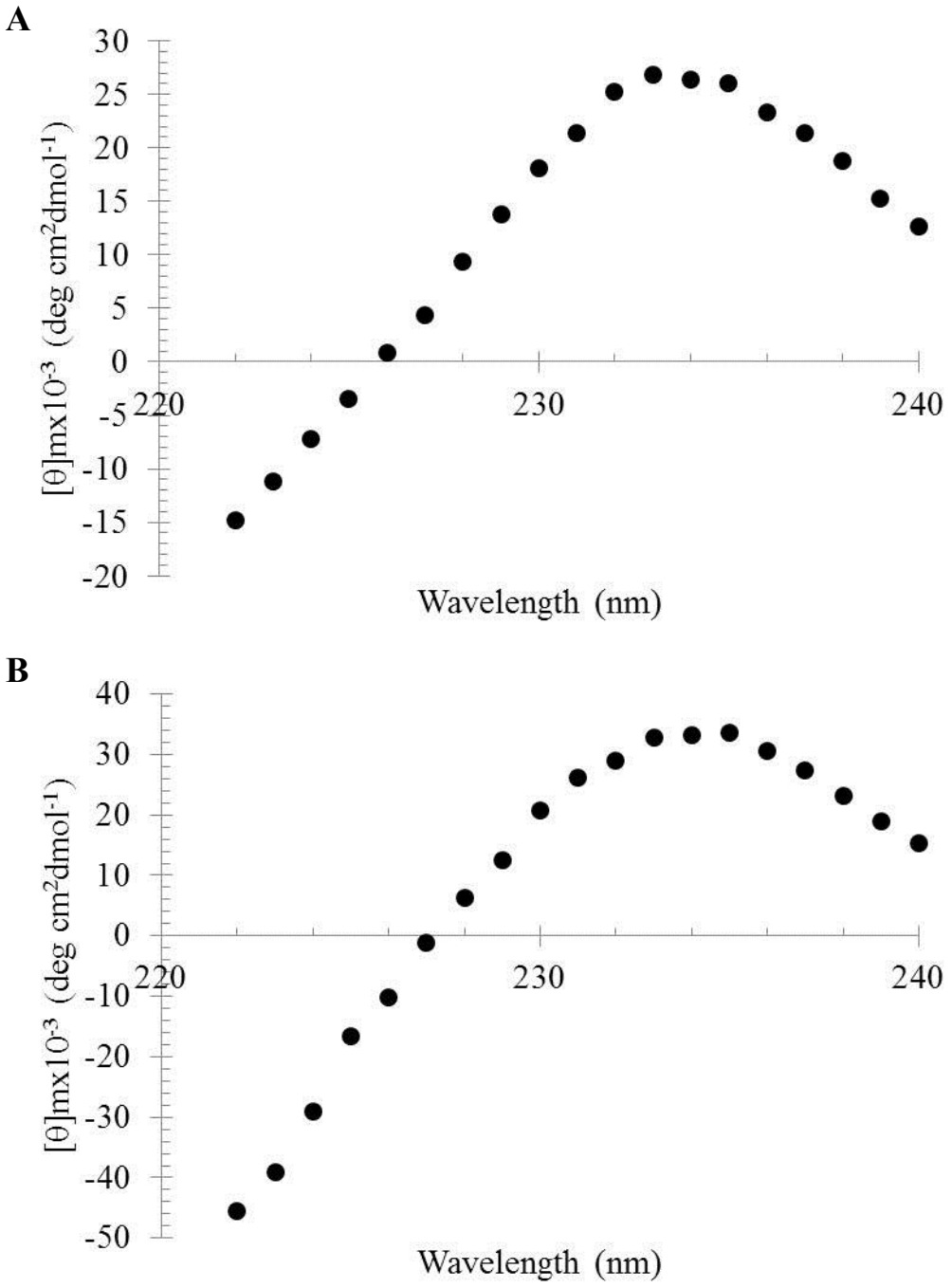

Figure 5. Circular dichroism spectra of RNase Sa 7S and 8S obtained between 222-240 nm wavelengths. 7S (A) and 8S (B) are in the folded state as indicated by the absorbance peak observed at 233 nm.

$$y = f_F y_F + f_U y_U \quad (13)$$

$$f_F + f_U = 1 \quad (14)$$

$$\therefore f_U = \frac{(y - y_F)}{(y_U - y_F)};\ f_F = 1 - f_U$$

where y is the ellipticity measured by CD, y_N is the y-intercept of the pre-transition region, and y_D is the y-intercept of the post-transition region. The slope of the pre- and post-transition regions is typically non-zero. In those cases, the equation for a line is substituted for the y_N or y_D values (e.g. $y_i = mx + y_{F,}$ for y_F). The line of the pre-transition region along its slope is treated as 100 % folded and the line of the post-transition region along its slope is treated as 0% folded as previously described.[7, 167] Data are normalized between 0% - 100% folded. The fraction folded for each set is averaged to produce a single curve at each pH (Figure 6). The free energy of unfolding, Δ(ΔG), are calculated as previously described (see also Materials and methods).[8, 37, 167] Briefly, T_M, ΔH, and the heat capacity (ΔCp) are used to determine the free energy of unfolding of the proteins using equation 4. The change in stability is more similar for Ile→Ala controls when the ΔCp used in calculations is the heat capacity change calculated by Fu *et al*. for 7S and 8S, or 1.68 and 1.07 kcal/mol/K, respectively.[44] Values for T_M, ΔH, ΔG and Δ(ΔG) are reported in Table 5.

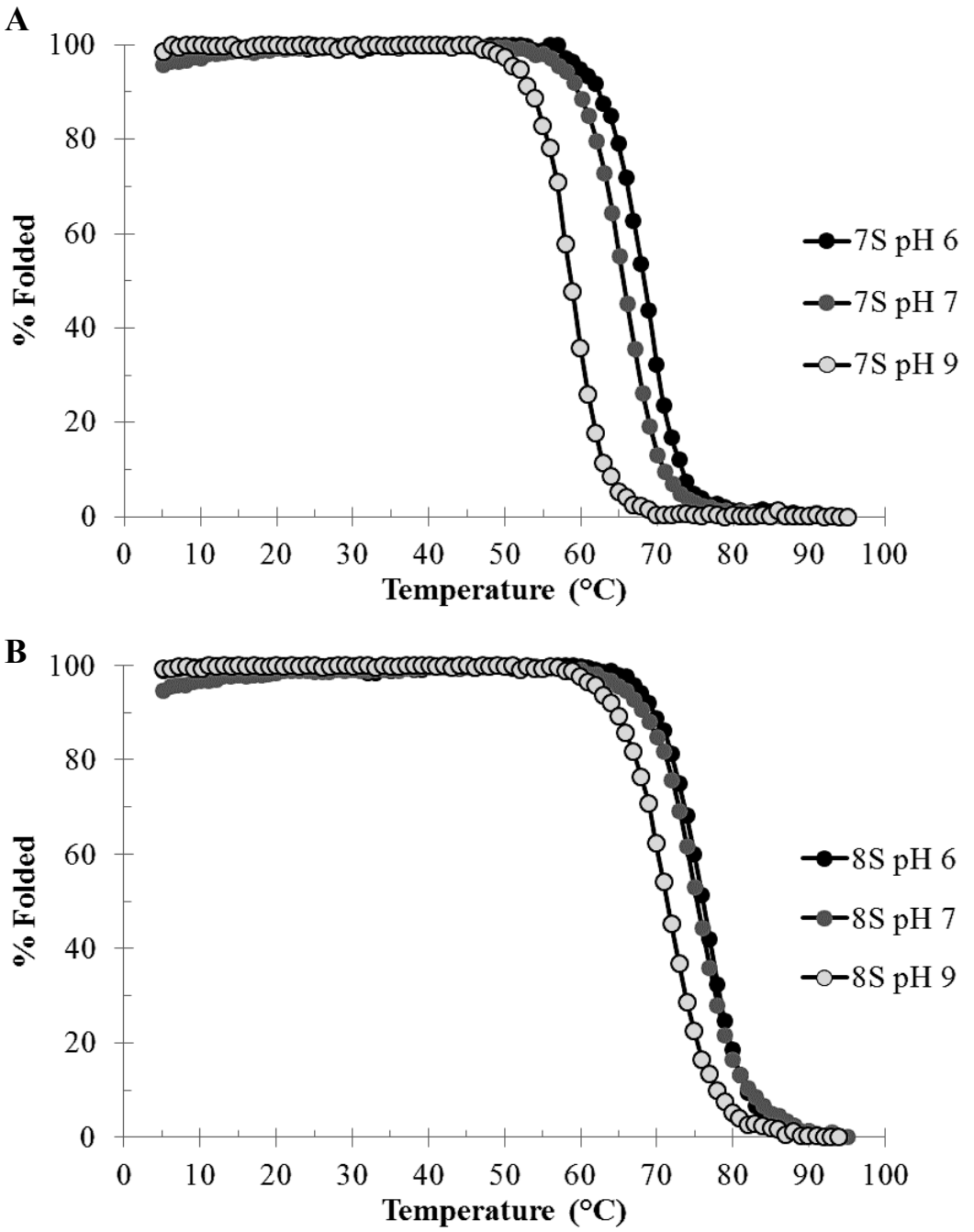

Figure 6. Thermal unfolding curves of RNase Sa 7S and 8S. The thermal unfolding curves of 7S (A) and 8S (B) for pH 6 (black), 7(grey), and 9 (open). Data were analyzed as previously described (see also Materials and methods).[37] Calculations are based on thermodynamic parameters reported in Table 5 and lines are added to guide the eye.

Table 5. Parameters characterizing the thermal denaturation of RNase Sa 7S and 8S at pH 6, 7, and 9.

Mutant	pH[a]	T_M[b] (°C)	ΔH[b](kcal/mol)	ΔG(kcal/mol)[c]
	6.0	68.8 ±0.8	98.0 ±4.1	0.9 ±0.2
7S	7.0	65.4 ±0.8	89.2 ±5.3	0.0 ±0.0
	9.0	59.1 ±0.6	99.0 ±3.4	-2.0 ±0.1
ΔG_{7SpH9}-ΔG_{7SpH6}[d]				-2.9 ±0.3
	6.0	75.9 ±0.8	89.4 ±3.2	0.2 ±0.2
8S	7.0	75.1 ±0.6	81.6 ±4.9	0.0 ±0.0
	9.0	71.3 ±0.3	83.6 ±4.0	-0.9 ±0.1
ΔG_{8SpH9}-ΔG_{8SpH6}[d]				-1.1 ±0.3
Stability contribution of a buried anion[e]				-1.8 ±0.6

[a] pH values are measured within ±0.01units.
[b]The melting temperature, T_M, is the midpoint of the thermal unfolding curve. ΔH is the estimated enthalpy change at the T_M. Values reported are the average of 4 independent replicates (n = 4) for pH 6 and 9, and 12 independent replicates for pH 7 (n = 12).
[c]The free energy of unfolding was calculated as previously described using ΔCp values 1.68 and 1.07 for 7S and 8S from Fu *et al*., respectively. The free energy was calculated at the T_M of each variant at pH 7 as the reference temperature "T" in the modified Gibbs-Helmholtz equation, giving $\Delta G = 0.0$ at pH 7.
[d]Values represent the effect of pH on stability over the range in which Asp79 ionizes and was calculated by subtracting ΔG at pH 6 from ΔG at pH 9 for each variant.
[e]The stability contribution of a buried anion is the difference in the pH effect on stability between 8S and 7S $\Delta(\Delta G_{7SpH9-6}) - \Delta(\Delta G_{8SpH9-6})$.

Contribution to stability of a buried anion

The pK of the native buried Asp79 of 7S is 7.2.[20, 79] Aspartic acid has a neutral charge below the pK and a negative charge (anionic) above the pK. The stability contribution of the carboxyl anion was calculated by monitoring thermal denaturation of 7S at pH 6,7, and 9. At pH 6, Asp79 will be completely protonated and uncharged. At pH 9, Asp79 will be completely deprotonated and anionic. The stability effect of ionization is calculated by subtracting the free energy of unfolding at pH 9 from the free energy of unfolding at pH 6. The total contribution to stability from the ionization of

buried Asp79 in 7S was calculated as -2.9 kcal/mol. To measure the intrinsic change in stability (background stability) in the absence of Asp79 between pH 6 - 9, the previous approach was repeated for 8S. The 8S variant contains a D79F mutation in addition to all other 7S mutations. The pH effect on stability for 8S between pH 6 and 9 was calculated as -1.1 kcal/mol. Subtracting the pH effect on stability for 8S from the stability estimated for 7S over the pH range of 6 to 9 gives the contribution to stability of the buried anion of -1.8 kcal/mol (Table 5).

Discussion

In RNase Sa WT, the aspartic acid at position 79 is 89% buried.[20] As a result, the pK of Asp79 has been elevated from 3.9 to 7.4, which shifts the carboxyl functional group of Asp79 to a more protonated and neutral state at physiological pH.[20, 79] To determine the stability contribution of Asp79, the free energies of unfolding for Asp79 mutants were studied in RNase Sa WT (WT).[20] The difference in free energy ($\Delta(\Delta G)$) between the WT and the WT D79A and D79F mutations is comparable and increased protein stability by 3.3 and 3.7 kcal/mol, respectively.[13, 20] The total contribution to stability from the ionization of Asp79 in RNase WT was measured at pH 3.0 and pH 8.5.[20] The wild-type has 8 residues that have pK values within 1 pH unit of pH 3 (Table 4, Figure 4). Therefore, the magnitude of the calculated change in stability from the ionization of Asp79 may include contributions from the variable ionization states of those 8 residues at low pH. To abate any variance that may result from those ionizable

groups in free energy calculations in this study, RNase Sa 7S and 8S are studied over a limited pH range of 6 - 9 in which only Asp79 fully ionizes.

The change in stability for 7S from pH 6-9 is -2.9 kcal/mol. Therefore, the shift in pH from 6 to 9 is destabilizing. The difference in free energy between pH 6 - 9 in the 8S variant was calculated as -1.1 kcal/mol. The value differs from the -4.0 kcal/mol difference that was measured between pH 3 – 8.5 in the WT D79F mutant (Table 5). The difference between the 8S variant and WT calculations for WT is that WT calculations used the average T_M of all mutants as the reference temperature and $\Delta(\Delta G)$ values were the difference between mutants and the WT at each pH.[20] By using both the T_M and stability of 7S and 8S at pH 7 as a reference, any inherent difference in force contributing to stability that was not a result of the ionization of Asp79 (background stability contribution) is subtracted out (Table 5). This includes packing density differences that result from removing the side chain of Asp when making a D79A mutation or substitution of the aromatic ring of Phe for Asp in 8S.

As previously stated, the pK of Asp79 is 7.4, and no other group in 7S fully ionizes between pH 6 – 9 (Figure 4). Having a pK isolated within a range of ±1 pH units provides the unique opportunity to determine the contribution of not just a buried ionizable residue, but the ion itself in the nonpolar environment of the protein interior. This is in contrast to the traditional approach testing the stability contribution of buried ionizable residues that uses mutagenesis to change the ionizable residue to different non-ionizable residues. Careful consideration of the contributing forces after mutation must be considered. For example, the contribution of a single methyl group to protein

stability has been determined to be ≈1.5 kcal/mol, and that contribution has to be considered in any mutation that includes methyl group removal.[138, 173, 174] Studies have indicated that the forces contributing to protein stability are additive.[24] By using the change in stability at pH 7 as the standard reference in our models, variance is mitigated. Intrinsic additive changes in stability are subtracted out for calculations within each mutant, which may not occur when subtracting stability changes between a wild-type and mutant at two different pH. From that, a true comparison can be made between the changes in stability for 7S and 8S at pH 6 and pH 9 by using the T_M of each parent. Thus, the calculated stability contribution of the carboxyl anion of Asp79 in RNase Sa 7S is destabilizing and has a magnitude of -1.8 kcal/mol. The stability contribution partially results from the desolvation of the charge, but also includes electrostatic interactions with other charged groups in 7S. The magnitudes of electrostatic contributions have been calculated and are reported in Chapter VI.

CHAPTER IV

THE STABILITY EFFECT OF BURYING IONIZABLE GROUPS IN STABILIZED RNASE SA MUTANTS, 7S AND 8S

Introduction

Protein stability is the additive contribution of all forces acting to fold and unfold a protein and is described by the free energy change $\Delta(\Delta G)$ in the reaction shown in equation 1. The forces contributing to the folded state include: the hydrophobic effect, hydrogen bonding, van der Waal's interactions, and stabilizing electrostatic interactions like ion pairs.[58] The largest contributor to destabilization is conformational entropy. The burial of ionizable groups in the protein interior is also destabilizing. The desolvation penalty of moving ionizable groups from polar solvent to the protein interior has been calculated to be ≈19 kcal/mol.[4] This penalty must be overcome if polar residues are to be buried in the hydrophobic protein interior as proteins fold. Polar groups minimize the penalty for being buried by addressing the charged state of the side chain in one of three ways: 1) hydrogen bonding, 2) non-covalent electrostatic interactions (including van der Waal's interactions), or 3) shifting the pK to neutralize the charge. In doing so, the polar groups can be more readily buried as chemically they more resemble the nonpolar environment of the protein core. In some cases, buried polar residues contribute more to stability than buried hydrophobic residues. Pace estimated that buried polar groups can contribute up to 30 cal/(mol $Å^3$) more to stability than hydrophobic groups when comparing Asn → Ala to Leu → Ala or Ile → Val mutations.[138]

The number of buried polar groups generally increases as protein size increases.[19, 132] This is thought to be an evolutionary optimization of protein stability and enzyme catalysis. For example, with increasing numbers of hydrophobic residues buried and the ratio of exposed residues to buried residues decreasing as protein size increases, one would expect protein stability to increase. In actuality, protein stability stays relatively unchanged, most likely as a result of burying more ionizable groups as size increases.[14, 132] The level of burial has been calculated by measuring the average surface area buried for different amino acid classes.[57] Polar groups on average comprise 22% of amino acids in proteins and approximately 32% of those are buried (Table 2).[57, 127] Furthermore, many algorithms that predict protein folding and structure use the lowest free energy to direct the folding pathway in their protein folding software. Therefore, understanding the level of stability imparted by buried charges will enhance the accuracy of predictive programs and will also add a deeper understanding of the contribution these groups make to protein structure and function. Thus, the stability contribution of buried ionizable residues is of great interest.

Since ionizable group burial is destabilizing, our model for testing the effects of buried ionizable groups is a stabilized variant of RNase Sa. Using site-directed mutagenesis, Fu *et al*. made seven stabilizing mutations in RNase Sa that optimized 1) protein solvent interactions on the surface and 2) β-turns that "locked" RNase Sa in a more folded state-like conformation or decreased steric strain (see also Materials and Methods).[36] Together, the 7 mutations provide a net increase to stability of 5.2 kcal/mol (Table 3) and the variant is named RNase Sa 7S (7S).

Two criteria are used to determine the buried residues to mutate to ionizable groups in 7S: 1) accessible surface area (ASA) and 2) the population of individual amino acid type. Buried is defined as those residues with side chains that have a 0% solvent-accessible surface area, as determined by an in-house computer program *pfis* (see also Materials and methods).[114, 164] There are 10 residues in 7S that are ≈100% buried. Ile had the highest population (n=3) and are located at positions Ile70, Ile71, and Ile92. Consequently, these residues were chosen as candidate positions for substitution with polar ionizable groups to minimize variability when making substitutions.

Inspection of the positions of Ile70, Ile71, and Ile92 within the putative crystal structure of 7S (Figure 1, see also Chapter I) show that Ile70 and Ile92 are closer in space to one another than either of those positions to Ile71 (Figure 7). The side chain of Ile71 is on the opposite face of the 7S β-sheet. Additionally, positions Ile70 and Ile92 are in much closer proximity to a native 89% buried aspartic acid at position 79 (Asp79), which lies on the same side of the β-sheet. Therefore, positions 70 and 92 are in a different local microenvironment than position 71. Consequently, this system allows us to test for the stability contribution of different microenvironments.

Site-directed mutagenesis was used to test the effects that buried substitutions at positions 70, 71, and 92 have on the stability of 7S, a stabilized variant of RNase Sa that can tolerate buried ionizable mutations more than RNase Sa WT. At each position, Ile is replaced with Ala, Asp, or Lys. Alanine serves as a small structural and internal control. Packing of nonpolar groups is important in the protein interior and an Ile→Ala mutation removes 3 -CH2- groups which has been shown in multiple studies to contribute

approximately 3 kcal/mol.[2, 55, 116, 139, 140, 172, 173] If any of the three candidate positions is sensitive to differences in core packing, a change in the magnitude of the contribution to stability will be observed. Additionally, the validity of any measurement made at each location is enhanced when Ile→Ala mutations result in a change in stability of ≈3 kcal/mol. Aspartic acid was chosen as the acidic substitution (negative charge group) because the side chain has a smaller molecular volume than glutamic acid (Glu). Additionally. the molecular mass of Asp (≈115 Da) is similar to Ile (≈113 Da) and the molecular mass of Glu (≈129 Da) is larger than Ile. The choice of Asp helps to minimize the variability that would result from attempting to pack the larger Glu in an area that natively holds Ile during folding. The same reasoning is used for the choice of the basic residue (positive charge group) Lys. Arginine has a large and bulky guandino group on the δ-carbon of the side chain, whereas Lys has an amine connected to the ε-carbon. Thus, the molecular volume of Lys is smaller and closer to Ile than that of Arg.

The close proximity of the native buried Asp79 of 7S to positions 70 and 92 versus that of 71 allows us to determine the stability effect of having two ionizable residues buried in close proximity. Both the 70 and 92 positions are within 6 angstroms (Å) of the 79 position. Ile71 is 10 Å away from the carboxyl of Asp79 and is separated by the 7S β-sheet. Taken together, Ile70 and Ile92 are in different microenvironments than Ile71. To test the effects on stability of having two buried ionizable groups in close proximity, all buried ionizable mutations were made both in 7S and in RNase Sa 8S (8S), which has all of the 7S mutations plus a D79F mutation. Positive free energy

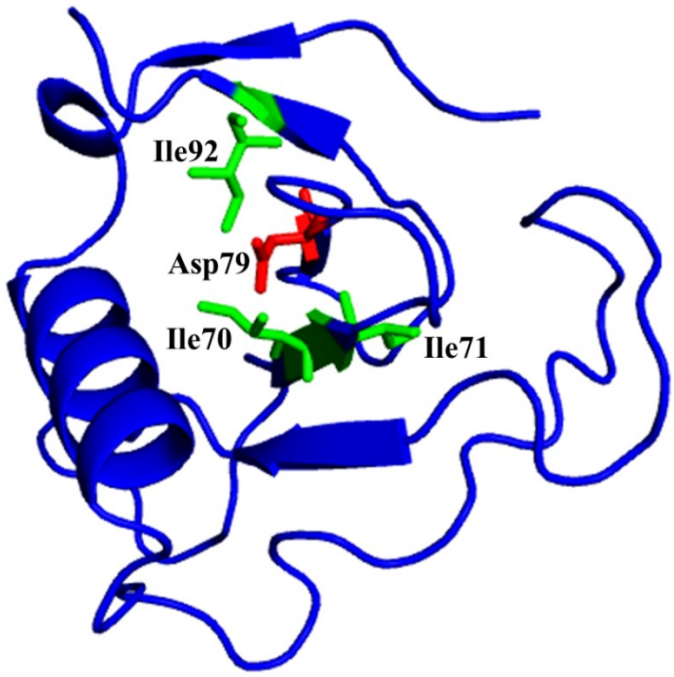

Figure 7. Ribbon diagram of 7S with native buried isoleucines 70, 71, 92, and aspartic acid 79. Ile70, Ile71, and Ile92 (green) have 0% solvent-accessible surface area. Ile70 and Ile92 are on the same side of a 5-strand β-sheet. The distances between the δ-carbon of Ile70, Ile71, Ile92 and the carboxyl carbon of Asp79 (red) are 6.2, 10.2, and 5.5 Å, respectively. The shortest distances between the nearest $-CH_2-$ group and Asp79 for Ile70, Ile71, and Ile92 are 4.3, 8.1. and 5.5Å, respectively. The crystal structure is modified from the original structure of 7S I71A by *in silico* mutagenesis of Ala71 to Ile. The program PyMol was used for structural analysis and modeling.[154]

differences denote an increase in stability. In RNase Sa WT, the D79F mutation increases the stability of WT by 3 kcal/mol.[20] In 8S, the increase in stability due to the D79F mutation measures 2.6 kcal/mol at pH 7. In all, the 7S and 8S mutants provide an excellent model system to measure the contribution to stability of buried ionizable groups and the interactions between them.

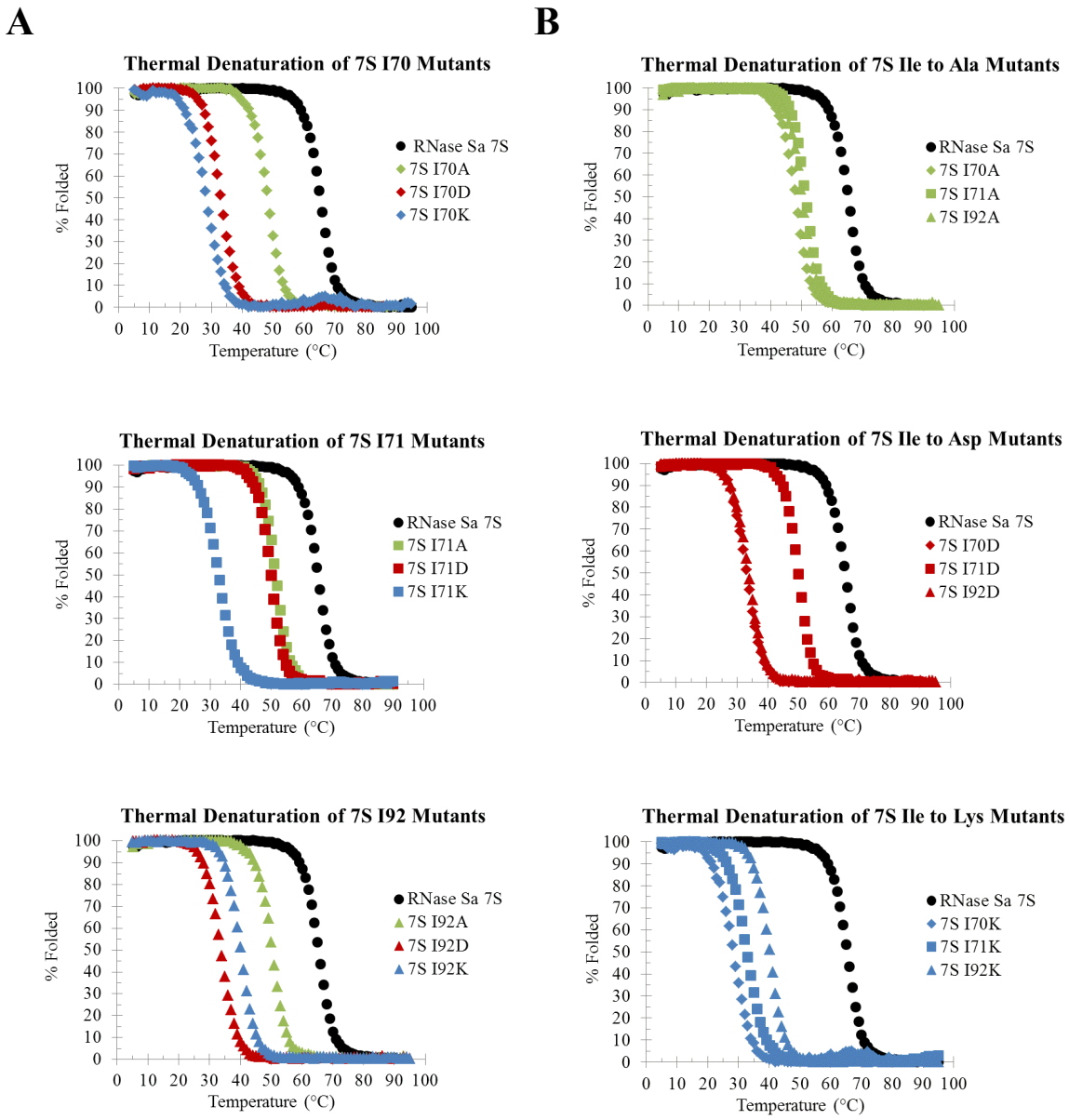

Figure 8. Thermal unfolding curves of RNase Sa 7S buried ionizable mutants. Fraction folded is on the y-axis and temperature (°C) is on the x-axis. Thermal unfolding curves of ionizable mutants separated by A) substitution position and B) amino acid mutation. In (A), Ile70 mutants are in the top panel, Ile71 mutants are in the middle panel, and Ile92 mutants are in the bottom panel. Each panel gives the thermal unfolding curve for RNase Sa 7S (black), substitutions of Ala (green), Asp (red), and Lys (blue). In (B), Ala mutants (green) are in the top panel, Asp mutants (red) are in the middle panel, and Lys mutants (blue) are in the bottom panel. Each panel has curves for mutations at position 70 (diamonds), 71 (squares), and 92 (triangles). Curves were obtained by monitoring the CD absorbance at 234 nm.

Table 6. Parameters characterizing the thermal denaturation of RNase Sa 7S buried ionizable group mutations.

7S Mutant	T_M(°C)[a]	ΔH(kcal/mol)[a]	$\Delta(\Delta G_{7SMut-7S})$ (Avg T_M) (kcal/mol)[b]
I70A	48.7 ±0.6	80.0 ±3.2	-3.8 ±0.1
I70D	34.3 ±0.1	75.8 ±1.2	-6.5 ±0.3
I70K	28.6 ±0.5	62.9 ±4.9	-6.9 ±0.1
I71A	51.9 ±0.0	90.9 ±1.6	-3.0 ±0.0
I71D	50.7 ±0.1	90.0 ±0.4	-2.3 ±0.0
I71K	33.0 ±0.6	66.0 ±4.1	-6.0 ±0.2
I92A	50.5 ±0.3	84.8 ±1.7	-3.4 ±0.1
I92D	34.1 ±0.6	71.4 ±1.6	-6.5 ±0.3
I92K	40.1 ±0.3	79.7 ±1.7	-4.3 ±0.1

[a]The melting temperature, T_M, is the midpoint of the thermal unfolding curve in Figure 8. ΔH is the enthalpy change at the T_M. Values reported are the average of a minimum of 4 independent replicates ($n \geq 4$) for the mutant indicated.
[b]$\Delta(\Delta G)$ = ΔG (variant) - ΔG (7S) at pH 7. ΔG was calculated as previously described using 1.68 kcal/mol/k as the ΔCp value from Fu *et al*. and the average T_M of each 7S variant type as the reference temperature.[44] The mean standard deviation is ±0.6 kcal/mol.

Results

Stability effects of buried ionizable mutants in RNas Sa 7S

Thermal unfolding of each variant was followed by circular dichroism spectrometry (CD) at 234 nm. All the mutants indicated two-state unfolding during thermal denaturation (Figure 8). Additionally, all 7S variants were less stable than 7S, as evidenced by the shift of the state-transition region to lower temperatures (Figure 8). The melting temperature, the change in enthalpy, and the change in stability can be calculated from the thermal denaturation curves and are reported in Table 6.

A summary of the change in stability of RNase Sa 7S buried ionizable group mutants follow (Table 6). The change in stability for Ile→Ala mutant controls is destabilizing and has a magnitude of -3.8 kcal/mol for I70A, -3.0 kcal/mol for I71A, and -3.4 kcal/mol for I92A. The change in stability for Ile→Asp mutants is -6.5 kcal/mol for I70D, -2.3 kcal/mol for I71D, and -6.5 kcal/mol for I92D. The change in stability for Ile→Lys mutants is -6.9 kcal/mol for I70K, -6.0 kcal/mol for I71K, and -4.3 kcal/mol for Ile92.

Stability effects of buried ionizable mutants in RNase Sa 8S

The difference between 7S and 8S is that 8S has an Asp→Phe mutation that replaces the native 89% buried Asp79 resulting in a stabilizing free energy change of 2.6 kcal/mol at pH 7 (Table 3). Of interest was the change in stability for buried ionizable mutants in 8S when Asp79 is absent, as well as the difference ($\Delta\Delta G_{8S-7S}$) in stability between 7S and 8S. By subtracting the stability contribution between buried ionizable group mutants between 7S and 8S, any excess free energy in addition to polar group burial (e.g. due to electrostatic interactions or cavitation) can be determined for 7S. To that end, the conformational stability was also measured for 8S buried ionizable group variants. The thermal denaturation curves of 8S buried ionizable mutants are reported in Figure 9. The T_M, ΔH, and stabilities of 8S buried ionizable mutants are reported in Table 7.

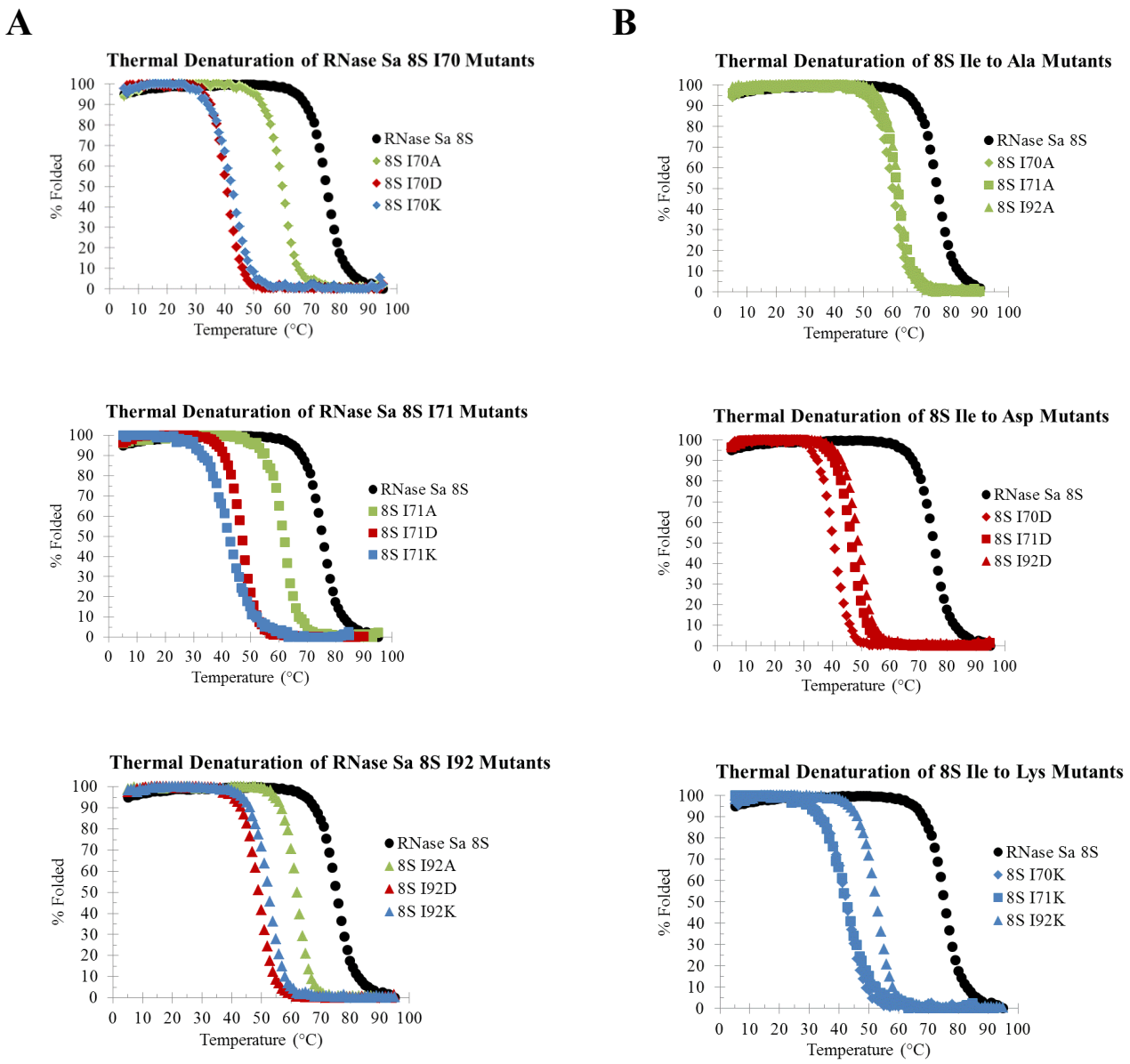

Figure 9. Thermal unfolding curves of RNase Sa 8S buried ionizable mutants. Fraction folded is on the y-axis and temperature (°C) is on the x-axis. Thermal unfolding curves of ionizable mutants separated by A) substitution position and B) amino acid mutation. In (A), Ile70 mutants are in the top panel, Ile71 mutants are in the middle panel, and Ile92 mutants are in the bottom panel. Each panel gives the thermal unfolding curve for RNase Sa 8S (black), substitutions of Ala (green), Asp (red), and Lys (blue). In (B), Ala mutants (green) are in the top panel, Asp mutants (red) are in the middle panel, and Lys mutants (blue) are in the bottom panel. Each panel has curves for mutations at position 70 (diamonds), 71 (squares), and 92 (triangles). Curves were obtained by monitoring the CD absorbance at 234.

Table 7. Parameters characterizing the thermal denaturation of RNase Sa 8S buried ionizable group mutations.

8S Mutant	T_M(°C)[a]	ΔH(kcal/mol)[a]	Δ(ΔG) (AvgT_M) (kcal/mol)[b]	ΔΔ(ΔG) (T_M°C) (kcal/mol)[c]
I70A	59.9 ±0.2	79.4 ±4.0	-3.3 ±0.1	0.5 ±0.2
I70D	40.2 ±0.1	77.6 ±1.0	-6.9 ±0.1	-0.4 ±0.4
I70K	42.5 ±0.3	60.3 ±0.9	-6.2 ±0.1	0.7 ±0.2
I71A	61.5 ±0.1	83.2 ±2.1	-2.9 ±0.1	0.1 ±0.1
I71D	46.4 ±0.0	77.9 ±1.1	-5.3 ±0.1	-3.0 ±0.1
I71K	46.2 ±0.0	57.3 ±0.0	-5.5 ±0.1	0.5 ±0.3
I92A	62.0 ±0.1	98.6 ±0.8	-2.7 ±0.1	0.7 ±0.2
I92D	49.1 ±0.1	78.4 ±2.9	-4.2 ±0.0	2.3 ±0.3
I92K	52.2 ±0.4	68.5 ±3.3	-4.2 ±0.1	0.1 ±0.2

[a]T_M is the melting temperature, determined as the midpoint of the thermal unfolding curve (Figure 9), and ΔH is the enthalpy of unfolding at the T_M. Values are calculated from the average of a minimum of 4 independent replicates ($n \geq 3$).
[b]Δ(ΔG) = ΔG (variant) - ΔG (8S) at pH 7. ΔG was calculated as previously described using 1.07 kcal/mol/K as the ΔCp value from Fu *et al*. and the average T_M of each 8S variant type as the reference temperature. The mean standard deviation is ±0.7 kcal/mol.
[c]ΔΔ(ΔG) is the stability difference between the same variant in 8S or 7S calculated using the average T_M of each 8S or 7S variant types at pH 7, respectively.

A summary of the change in stability for 8S buried ionizable mutants are reported above (Table 7). The change in stability for Ile→Ala mutant controls is destabilizing and has a magnitude of -3.3 kcal/mol for I70A, -2.9 kcal/mol for I71A, and -2.7 kcal/mol for I92A. The change in stability for the Ile→Asp mutations is -6.9 kcal/mol for I70D, -5.3 kcal/mol for I71D, and -4.2 kcal/mol for I92D. The change in stability for the Ile→Lys mutants is -6.2 kcal/mol for I70K, -5.5 kcal/mol for I71K, and -4.2 kcal/mol for I92K.

Stability differences between buried ionizable mutants of 7S and 8S

The stability difference between 7S and 8S was calculated to be 2.6 kcal/mol by Fu. *et al*. at pH 7 (Table 3).[44, 164] In the absence of any other contributing forces, the difference between 7S and 8S mutants at the same positions should be maintained. To investigate if any other stabilizing or destabilizing forces are contributing to the stability of 7S buried ionizable mutants, the stability differences between 7S and 8S were calculated (Table 7). The T_M of 8S is ≈10°C higher than the T_M of 7S, and calculations made at the 8S T_M's would underestimate the contribution to stability of mutations in 7S. Furthermore, using the T_M's of 7S in 8S calculations would overestimate the stability of 8S mutants. Consequently, the stability for each variant was calculated using the average T_M for each variant type in the protein from which it originated at pH 7, respectively. For example, the T_M used for Ile→Ala stability calculations in the 7S background was 50.3°C and the T_M used for the same mutations in 8S was 61.1 °C, which are the average T_M's for all Ile→Ala variants in 7S or 8S, respectively. Additionally, the stability values calculated using the average T_M's were carried through in subsequent calculations in which 7S variant stabilities were subtracted from 8S stabilities.

The change in stability between 8S and 7S buried ionizable mutants follow (Table 7). The stability difference for Ile→Ala mutants is 0.5 kcal/mol for I70A, 0.1 kcal/mol for I71A, and 0.7 kcal/mol for I92A. The stability difference for Ile→Asp mutations is -0.4 kcal/mol for I70D, -3.0 kcal/mol for I71D, and 2.5 kcal/mol for I92D. The stability difference for Ile→Lys mutations is 0.7 kcal/mol for I70K, 0.5 kcal/mol for I71K, and 0.1 kcal/mol for I92K.

Discussion

Buried residues have side chains with 0% ASA. Using *pfis* to calculate the ASA, 10 residues were identified in RNase Sa. The individual residue with the highest occurrence in the buried residue population was isoleucine, n = 3. Those Ile residues are located at positions 70, 71, and 92 in both RNase Sa 7S and 8S. In 7S, positions Ile70 and Ile92 are in close proximity to the native 89% buried Asp79, whereas Ile71 is oriented away from Asp79 on the opposite face of the RNase Sa β-sheet (Figure 7).

To study the stability effects of buried ionizable groups at each position, site-directed mutagenesis was used to substitute Ala, Asp, and Lys at positions 70, 71, and 92 of 7S and 8S. In an effort to minimize variance in the forces contributing to stability in buried ionizable mutants, candidate substitutions were rationally chosen.

Alanine was chosen as a control to test if Ile was necessary for the protein to fold. If Ile at any candidate position is necessary for 7S or 8S folding, substitution with Ala would result in non-reversible unfolding or major structural rearrangement of 7S. Thermal unfolding curves (Figure 8B Top, 9B Top) and the *in silico* structural alignment of the crystal structure of 7S and 7S I71A show that 7SI71A is folded below its T_M and in a similar structural topology (Figure 1D).

The difference between Ala and Ile is 3 hydrophobic carbon groups. Previous studies have shown that burial of a single -CH_2- group contributes 1.1 kcal/mol to stability.[39, 50, 52, 173] The change in stability for a buried Ile→Ala mutation was previously measured as -3.1 ± 1.2 kcal/mol.[39] The Δ(ΔG) for all 7S and 8S Ile→Ala mutants are in good agreement, and range between -2.7 – -3.8 kcal/mol (Table 6, 7).

Additionally, the similarity in stability changes for the Ile→Ala helps to buttress the validity of the changes observed for the Asp and Lys substitutions.

Aspartic acid was chosen as the acidic substitution (negative group) because the molecular size of Asp is similar to Ile. Additionally, the side chain of Asp and the Ala control differ only by a carboxyl. If Glu were used as the acidic substitution, the removal of an additional -CH_2- group and core packing would have to be considered. The contributions to stability for Ile→Asp mutants in 7S and 8S were measured and gave comparable results (Table 6, 7). In 7S, mutations I70D and I92D were highly destabilizing and each gave a change in stability of -6.5 kcal/mol. The I71D mutation was less than half as destabilizing at -2.3 kcal/mol. The results are intriguing when compared to the changes in stability observed for 8S. In 8S, I70D, I71D, and I92D are -6.9, -5.3, and -4.2 kcal/mol, respectively. The expectation being that the removal of the native buried Asp79 in 8S would decrease the destabilizing contribution of the direct interaction of Asp79 with I70D and I92D in 7S. The hypothesis was that increased destabilization was a result of charge-charge repulsions between the buried charge mutations and the native Asp79 in 7S. Interestingly, the I71D mutation, which is removed from the local environment of Asp79, was more destabilizing in 8S than it was in 7S by -3.0 kcal/mol (Table 7).

The choice of basic residue for substitutions is limited to Lys and Arg. Lys was chosen because it has a surface area that is less bulky and a molecular volume that is closer to Ile than Arg. As with the Asp mutations discussed above, the results for Ile→Lys mutations were variable. All mutations were highly destabilizing, but the range

of the change in stability is from -4.2 – -6.9 kcal/mol. In both 7S and 8S, the I70K mutation gave the largest change in stability with a difference of -6.5 and -6.2 kcal/mol, respectively. In general 8S Ile→Lys mutants were ≈0.5 kcal/mol more stable at every position (Table 7). Taken together, these data suggest that the contribution to stability is context dependent and based on the local environment of the groups.

The stability difference for the same variant in 7S and 8S is calculated by subtracting the Δ(ΔG) of 7S from Δ(ΔG) of 8S, and allows for a comparative interpretation of the response of the proteins to different mutations. For instance, the variant stability difference for all the Ile→Ala mutations in 8S is 0.1 – 0.7 kcal/mol more stable than the same mutations in 7S (Table 7). The indication is that the hydrophobic core of 8S is slightly less tightly packed than 7S. The magnitudes of the change in stability for the other substitutions vary. The variant stability difference for Ile→Lys mutations at every position in 7S and 8S are within a narrow value range of 0.1 – 0.7 kcal/mol (Table 7). Therefore, 8S tolerates buried Lys mutants slightly better than 7S, as indicated by higher stabilities at each location, but the overall similarity in the change in those values indicates the tolerance is independent of the microenvironment. In contrast, the stability contribution of making Ile→Asp mutations in 7S and 8S varies by position (Table 7). The 7S and 8S variants show similar stabilities for I70D. 8S is less tolerant of the I71D mutation by -3.0 kcal/mol, but more tolerant to I92D by 2.3 kcal/mol.

There may be a few reasons for these results. Recent studies by Fu *et al*. suggest that the denatured state of 8S retains more structure than 7S, possibly because the denatured state of 7S is more rigid.[44] Thus leading to the possibility that the increased

stability values calculated for variants in the 8S background result from residues remaining more buried upon unfolding. Additionally, the charged state of buried ionizable groups may differ between positions leading to alternate ionizable-hydrophobic group or ionizable-ionizable group interaction dynamics or changes in the localized or global dielectric. The pK of ionizable groups has been shown to shift when transferred to the hydrophobic core of proteins.[10, 13, 76] The pK's of all 7S and 8S mutants were determined and are discussed in Chapter VI, wherein a positive correlation is reported between the magnitude of the pK shift and $\Delta(\Delta G)$. Additionally, The structure of buried ionizable group variants could allow solvent access to the charged groups' side chains. For example, the long side chain of Lys could rotate and orient itself in such a way that the ionizable group is solvent accessible. Knowing the structure of 7S and 8S variants is paramount to investigate these possibilities. Spectral analysis of the proteins show normal absorbance peaks observed by CD at 234 nm and UV-Vis at 278 nm (data not shown), indicating that buried aromatic rings remain solvent inaccessible and the overall fold remained intact. Crystal structures for some 7S and 8S variants were determined and structural analysis is discussed in Chapter V.

CHAPTER V

STRUCTURAL ANALYSIS OF RNASE SA VARIANTS 7S I71A and 8S I71D

Introduction

The forces that contribute to protein stability are additive.[24] Thus, comparative studies must necessarily account for variance between model systems. Mutations in proteins can induce structural changes that affect and change: 1) the folding pathway as the protein moves towards the folded state and 2) solvent access to the protein interior and 3) many other aspects of protein stability and function that are dependent on the relationship of residues with their environment. All are important factors that contribute to the free energy of unfolding and stability calculations. The focus of this work is to measure the stability effects that buried ionizable groups have on protein stability, including whether buried charge mutations induce structural changes that could result in differences in distances between those groups or solvent access. Coulomb's Law (equation 5) relates the distance between ions to the free energy of the interaction between them. The solvation state of ionizable amino acids can affect the pK of the ionizable portion of the side chain. In the solvent inaccessible protein interior, the pK of ionizable groups will shift in order to neutralize the charged species, thereby inducing a state that is more similar to the protein interior.[10]

Studies on the effect that mutations have on protein stability indicate that proteins are typically structurally tolerant to mutations.[61] For instance, studies in T4 lysozyme buried charge mutants concluded that structure was unaffected by the destabilizing mutations.[143] This also holds true for other proteins that exhibit two-state

unfolding even when mutations are highly destabilizing.[88] The crystal structures of mutants of bovine trypsin inhibitor that removed disulfide bonds are similar in structure to the parental protein, even though the change in stability was 3 – 4 kcal/mol.[175]

In recent studies of SNase, buried ionizable group contributions to stability were measured by making substitutions at different positions in the protein.[150-152] The authors found that: the pK of Glu residues is generally increased to ≈7, Lys residues could be shifted to as low as ≈6, and Arg residues exhibited no change in pK.[77, 150, 151] The contribution to stability of the ionization of buried Glu was determined to be between 3-7 kcal/mol.[151] The contribution of ionization of buried Lys to the stability of SNase was estimated to be between 2-7 kcal/mol.[150] Lastly, the contribution to stability of buried and charged Arg was reported to be between 2-10 kcal/mol.[77] These results may need to be approached critically as, 1) the authors defined "buried" groups "...as those in which the C_α–C_β vector of a side chain points toward the protein interior," and was not based on solvent accessible surface area of the side chain, 2) the authors previously showed that SNase has a protein interior that appears to be accessible to liquid water , 3) the protein interior of both SNase and the stabilized mutants used in their studies might have a high average dielectric constant, and 4) packing density within the protein core of SNase appears to be dynamic upon buried group ionization.[78, 149, 152, 155, 156]. Fitch *et al*. showed that buried ionizable groups in SNase allow for water access to the protein core, resulting in altered pKs of buried ionizable groups.[149] Additionally, Uversky *et al*. report that SNase forms folding intermediates at different salt concentrations, in the presence of anions at low pH, and when self-associating.[157, 158] Thus, the wide range of

free energy values calculated for contributions to stability in SNase ionizable group mutants may be a consequence of inadvertently measuring the stability contributions in an intermediate state induced by the presence of a buried ion mutant.

Here, the crystal structures of our model proteins were obtained to test for changes in structure or solvent access. The eponymous *Streptomyces aureofaciens* enzyme RNase Sa is a 96 amino acid guanylic acid specific endonuclease.[160] The three-dimensional structure of RNase Sa has been resolved with high resolution by X-ray crystallography (Figure 1, 1rgg.pdb: molecule B).[176] The secondary structure consists of an α-helix, a 6-strand β-sheet, 2 β-turns between β-strands 4 - 5 and 5 – 6, and random coil. The positions of each secondary structure are: 1) 9 – 25 for the α-helix, 2) 3 – 8, 35 – 37, 52 – 57, 68-73, 78 – 82, 88 - 93 for β-strands 1-6, respectively, 3) 74 – 77 and 83 – 88 for β-turns, and 4) 26 – 34, 38 – 51, 58 – 67 for random coil. RNase Sa forms one disulfide bond between cysteine residues at positions 7 and 96.[37]

Since buried ionizable mutants were correctly hypothesized to decrease protein stability (Chapter IV), our model system for studying the structural effects of buried ionizable group mutants is RNase Sa 7S which contains 7 stabilizing mutations. Using site-directed mutagenesis to optimize β-turns, the stability of RNase Sa was increased by relieving strain with Gly substitutions at the *i*+2 position and directing backbone geometry with Pro substitutions at the *i*+1 position.[36, 177] These substitutions increase the free energy of the unfolded state, fixing RNase Sa in a more folded conformation. Each optimizing mutation increased stability by ≈1 kcal/mol. Two lysine mutations on the surface improved surface-solvent interactions, and five Gly and Pro mutations in β-

turns optimized protein geometries to together increase conformational stability. The 7 mutations provide a stability increase of 5.2 kcal/mol.[36] An additional mutation, D79F, further increases the stability of 7S by 2.6 kcal/mol and together make 8 stabilizing mutations and the model protein 8S.

Results

X-ray crystallography and structural determination was performed in the Kazufumi Takano Lab at the Graduate School of Life and Environmental Sciences, Kyoto Prefectural University, Kyoto, Japan. Briefly, protein crystals were formed by the hanging drop method before X-ray diffraction. The structures for the mutants 7S I71A and 8S I71D are discussed below.

No structure of 7S exists, however, a structural alignment of 7S I71A (1.8 Å resolution) with RNase Sa WT (1.7 Å resolution) shows that backbone topology is comparable when position 71 is reverted back to Ile by *in silico* mutagenesis (Figure 1C, D).[176] Using a solvent radii (1.4 Å) based on results from Lee and Richards, the accessibility of residues in 7S I71A can be observed by molecular modelling in PyMol (Figure 10).[126, 154] The side chains of Ile70, Ala71, and Ile92 are completely solvent inaccessible. The in-house program *pfis* is used to determine the ASA of the side chains in 7S I71A,and *pfis* analysis reveals that Asp79 is 89.2% buried. Consequently, this value is in agreement with the close proximity of the side chain of Asp79 to solvent water observed in the crystal structure (Figure 10). The observation of the mostly buried

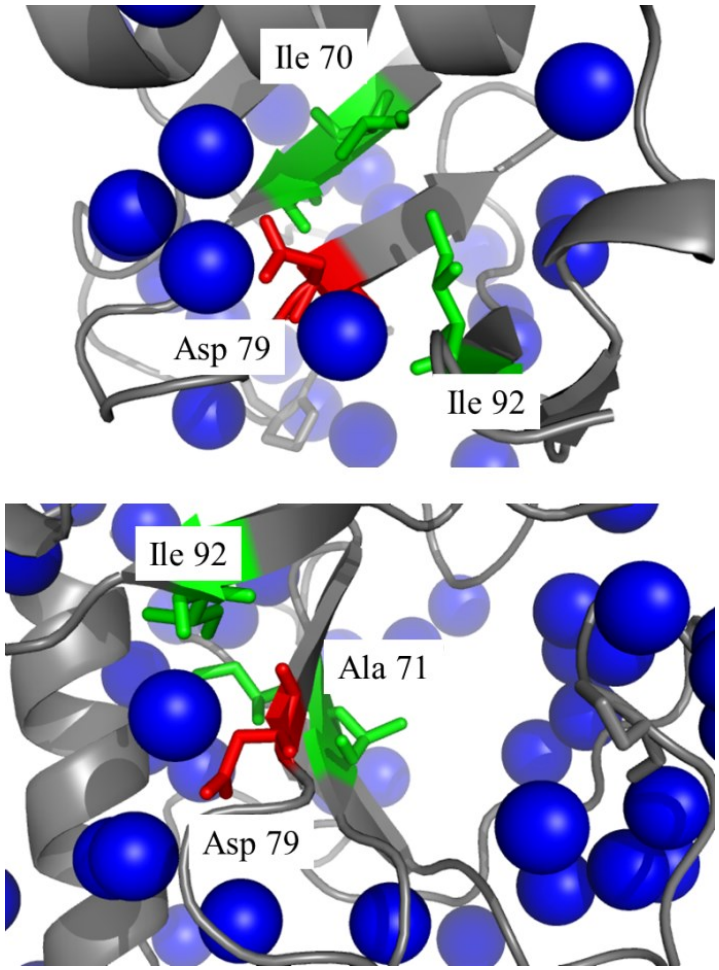

Figure 10. Molecular modelling of solvent access of the interior of RNase Sa 7S mutant I71A. The ribbon diagram of RNase Sa 7S mutant I71A is shown (grey). Buried residues Ile70, Ala71, and Ile92 (green) are buried and are inaccessible to solvent water (blue). The spheres used to determine solvent access have a van der Waal's radius of 1.4 Å previously used by Lee and Richards.[126] The close proximity of the Asp79 carboxyl to solvent agrees with *pfis* data for WT that gave a side chain ASA of 10.8%.

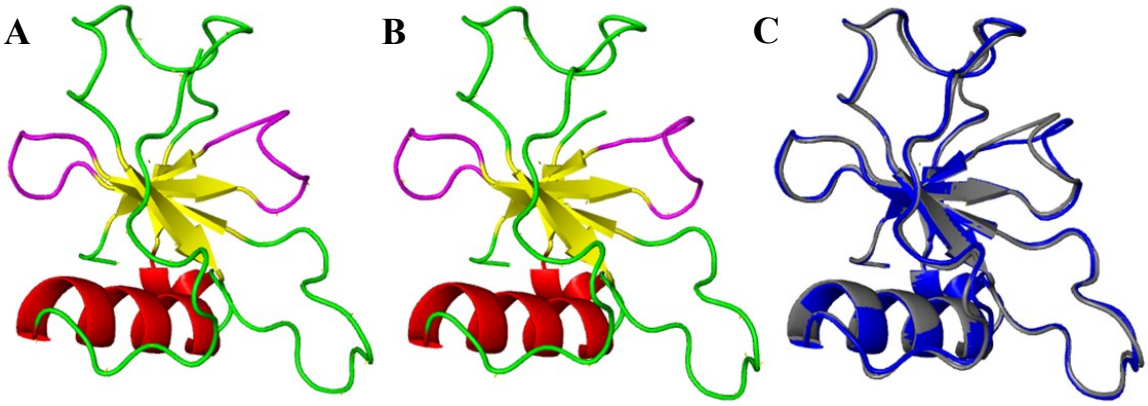

Figure 11. Ribbon diagrams of the crystal structures and structural alignment of RNase Sa mutants 7S I71A and 8S I71D. Secondary structures of RNase Sa mutant A) 7S I71A and B) 8S I71D are colored to differentiate between helices (red), β-strands (yellow), β-turns (magenta), and random coil (green). The structures for 7S I71A and 8S I71D have a resolution of 1.8 Å and 2.5 Å, respectively. C) A structural alignment of 7S I71A (grey) and 8S I71D (blue) was performed using the three dimensional modelling software PyMol.[154] A structural alignment comparison is made for WT in Figure 1.

Asp79 is further supported by a comparison to the crystal structure of RNase Sa WT (Figure 1).

To date, the structures of 7S I71A and 8S I71D have been resolved. Both three dimensional structures and an alignment between these structures are in Figure 11. The structure of 8S I71D was obtained at a resolution of 2.5 Å. Analysis of the solvent accessibility of the protein interior is similar to 7S I71A in that the side chains at positions 70, 71, and 92 are solvent inaccessible. The van der Waal's radius of water molecules are 2.8 Å, which is within the resolvable limit of detection.

Discussion

The crystal structures of the RNase Sa mutants of 7S and 8S allow for a comparison of both structure and solvent access of the protein interior. Both the former and latter are comparable to RNase Sa WT when studied by molecular modelling software. The indication is that the structure of RNase Sa 7S and 8S buried ionizable mutants remain intact, even when the mutations are highly destabilizing. Additionally, the lack of solvent access indicates that the differences in pK values reported in Chapter V are a result of the Born effect and that the pK of the group shifts in a context dependent manner. Additionally, analysis of the crystal structures allows for the study of side-chain geometries that may indicate the formation of ion pairs or salt bridges that may further explain the stability differences that are measured between 7S and 8S mutants. The locations of the mutations in 7S I71A and 8S I71D are out of the local microenvironment of the native buried Asp79 or Phe79, respectively. Thus, they would be outside of the range of a direct electrostatic interaction with Asp 79. Additional structures need to be obtained and analyzed in order to get information on the structural effect of mutations made close to position 79.

CHAPTER VI

DETERMINATION OF THE pK OF BURIED IONIZABLE RESIDUES

Introduction

The desolvation penalty for burying an ionized group into the hydrophobic core of a protein was previously calculated as high as -19 kcal/mol.[4] Despite the large unfavorable Born self-energy, proteins readily bury polar-charged amino acids during folding. Furthermore, some studies indicate that the larger proteins become, the more ionizable groups are buried.[14, 132] There are multiple strategies that proteins use to mitigate the large destabilizing force attributed to burying charges. The strategies include: cavitation to allow water penetration into the protein core and allow solvation of the group, non-covalent interactions in the form of ion pairing or salt bridges, hydrogen bonding to decrease the intensity of the charge, and/or by shifting the dissociation constant of the ionizable groups towards a more neutral pK. Neutralization of the charge makes the side chains more similar to the nonpolar protein core and less like polar aqueous solvent.

The acid dissociation constant (pK) describes the point at which an ionizable group is half ionized. That is, that the ionizable group exists in two populations of equal concentration in solution, one that is ionized and the other that is not ionized. The relative fractional populations of each species can be changed by altering the pH of the environment of the ionizable group. The relationship of the populations can be calculated using the classic Henderson-Hasselbaulch relationship (equation 6). An

ionizable species will be protonated below the pK and deprotonated above the pK of the group, and the charge state upon protonation/deprotonation is dependent on the amino acid and its environment.

The three major classes of amino acids are nonpolar, polar-uncharged, and polar-charged. The designation of the polar groups as "charged" and "uncharged" is based on the ionization state of their side chains in solution at physiological pH = 7.4. The ionization state, in turn, is based on the pK of side chain's functional group. The polar-charged groups are further characterized as acidic and basic depending on having a negative or positive charge at pH = 7.4, respectively. The acidic residues are aspartic acid (Asp: D) and glutamic acid (Glu: E) and the C-terminus carboxyl. All contain a carboxylic acid functional group that ionizes (…-COO-[H]). The basic residues are lysine (Lys: K) and arginine (Arg: R) and the N-terminus, and all contain an amine group that ionizes (…-NH_2-[H^+]). Excluding Arg and the N-terminus, the intrinsic pK value for the groups was determined in blocked pentapeptides with an Ala-Ala-X-Ala-Ala motif in order to make the calculation in a more protein-like environment.[13, 76] The pK of solvated Asp, Glu, and the C-terminus are estimated as 3.9, 4.3, and 3.5, respectively. The pK of Lys in the pentapeptide motif was 10.4, and the pK of the N-terminus of RNase Sa is 9.1.[13, 79] The value for free arginine was previously calculated in phase solubility studies as 12.5.[75]

Here, buried ionizable mutations are made in stabilized variants of RNase Sa, RNase Sa 7S (7S) and RNase Sa 8S (8S) that can tolerate buried charges and allow for measurement of their stability contributions. 7S is named from the 7 stabilizing

mutations that were made by optimizing β-turn geometry.[36] A D79F mutation increased the stability of 7S by 2.6 kcal/mol and is the eighth mutation in RNase Sa 8S.[20, 44] Buried residues are those that have 0% solvent-accessible surface area (ASA). In 7S and 8S, three positions with 0% ASA were chosen for substitutions with buried ionizable groups: Ile70, Ile71, and Ile92 (see also Materials and Methods).

The magnitude of the apparent change in stability of buried ionizable groups is dependent on the ionization state of the charge (Chapter III). Furthermore, differences in the stability of buried ionizable groups at different positions within RNase Sa 7S and 8S (Chapter IV) may be a result of different ionization states of buried ionizable group mutations. For that, the pK of the side-groups of buried ionizable residues is necessarily examined here.

The pK of buried side groups can be determined in folded proteins by plotting the free energy of unfolding (ΔG) vs. pH. If the ΔG is dependent on the ionization of an ionizable group, the resultant curve is fit with equation 9:

$$\Delta G_{H^+} = \Delta G_{H^+ \to \infty} + RT\left(\ln \sum_{i=1}^{n} \frac{1+\frac{K_{iF}}{[H^+]}}{1+\frac{K_{iU}}{[H^+]}}\right) \quad (9)$$

where ΔG_{H}^{+} is the free energy of unfolding, $\Delta G_{H+ \to \infty}$ is the free energy change when all ionizable groups are protonated (the y-intercept from linear extrapolation), R is the gas constant, T is the temperature in °K, K_{iF} is the dissociation constant for group "*i*" in the folded state, and K_{iU} is the dissociation constant of the group in the unfolded state (the

estimated value from the guest pentapeptide studies). The ΔG values for 7S and 8S are calculated by analysis of thermal denaturation curves over a pH range as determined by CD spectrometry at 234 nm (see also Materials and Methods). This allows for the determination of the charged state of buried ionizable residues in RNase Sa stabilized mutants. Thus, the resultant change in stability can be compared for mutants in the ionized and non-ionized states.

Results

pK of buried ionizable groups in 7S

Thermal unfolding curves for 7S buried ionizable group mutants were obtained by monitoring the CD absorbance of mutants at 234 nm over a temperature range of -5 – 95°C (see Materials and Methods). A thermal unfolding curve was obtained in buffers at a pH of 1, 1.5, and each pH from 2 - 10. A representative graph of the fraction folded at each pH is shown in Figure 12 for 7S Ile71 mutants. Dependent on preliminary results, some curves were repeated starting at sub-zero temperatures (-5°C) to obtain pre-transition data points in the thermal unfolding curve (e.g. 7S I71D and 7SI71K, Figure 12B, C).

The fraction folded and the stability are calculated as described (see Materials and Methods), and the stability of 7S and variants over a pH range are reported in Table 8. For 7S and all variants, the greatest stability is obtained at pH 5. 7S I70K is unstable at any pH below 5 or above 9. Consequently, the pK of 7S I70K was not determined. The ΔG is used to calculate the pK of buried ionizable groups. The 7S ΔG values are

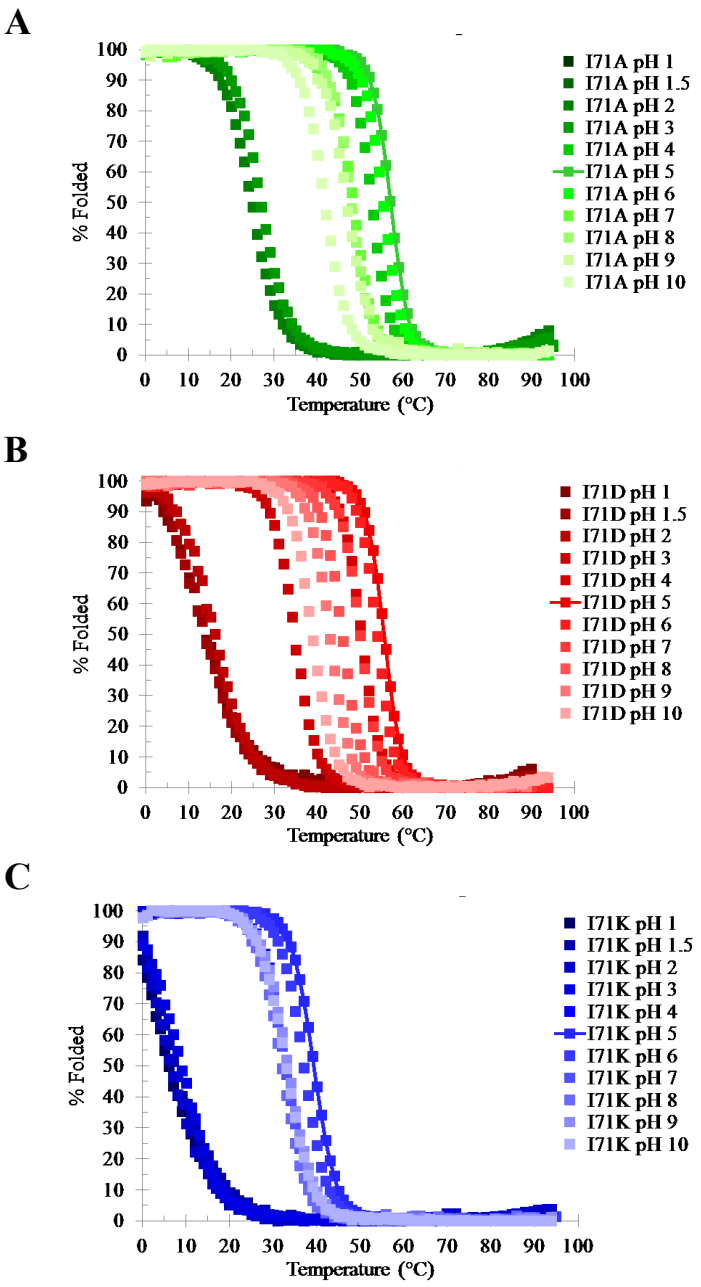

Figure 12. Representative unfolding curves of 7S Ile71 mutants over a pH range of 1 – 10. Thermal unfolding curves of A) 7SI71A (green), B) 7SI71D (red), and C) 7SI71K (blue) are shown. A color gradient is used to guide the eye from low pH values (dark) to high pH values (light). The pH value corresponding to the highest stability is marked with a line. Fraction folded (x-axis) was monitored by CD absorbance at 234 nm per 1°C temperature step (y-axis). Pre-transition data points for 7S I71D and I71K extend to -5°C (data not shown).

Table 8. Free energy of unfolding (ΔG) for buried mutants over a pH range of 1 – 10.

7S Mutants	pH[a]										
	1	1.5	2	3	4	5	6	7	8	9	10
7S	-5.2	-5.7	-5.3	-2.9	-0.1	1.1	0.9	0.0	-0.7	-2.0	-2.6
I70A	-8.0	-7.8	-8.1	-4.3	0.1	1.5	0.9	0.0	-0.9	-2.1	-2.9
I70D[b]	-4.8	-4.3	-3.7	-0.7	2.5	3.0	1.7	0.0	-2.6	-5.9	-
I70K[c]	-	-	-	-	-	-	1.4	0.0	-	-0.7	-
I71A	-6.7	-6.3	-6.0	-3.1	0.3	1.6	1.1	0.0	-1.1	-1.0	-2.6
I71D	-8.3	-8.6	-8.0	-4.4	0.0	1.6	1.1	0.0	-1.3	-1.9	-3.2
I71K	-5.1	-4.8	-5.3	-4.9	0.0	1.4	0.8	0.0	-0.3	0.0	0.0
I92A	-7.7	-7.5	-8.1	-4.5	-0.1	1.4	1.0	0.0	-1.2	-2.0	-3.2
I92D	-4.6	-5.3	-6.0	-1.7	1.7	2.6	1.6	0.0	-1.5	-3.2	-4.3
I92K	-7.1	-6.7	-7.4	-3.4	0.0	1.1	0.7	0.0	-0.6	-1.6	-2.4
8S Mutants	pH[d]										
	1	1.5	2	3	4	5	6	7	8	9	10
8S	-7.6	-8.5	-7.1	-4.3	-1.7	-0.3	0.2	0.0	-0.4	-0.9	-1.5
I70A	-9.4	-8.7	-8.0	-4.6	-1.8	0.6	0.1	0.0	0.2	-1.0	-1.5
I70D	-5.6	-5.8	-4.5	-1.9	1.2	2.7	1.8	0.0	-1.1	-3.6	-6.9
I70K[e]	-	-	-	-4.8	-2.4	-1.2	-0.4	0.0	0.4	1.1	0.8
I71A	-8.2	-8.5	-7.7	-5.1	-1.6	0.4	0.5	0.0	-0.4	-0.7	-2.2
I71D	-5.2	-5.8	-5.1	-2.3	1.1	2.4	1.9	0.0	-1.1	-2.6	-4.1
I71K[e]	-	-	-7.7	-4.2	-0.9	0.0	0.2	0.0	0.1	0.5	0.9
I92A	-8.6	-9.7	-8.3	-6.1	-2.2	0.3	0.4	0.0	-0.1	-0.9	-1.3
I92D	-4.6	-5.9	-5.9	-3.8	-0.6	0.8	0.6	0.0	-0.6	-1.3	-1.9
I92K	-6.4	-7.0	-6.3	-3.8	-1.1	0.4	0.5	0.0	-0.4	-0.7	-0.9

[a]Calculated using the Gibbs-Helmholtz equation and the measured T_M and ΔH (Materials and Methods). The ΔCp value (1.68 kcal/mol/K) was previously determined by Fu *et al*. The T_M of each mutant at pH 7 was used as the reference temperature, making all pH 7 values zero.
[b]The thermal unfolding curve for the 7S I70D pH 10 sample did not reach 100% folded at the lower temperature limit (-5°C) of the CD spectrometer. Consequently, no data were obtained.
[c]The thermal unfolding curves for 7S I70K at pH 1 – 5, 8, and 10 were not resolved and no data were obtained.
[d] Calculated using the Gibbs-Helmholtz equation and the measured T_M and ΔH (Materials and Methods). The ΔCp value (1.07 kcal/mol/K) was previously determined by Fu *et al*. The T_M of each mutant at pH 7 was used as the reference temperature, making all pH 7 values zero.
[e]The thermal unfolding curves for 8S I70K pH 1 - 2 and I71K pH 1 – 1.5 did not reach 100% folded at the lower temperature limit of the CD spectrometer. Consequently, no data were obtained.

subtracted from the mutant ΔG values (Δ(ΔG)) and plotted at each pH studied. Representative ΔG vs. pH plots with fits for 7S Ile92 and 8S Ile70 mutants are in Figure 13, and the calculated pK values for each buried ionizable group mutant are listed in Table 9.

An observed shift in pK was not apparent for each residue type. For instance, the calculated pK for 7S I70D and 7S I 92D were both elevated to 9.6 and 7.2, respectively, whereas the pK of 7S I71D seems unaffected. Lys mutants in 7S also give pK variances. The apparent pK of 7S I71K was depressed by -2.7, but the pK of 7S I92K was unchanged. The differences in pK for buried Asp and Lys mutants in 8S also seem location specific. The change in pKs for 8S I70D, I71D and I92D are 8.5, 7.2, and unchanged, respectively. 8S I70K and I71K have depressed pKs of 7.4 and 8.4, but the estimated pK 8S I92K is unaffected. The ΔpKs, the charged state at pH 7 based on estimated pKs, and the relative magnitudes of the pK shifts are reported in Table 9. The ΔpK is calculated by subtracting the pK of the group in the folded state from the pK of the group from experimental data in blocked pentapeptides (Table 1).[13, 76]

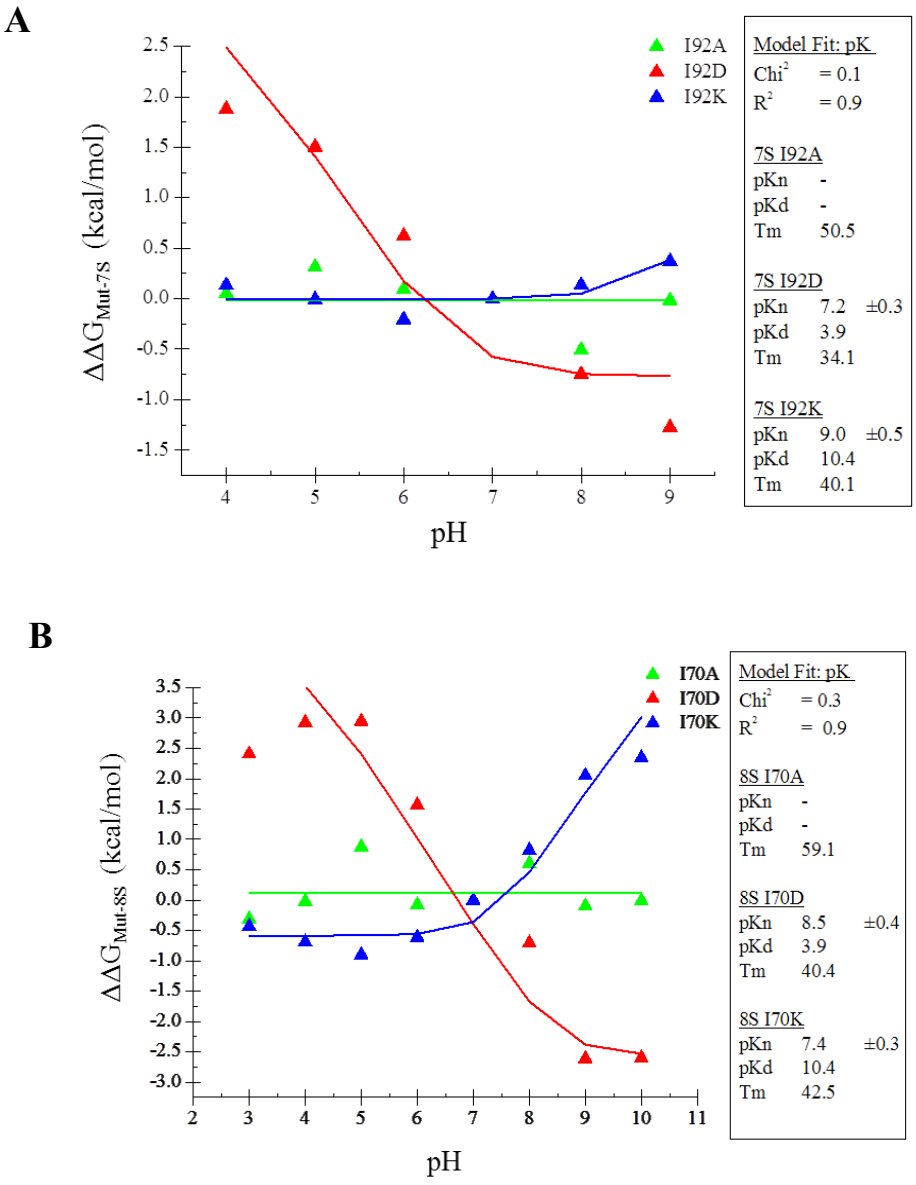

Figure 13. Representative pK analysis curves. Plot of Δ(ΔG) *versus* pH for A) 7S Ile92 mutants and B) 8S Ile70 mutants. Values for $\Delta(\Delta G_{MutX\text{-}X})$ were calculated by subtracting the 7S or 8S ΔG values from the ΔG of each variant at pH 3 – 10. Values are reported in Table 8. The pK of ionizable groups in the folded state (pKn) for Ile→Ala (green), Ile→Asp (red), and Ile→Lys (blue) were estimated as previously described (see also Materials and Methods).[99] The pK of groups in the unfolded state (pKd) were from studies in pentapeptides as reported in Grimsley *et al*. and Table 1.[13] The fits for Ile→Ala mutants (green line) show a negligible difference in the free energy of unfolding as indicated by the near zero Δ(ΔG) values for all pH tested. The fits of Ile→Asp (red line) and Ile→Lys (blue line) mutants show inflection points at the pKn and pKd, respectively (inset).

Table 9. Estimated pK values of buried ionizable mutants of RNase Sa 7S and 8S from analysis of Δ(ΔG) vs pH plots.

7S Mutant	pK_{pp}[a]	pK[b]	ΔpK[c]	Charge at pH 7	Shift[d]
I70D	3.9	8.4 ±0.4	4.5	neutral	↑↑↑↑↑
I71D	3.9	3.9 ±0.0	0.0	negative	--
I71K	10.4	7.7 ±0.3	-2.7	neutral	↓↓↓
I92D	3.9	7.2 ±0.3	3.3	neutral	↑↑↑
I92K	10.4	10.4 ±0.0	0.0	positive	--
8S Mutant	pK_{pp}[a]	pK[b]		Charge at pH 7	Shift[d]
I70D	3.9	8.5 ±0.4	4.6	neutral	↑↑↑↑↑
I70K	10.4	7.4 ±0.3	-3.0	neutral	↓↓↓
I71D	3.9	7.2 ±0.4	3.3	neutral	↑↑↑
I71K	10.4	8.4 ±0.4	-2.0	positive	↓↓
I92D	3.9	3.9 ±0.0	0.0	negative	--
I92K	10.4	10.4 ±0.0	0.0	positive	--

[a]pK_{pp} is the pK determined from studies in guest pentapeptides (Table 1).[13, 76]
[b]pK values are estimated from analysis of the fits of ΔG vs. pH curves for each mutant indicated.
[c]Values are calculated by subtracting pK_{pp} from pK ($\Delta pK = pK_{pp}-pK$).
[d]Graphical representation of ΔpK. Arrows represent 1 pK unit. Up arrows indicate increased pK and down arrows indicate decreased pK.

The free energy of unfolding is determined for 7S and 8S buried ionizable mutants at pH 6, 7, and 9 in order to gauge the magnitude of the effect of the pK shifts of buried ionizable mutants on the stability of 7S and 8S (Figure 14). The Δ(ΔG)s are calculated for: 1) the difference between each variant at each pH and their parent (7S or 8S) at pH 7, and 2) the stability difference between each variant at pH 6 and 9 from itself at pH 7. To estimate the change in free energy due to the mutation alone in the absence of other contributing factors, the Δ(ΔG) of 7S or 8S is subtracted from Δ(ΔG) of the mutant (Figure 14). By comparing ΔpK and the differences in stability for 8S and 7S, a

A

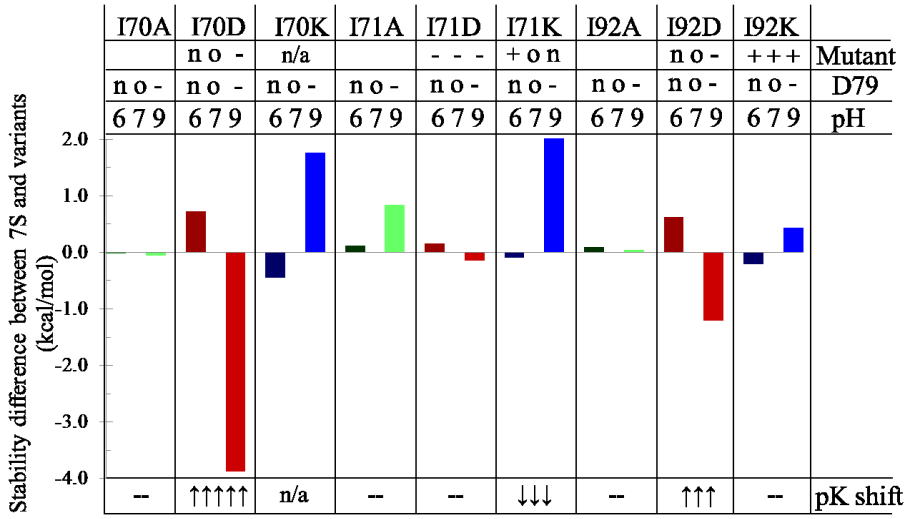

B

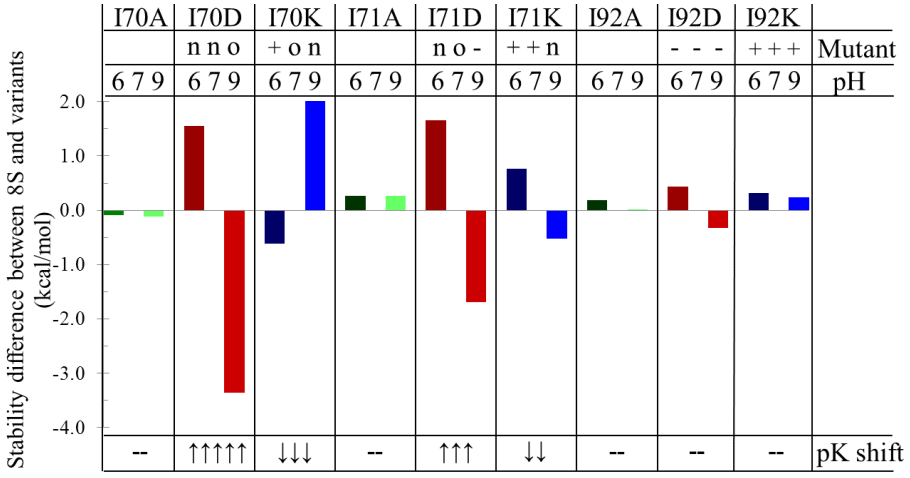

Figure 14. The effect of ionization on the stability of buried ionizable mutants. The ionization effect on variant stability over the pH range of 6 - 9 was calculated for buried ionizable variants in A) 7S and B) 8S by subtracting the free energy difference between each mutant and its parent ($\Delta(\Delta G)$) at pH 7 from the $\Delta(\Delta G)$ at each pH indicated. The reference temperature for each mutant is the T_M of that mutant at pH 7(Table 6, 7). Consequently, the stability difference at pH 7 is zero for all mutants. Bars are colored for consistency for Ile→Ala mutations (green), Ile→Asp mutations (red), Ile→Lys mutations (blue), pH 6 (dark), and pH 9 (light). The charged state for the mutant residues (Mutant) is indicated as positive (+), negative (-), neutral (n), or near/at the ionization point (o) at the indicated pH studied (pH). The charged states are based on values from Table 9. The magnitude of the shift in pK is indicated (bottom of chart) for each mutant. Each arrow indicates a shift of 1 pH unit. Up arrows indicate an increase in pK, and down arrows indicate a decrease in pK. A double dash indicates no observable change in pK. For 7S buried ionizable mutations, the charged state of Asp79 is included. The pK of 7S I70K was not determined (see text Chapter VI).

Table 10. The free energy difference between buried mutants of RNase Sa 7S and 8S at pH 6,7, and 9.

Mutant	Difference in pH stability effects between 7S and 8S (kcal/mol)[a] pH		
	6	7	9
I70A	-0.1	0.0	-0.1
I70D	0.8	0.0	0.5[b]
I70K	-0.2	0.0	0.3
I71A	0.2	0.0	-0.6
I71D	1.5[b]	0.0	-1.5[bc]
I71K	0.9[bc]	0.0	-2.5
I92A	0.1	0.0	0.0
I92D	-0.2[c]	0.0	0.9[bc]
I92K	0.5[bc]	0.0	-0.2[bc]

[a]Values are the free energy difference between 7S and 8S variants at different pH and are calculated by subtracting the free energy measured between pH values for 7S variants and the parent from the same in 8S.
[b]The buried ionizable group is in the ionized form in 7S at the indicated pH
[c]The buried ionizable group is in the ionized form in 8S at the indicated pH.

general correlation is observed between the magnitudes of the shift in pK and the change in $\Delta(\Delta G)$. That is, the greater the estimated shift in pK observed, the greater the magnitude of the calculated stability change and vice versa (Figure 14). Additionally, the effect on stability of the charged state of each mutant was studied. As expected and in each case where the pK of the ionizable group is shifted, the ionized form of the residues is estimated to be destabilizing (Figure 14).

8S and 7S differ in that 7S has a native 89% buried Asp 79 and 8S has a Phe.[44, 164] The pK of 7S Asp79 is 7.4.[164] For 7S variants, the difference in free energy values between the variants at pH 6 and 9 and their parent was calculated and includes any

contribution to stability from an interaction between buried ionizable mutants and Asp79. Those contributions should not exist in the stability differences observed for 8S variants over the same pH range. The values for the differences between 7S and 8S are reported in Table 10. The largest difference was measured for Ile→Asp mutants at position 71 at 3 kcal/mol. The smallest differences occur when the mutant is an Ala.

Discussion

There is typically a large and unfavorable desolvation penalty for burying charged groups in the mostly hydrophobic interior of proteins.[4, 81] Yet despite the unfavorable environment of the protein interior, ionizable groups are often buried.[10, 58, 132] One way that buried ionizable groups respond to being removed from polar water is by altering the pK of the ionizable group on the side chain to neutralize the charge.[10, 13]

To gain insight into the magnitude of the stability contribution of buried ionizable groups, the charge on the groups must be determined. The dissociation constant of the proton (pK) of ionizable groups is the solution pH value at which the group is half ionized. Below the pK, groups are protonated and above the pK, groups are deprotonated. Whether protonation or deprotonation results in ionization depends on the group in question. Aspartic acid is negatively charged above and Lys is positively charged below their respective pKs.

The pKs of the buried ionizable groups of 7S and 8S are estimated indirectly by analyzing CD thermal unfolding curves for buried ionizable group mutants over a pH range to determine the change in free energy at each pH (see Materials and Methods).

The change in free energy for the 7S parent is subtracted to give Δ(ΔG). By fitting Δ(ΔG) vs. pH with equation 9, the pK of the group is estimated (Table 8, Figure 13).

In 7S, I70D and I92D both had elevated pKs of 8.5 and 7.2, respectively. The large shift in pK helps keep the side chains uncharged at physiological pH, and the pK value of 8.5 is among the highest ever recorded for Asp in a protein. The I71D variant was estimated to have no change in pK in 7S. The two former charges are buried in close proximity to the native Asp79 (<6Å), whereas I71D is approximately twice the distance away (10 Å) and is separated from Asp79 by the 7S β-sheet. To test if the proximity to Asp79 affects the change in magnitude observed in the pK values for Asp70, Asp92, and Asp71, the pKs of the groups were also determined in 8S in which Asp79 is absent. The I70D mutation was estimated to have an elevated pK of 8.5. Interestingly, the I92D mutation showed no observable change in pK, but the I71D mutation was measured to have an elevated pK of 7.2. Thus, the apparent pK of Ile70 is comparable in the presence of Asp79, whereas the I92D pK is highly elevated in 7S (3.9 to 7.2) and unaffected in 8S. I70D is 6 Å away from Asp79 and I92D is 5 Å away. Classically, a distance of ≤5 Å is considered to be within the range of direct contact. Therefore, the difference in the pK shift response of I70D and I92D may result from the difference in distance from the Asp79 carboxyl.

The pK of I71D appeared unperturbed in 7S, but elevated in 8S. Since 8S is more stable than 7S, one possibility is that the unchanged pK of 7S I71D may be due to solvent access of the side group. A fully solvated I71D may explain the empirically estimated pK of 3.9. The location of the I71D mutation lies in the RNase Sa active site

and is buried by random coil (Figure 7). The 8S protein is more stable, and the protein has been suggested to be more structured in the unfolded state by Fu *et al*., further supporting the hypothesis that 7S I71D may be solvated in the less stable (more dynamic) 7S variant. Structural data is needed for any further study of the role of water access to buried ionizable groups.[44] This is especially true, since additional analysis of the pK shifts of Lys mutants show a decrease in pK for Lys at position 71 in both 7S and 8S (Table 9). Taken together, the change in pK for these groups is likely dependent on their location within a protein and possibly on the composition of the protein itself. Additional variance may result from electrostatic interactions, as there is an apparent difference in the change in stability for acidic and basic residues at that position.

Arginine groups at positions 65 and 69 are within the active site and help bind and orient RNA for catalysis of the endonuclease reaction of RNase Sa.[133, 135, 160, 176] Arg is positively charged at all pHs studied and the close proximity of these Arg to position 71 may result in the depressed pK values estimated for Lys. The side chain of Asp is ≈4 Å shorter than Lys, and the closest Arg (Arg69) is 9 Å away from the C_β of the position 71 side chain. Therefore, the Lys71 variants can be closer to Arg69 than the Asp71 mutants resulting in the decrease in pK value. I71D mutations show differences in pK between 7S and 8S (Table 9) and solving the structure of 7S and 8S variants may provide additional insight into possible reasons for the differences observed.

The pK shifts for lysine mutations also vary between 7S and 8S. For example, the I70K mutation was stable enough to study in a narrow range of $6 < pH < 9$, but thermal unfolding data for the full pH range of 1 – 10 is likely needed to estimate any

shift in the pK value. In 8S, I70K was unstable below pH 3, but the difference in the free energy of folding could still be fit to determine a decrease in pK from 10.4 to 7.4 (Table 8, Figure 13B). At position 71, the pKs of Lys mutations were decreased in 7S and in 8S from 10.4 to 7.7 and 8.4, respectively. At position 92, the pK of mutant Lys residues were unaffected in both 7S and 8S. Consequently, this suggests that the pK of Lys residues at position 71 and 92 are only marginally affected by the presence of Asp79, as the pK values change only slightly, if at all, between the 7S and 8S variants (Table 9).

A comparison of the magnitude of the shift in pK and the change in stability for buried ionizable mutants appear to be related. That is, as the shift in pK for a group gets larger, so does the estimated destabilization (Table 9, Figure 14). To determine the change in stability due to the buried mutant alone, the stability of 7S at pH 6, 7, and 9 was subtracted from the stability of each mutant at the same pH. The difference was then subtracted from the same calculated value in the equivalent 8S variant. As a result, the contribution from the burial of the native Asp79 is subtracted out. That leaves only the contribution to stability of the buried mutant and any interaction conferred by the presence of Asp79 on the group in the case of 7S. The resultant free energy differences between 7S and 8S variants at pH 6 and 9 are reported in Figure 14.

From the results of the pK shift analysis, the apparent changes in stability for each mutant appear to be related to the charge state, as comparing the stabilities over pH ranges in which the buried mutants ionize give increases in stability upon deionization or decreases in stability upon ionization (Figure 14). The magnitude of any charge-charge

interactions between buried ionizable mutants and Asp79 may be estimated by subtracting the change in stability in 7S from the change in stability in 8S when using the T_M of each mutant at pH 7 as a reference temperature. The contribution from burying the ionizable group and Asp79 are subtracted out, leaving only any free energy not attributable to desolvation of the charge group alone (Table 10) (e.g. coulombic interactions). As electrostatic interactions may only be a component of the values reported in Table 10, the free energy of electrostatic interactions between charge groups based on the distance between ions were calculated and are discussed in Chapter VII.

In all, the stability contribution of buried ionizable mutants in RNase Sa is context dependent, in that there are differences in the stability contributions between buried positions 70, 71, and 92 and for each mutation type studied. The magnitude of the shift in pK is appears to be related to the observed change in stability as a positive correlation between the two is observed. Simply put, the greater the estimated pK shift, the greater the calculated change in stability. Additionally, the ionization state of the residues determines the magnitude of the stability conferred at each location.

As expected, buried ionizable residues appear to be more destabilizing when ionized. The free energy change attributed to buried ionizable mutants and the native buried Asp79 alone are negated when subtracting stability values for 7S and 8S variants, which allows for the estimation of additional contributing forces in 7S. For example, a charge-charge repulsion may exist between Asp79 and Asp92 mutants that does not exist for Asp71 mutants or in 8S. Therefore, any additional energy observed may be due to non-covalent electrostatic interactions. Previous studies have shown that after solvation

effects, coulombic interactions are a main determinant for pK and ionization-state changes.[10] For that, the magnitude of the stability contributions of coulombic interactions is calculated in Chapter VII.

CHAPTER VII

STABILITY CONTRIBUTIONS OF BURIED ELECTROSTATIC INTERACTIONS IN RNASE SA 7S

Introduction

Protein stability is the additive contribution of all forces acting to fold and unfold a protein.[58] The difference in stability between the folded state and the more unfolded state is marginal. That is not to say that the forces contributing to stability are small. Collectively, the forces can be quite large, and the marginality arises from the small difference between those large values. Minor changes in stability can therefore shift proteins between the folded and unfolded states. As a protein's form and function are intricately linked, estimating the contributing forces to protein stability is important.

The largest forces acting to maintain the folded state of many proteins are van der Waal's interactions and the hydrophobic effect. Van der Waal's attractions result from induced partial dipoles between molecules and are optimized in the hydrophobic core of proteins where amino acids are tightly packed. The hydrophobic effect arises as water attempts to both maximize hydrogen bonding with itself and minimize contact with hydrophobic side chains of the largely aliphatic non-polar amino acid residues.[39, 47, 101, 125] Pace *et al*. recently reported that on average hydrophobic interactions contribute 60 ±4% of the stabilizing force in proteins.[39] Hydrogen bonding also contributes free energy to the folded state of RNase Sa and is the collective contribution of all hydrogen bonds. Hydrogen bonds contribute on average ≈40% of the stabilizing free energy in

proteins.[101] It is estimated that there are approximately 1 hydrogen bond per residue in proteins, and each bond increases stability by ≈1 kcal/mol.[101, 111] Conversely, conformational entropy is the largest force contributing to the denaturation of proteins.[24] In a 100 residue protein, it is estimated that conformational entropy contributes ≈200 kcal/mol to stability.[24, 37] To recapitulate, large forces act to fold or unfold proteins and the stability difference between the states is marginal. Additionally, the marginality has been observed across protein families.[4-6, 24, 42, 61, 88]

In addition to the forces mentioned above, there are other forces contributing to the stability of globular proteins, including non-covalent electrostatic interactions like van der Waal's forces, ion pairing, and coulombic interactions.[24] In previous chapters, the total stability contribution of buried ionizable mutations was measured by analysis of CD thermal unfolding curves. Included in those values are additive contributions from the burial of a charge, effects from shifts in estimated pK values to mitigate charge, and charge-charge interactions. Of interest is the free energy contribution to stability of charge-charge interactions conferred by buried ionizable mutations in RNase Sa 7S and 8S.

One factor to consider in examining the stability effects of buried ionizable mutants is the microenvironment of the location of those groups in proteins.[58] For instance, the unfavorable Born self-energy for burying charged groups in the hydrophobic interior of a protein has been estimated as ≈-19 kcal/mol.[81] Despite this, proteins on average bury ≈1 ionizable amino acid for every 100 residues in small proteins.[132] Surprisingly, the average number of buried ionizable residues may increase

as protein size increases. Proteins with ≈300 residues were found to have an average of ≈4.5 buried ionizable groups.[116, 132] Further evidence is found in a recent study in which a 700 residue protein was reported to bury 65% more polar groups than a 100 residue protein.[19] In Chapter IV above, we observe that buried ionizable groups at different positions may result in different changes in stability. Thus, the magnitude of the change in stability must necessarily be dependent on more than just desolvation effects alone.

Additionally, electrostatic interactions between ionized groups can be stabilizing or destabilizing and can affect the free energies of the folded or unfolded states. One example of a non-covalent interaction is an ion pair. When an ion pair forms, two charges of opposite sign are in close proximity. In this scenario, the charges will experience an attractive force. If the attraction between the charges decreases the propensity of the protein to achieve an unfolded state conformation, then the protein will be kept in a more folded-like structure.[178] Another example is a salt bridge. A salt bridge in T4 lysozyme that exists between Asp70 and His31 contributes 3-5 kcal/mol to stability.[95] The magnitude of the stability was determined by measuring the stability over a pH range in which the groups ionize.[95, 178] In contrast, an ion pair can also be destabilizing by reducing conformational flexibility/increasing steric strain, which decreases the propensity for the folded state structure and assumes a more unfolded-like state.[178, 179] The previous forces are short range interactions between charged species that are in direct contact, typically less than 5Å. Even when they are not involved in ion pairs or salt-bridges, ions can experience charge-charge effects, such as attraction and repulsion. The magnitude of the free energy of those interactions can be estimated using

Coulomb's equation (equation 5), which relates the free energy of interaction between charged groups to their distance apart and the polarizability of the medium between them.

Taken together, the charge, the polarizability of the environment of the charges, and the distance between charges in proteins directly affect the free energy contribution of the interaction between multiple charges. From Coulomb's equation, the choice of dielectric constant value in the denominator is important in determining the overall magnitude of the stability contribution of electrostatic interactions. For example, in studies examining mutations in the protein interior of Staphylococcal Nuclease (SNase), multiple values for the effective dielectric constant were calculated over a large range from 9 – 40.[86, 151] Furthermore, recent studies of SNase using a mean-field Poisson-Boltzman distribution approach indicate that the dielectric constant changes depending on the ionization state of the ionizable group present and the value ranges between 14 – 30.[180] By examining a large group of proteins of different sizes and topologies, the range of values appears to be position-dependent with lower values representing the protein interior.[10, 151, 180] Based on the range of dielectric values for protein interiors from those studies, the value for the dielectric constant used here is 20, so as not to over- or underestimate its contribution to the magnitude in the change in stability. The resultant free energy for non-covalent electrostatic interactions is calculated by equation 10 (see Materials and Methods), and the distances and charges for RNase Sa variants are reported in Table 11.

Table 11. Free energy of electrostatic interactions between RNase Sa 7S ionizable groups and native buried Asp79.

Position	Residue	Distance (Asp79)[a]	Charge[b]	ΔG[c] (kcal/mol)
1	ASP	16.7	-0.5	0.10
14	GLU	16.9	-0.5	0.11
17	ASP	14.5	-0.5	0.09
25	LYS	12.4	1.0	-0.15
33	ASP	13.8	-0.5	0.09
40	ARG	23.9	0.5	-0.15
41	GLU	21.3	-0.5	0.13
53	HIS	10.5	1.0	-0.13
54	GLU	13.8	-0.5	0.09
63	ARG	28.1	0.5	-0.18
65	ARG	16.8	0.5	-0.10
68	ARG	17.9	0.5	-0.11
69	ARG	15.8	0.5	-0.10
74	LYS	12.2	1.0	-0.15
78	GLU	7.6	-0.5	0.05
79	ASP	0.0	-0.25	0.00
84	ASP	17.2	-0.5	0.11
93	ASP	10.9	-0.5	0.07
Total ΔG				-0.25

[a]The distance was measured from the group at position X to the carboxylic carbon of Asp79 using equation 9.
[b]The charge for the oxygen atoms of carboxylic acids in Asp and Glu or the amine of the guandino group of Arg is assumed to be equally distributed over the group due to electronic resonance. Therefore, the q-value is -0.5 or +0.5, respectively.
[c]The change in free energy is calculated using equation 10.

As mentioned in Chapter I and II, the spatial relationship between Ile70, Ile71, Ile92, and Asp79 provide a unique system for measuring the free energies of the electrostatic interactions of buried ionizable groups. The D79F mutation in 8S gives an additional means by which a free energy of interaction can be isolated, as the

contribution to stability from the Ile70, Ile71, and Ile92 ionizable mutants in the absence of Asp79 can be calculated.

By comparing the stability of 7S, 7S buried ionizable variants, 8S, and 8S buried ionizable variants, the contribution to stability from buried ionizable groups was calculated (Chapter IV). The change in stability for buried ionizable mutations in 7S is different than the change in stability for 8S (Chapter VI, Table 10). The previously estimated pK values of each ionizable group determine the charge (q_n) at pH 7 (Chapter VI, Table 9). Therefore, Coulomb's equation can be used in order to compare and quantify the contribution to stability of electrostatic interactions with buried ionizable mutations in the presence and absence of Asp79.

In the above chapters, we estimate the total stability effect of burying ionizable residues in the protein interior and go on to describe the stability effect of ionization of those groups in 7S and 8S. As the magnitude of the reported stability values is the additive contribution of different forces, of interest is what part of the total protein stability is from electrostatic interactions between ions. Here, we use Coulomb's Law to estimate the contribution to stability of ion-ion interactions in RNase Sa variants at pH 7. The pK values previously reported in Chapter VI are used to assign the charge on residue side-chains. Coulombic interactions are calculated for buried ionizable mutants in 7S and 8S to measure the effect of the native buried ionizable group on charge-charge interactions in variant proteins. To this end, the total stability changes for making buried ionizable mutations in 7S includes the stability contribution of coulombic interactions between Asp79, the buried ionizable mutants, and other ions in 7S. In 8S, the magnitude

of coulombic interaction contributions is limited to the interaction between the buried ionizable mutants and other ions in the protein.

As an alternate approach, we calculate the localized effect of buried ionizable mutants on the dielectric constant value using Coulomb's law. To do so, we operate under the premise that the structure of mutants is similar (Chapter V), and presume that mutant ionizable side-chains will: 1) be in a similar local environment to resolved structures, 2) the distances between ions will be similar to resolved structures, and 3) that the determined stabilities (Chapter IV) are due exclusively to charge-charge interactions. We use the free energy difference between 7S and 8S variants in order to account for both the background interactions between native ions and native ions and solvent.

Results

Free energy of electrostatic interactions between 7S buried mutants and Asp79

In Chapter III, the total stability contribution of the ionization of Asp79 was calculated to be 1.8 kcal/mol. The estimated contribution to that value from coulombic interactions is -0.25 kcal/mol and is reported in Table 11. The free energy of the coulombic interaction between buried ionizable mutants and 7S Asp79 was calculated as described above and are reported in Table 12. Taken alone, the interaction between each buried mutant and the native Asp79 ($\Delta G_{Mut\text{-}D79}$) is typically small. For instance, the maximum electrostatic contribution of buried Asp mutants ranges between 0.07 – 0.1

kcal/mol when both the buried mutant and Asp79 are ionized. Furthermore, Lys mutants contribute -0.15 to -0.19 kcal/mol when both Lys and Asp79 are ionized.

Table 12. The free energy of coulombic interactions in RNase Sa 7S buried ionizable mutants.

Variant	$\Delta G_{Mut\text{-}D79}$ (kcal/mol)[a]	ΔG_{pK} (kcal/mol)[b]	ΔG_{Total} (kcal/mol)[c]
7S	--	-0.25	-0.25
I70D	0.08	0.00	0.00
I70K	-0.17	-0.08	0.57
I71D	0.10	0.05	-0.28
I71K	-0.19	-0.10	0.57
I92D	0.07	0.02	-0.43
I92K	-0.15	-0.07	1.71

[a]The free energy of the electrostatic interaction between the buried ionizable group and the native buried Asp79 when both groups are ionized.
[b]The free energy of the electrostatic interaction at pH 7 using the experimental pK value (Table 9) to set the charge of the ionizable group and Asp79. When Asp or Lys is near the pK of the group, the charge is halved during calculations (e.g. Asp79 is given a -0.25 charge at pH 7).
[c]The total free energy of electrostatic interactions in the protein at pH 7 for each mutant. The buried ionizable mutant was used as the point of reference for measuring the distance used in Coulomb's equation.

Previously, the pK of the buried ionizable groups was determined (Table 9). Based on those values, the coulombic interaction for the buried ionizable groups is reported when the groups are in their experimentally determined charged state. The charge value (q_n) of Asp79 is -0.25 as the pK of the carboxyl functional group is 7.2 and will be half charged at pH 7. The same approach is used for all groups whose pK is within experimental error of pH 7, in that the charge value used in calculations is halved if near the pK. The pK of 7S I70D is 9.6 and the group is uncharged at pH 7, giving an

electrostatic contribution of zero. The contributions from 7S I71D, I 92D, I 71K, and I92K were 0.05, 0.02, -0.08, and -0.07, respectively.

Even though the electrostatic interaction between buried ionizable groups and Asp79 were destabilizing for the negatively charged Asp groups and stabilizing for the positively charged Lys groups, the overall contribution to stability for the groups (ΔG_{Total}) had the opposite effect. The stability contribution due to electrostatic interactions of 7S I71D and 7S I92D were 0.05 and 0.02 kcal/mol when interacting with Asp79 alone, but contributed -0.28 and -0.43 kcal/mol to protein stability overall, respectively. Conversely, 7S I70K, 7S I71K, and 7S I92K contributed -0.08, -0.10, and -0.07 kcal/mol when interacting with Asp79 alone, but were destabilizing and contribute 0.57, 0.57, and 1.71 kcal/mol to overall protein stability.

Free energy of electrostatic interactions of 8S buried ionizable mutants

The RNase Sa 8S variant has all of the same mutations as the 7S variant with an additional D79F mutation. Consequently, and unlike 7S, there can be no electrostatic interaction between 8S buried ionizable groups and Phe79. The overall contribution to protein stability of electrostatic interactions due to 8S buried ionizable group mutants in both in the ionized state ($\Delta G_{Total\ ion}$) and in the charge state based on experimentally estimated pKs ($\Delta G_{Total\ pK}$) is reported in Table 13. The pK of 8S I70K and 8S I71D are 7.4 and 7.2 and the charge value used in the calculation of $\Delta G_{Total\ pK}$ was -0.25, and 0.5, respectively. All other ionizable groups in 8S are ionized at pH 7. As with 7S, the total contributions to stability from buried ionizable group electrostatic interactions in 8S at pH 7 ($\Delta G_{Total\ pK}$) are typically between -1 and 2 kcal/mol (Table 13). The 8S I70D,

I71D, and I92D mutations contribute 0.0, -0.17, and -0.89 kcal/mol. The difference in stability for Asp mutations at position 70, 71 and 92 in 8S and 7S ($\Delta\Delta G_{8S-7S}$) were 0.0, 0.11, and -0.46 kcal/mol. Since positive changes in stability denote a decrease in

Table 13. The free energy of coulombic interactions of RNase Sa 8S buried ionizable mutants.

8S Mutant	$\Delta G_{Total\ ion}$[a] (kcal/mol)	$\Delta G_{Total\ pK}$[b] (kcal/mol)	$\Delta(\Delta G)$[c] (kcal/mol)
I70D	-0.61	0.00	0.00
I70K	1.21	0.61	0.04
I71D	-0.33	-0.17	0.11
I71K	0.57	0.57	0.00
I92D	-0.89	-0.89	-0.46
I92K	1.78	1.78	0.07

[a]The free energy contribution of electrostatic interactions in 8S when buried ionizable mutants are ionized.
[b]The free energy contribution of electrostatic interactions in 8S when the charged state of buried ionizable mutants is based on the experimental pK (Table 9) at pH 7. If mutant groups have a pK near pH 7, the charge value is halved to reflect partial ionization.
[c]$\Delta(\Delta G)$ = ΔG (8S variant) – ΔG (7S variant) using experimental pK values to determine the ionization state of the groups.

stability and negative values denote an increase in stability, Asp mutations in 8S can be more or less stable than those same mutations in 7S. The contribution to stability from electrostatic interactions of buried ionizable Lys mutations in 8S are generally stabilizing at 0.61, 0.57, and 1.78 kcal/mol. The difference in stability between buried Lys mutations in 8S and 7S is 0.04, 0.0, and 0.07 kcal/mol, at position 70, 71, and 92, respectively.

The localized effect of buried ionizable mutations on the dielectric constant

The dielectric constant is a relative measure of the polarizability of a medium. For example, in a vacuum, the dielectric constant is 1. For hexane, octanol, and ethanol, the values are 2, 10, and 25 respectively. For water, the value is 80. As the polarizability of the medium increases, so does the value of the dielectric constant. Similarly, as the dielectric value decreases, hydrophobicity increases. Of interest here is the localized effect on the dielectric constant from burying an ionized group in the hydrophobic interior of a protein.

Table 14. The localized effect of buried ionizable mutants on the dielectric constant value

Variant	Dielectric (D)[a]
7S	29
I70D	46
I71D	63
I92D	38
I70K	1
I71K	9
I92K	3

[a]The dielectric was calculated using Coulomb's law (Equation 10). The free energy term (ΔG) is fixed and is calculated by subtracting the stability of 7S variants from 8S variants (Chapter IV). The distances between ions are measured in the molecular modelling program Pymol and are based on the structure of 7SI71A.

Using Coulombs Law (Equation 10), we calculate the dielectric by: 1) presuming the difference in the change in stabilities between 7S and 8S variants is due to charge-charge interactions alone (Chapter IV), 2) using the resolved crystal structure of 7SI71A to determine ion-ion distances (Chapter V), and 3) using calculated pK values to assign charge to ionizable mutant side chains (Chapter VI). The calculated dielectric values are reported in Table 14. The dielectric constant of the protein interior of 7S is calculated as 29, the dielectric increases for all Ile→Asp variants, and decreases for all Ile→Lys variants studied. The average dielectric value for all variants is 27.

Discussion

The forces contributing to the stability of proteins are additive and the stability difference between the folded and unfolded states are marginal.[2, 4-9] Generally, the stability difference between folded states of globular proteins is in the range of 5-10 kcal/mol.[2, 9] Consequently, small changes in stability can shift a protein from one state to the other. Of interest here is the contribution that electrostatic interactions from buried ionizable residues have on protein stability and the constituent magnitude contributed by those forces to the total change in stability measured for buried ionizable mutants in Chapter IV and VI.

There are five general types of non-covalent charge-charge interactions in proteins: salt bridges, ion pairs, hydrogen bonds, van der Waal interactions, and coulombic interactions.[5, 9, 81, 87-92] Ion pairs and salt bridges form when oppositely charged ions interact. An ion pair occurs when the two oppositely charged ions are

within 5 Å and can be stabilizing or destabilizing.[10, 87, 91] Ion pairs in the protein interior have been shown to contribute between 2-6 kcal/mol to stability.[61] Salt bridges are formed between hydrogen atoms and negatively charged ions. In proteins, the majority of salt bridges are typically formed between the hydrogen group of Nitrogens or the charged basic residues and a negatively charged carboxylate.[88, 94] The difference between ion pairs and salt bridges is that that ion pairing involves two point charges and salt bridges involve the interaction of the partial dipole of a hydrogen with a free pair of electrons. The stability conferred by salt bridges has been experimentally determined to be in the range of 3 – 5 kcal/mol in the protein interior, and less on the solvent exposed protein surface.[10, 61, 92, 94-96] Since transferring charged residues into a hydrophobic environment is unfavorable, one would assume that the formation of ion pairs and salt bridges in the non-polar environment of the protein interior would mitigate the desolvation penalty, providing an attractive approach for increasing protein stability. This was shown not to be the case, as hydrophobic substitutions for one, two, or all three of a buried charge triad were found to increase stability in the Arc repressor of bacteriophage P22.[89] In the thermophile *Thermococcus celer* L30e protein, the magnitude of the stability contribution of charge-to-alanine mutations was shown to be context dependent.[97]

That is not to say that buried electrostatic interactions cannot be stabilizing. For example, the buried Asp33 in the same enzyme that forms 3 hydrogen bonds and when removed by mutation to Ala, decreases stability of RNase Sa by 6 kcal/mol.[79, 98] In contrast, RNase Sa Asp79 is buried and forms no hydrogen bonds or ion pairs to other

residues in the protein.[20] The buried Asp79 decreases the stability of RNase Sa WT by ≈3 kcal/mol.[20] The experimentally determined pK of Asp 79 is 7.2, and that of Asp33 is 2.4.[20, 79, 98] Buried Asp76 in RNase T1 forms three hydrogen bonds and has a pK of 0.5![99] Thus, mitigation of the desolvation of ionizable groups into the protein interior is a mixture of both pK shifts and electrostatic non-covalent interactions. Statistical analysis of proteins reveals that most native buried ionizable groups are involved in forming either ion pairs or salt bridges.[100] Experiments testing the response of protein stability to changes in pH show that electrostatic interactions collectively contribute a maximum of ≈10 kcal/mol, which is within the magnitude range of the stability difference between folded states.[2, 10, 24, 39, 51, 102, 103]

Since contributions to stability are additive and net stability is marginal, the change in stability due to electrostatic interactions is studied in RNase Sa variants that are able to tolerate buried groups without unfolding. The models used are derived from two highly stabilized variants of RNase Sa, 7S and 8S (Chapter I). Three buried isoleucines (Ile70, Ile71, and Ile92) were identified as candidates for buried ionizable group substitution using a computer program, *pfis,* which measures the solvent-accessible surface area of amino acid side chains. All three Ile's are 100% buried. Ile70 and Ile92 are 6 Å and 5 Å away from Asp79. Ile71 is 8 Å away from Asp79 with a side-chain geometry that points away from the buried Asp on the opposite face of the 7S and 8S β-sheet, further separating the residues. The buried D79F mutation in 8S provides a unique model to study the stability contribution of buried electrostatic interactions when

buried ionizable substitutions are made at positions 70, 71 and 92. Each Ile was individually mutated to ionizable residues Asp and Lys.

Coulomb's Law is used to calculate the electrostatic contribution to stability for each mutation. The 7S crystal structure was mutated *in silico* using the program PyMol (see also Materials and Methods). From that, the distances between all ionizable atoms are measured. Since the exact location of the charge is unknown for groups that exhibit electronic resonance, a reasonable estimation of the distance can be made by measuring to the carboxyl-carbon of acidic groups and assigning the group a half charge. The distance, charge, and dielectric constant of the protein interior are all that is needed to calculate the stability contribution of the electrostatic interaction between the proteins.

The charge of each ionizable group and mutant is based on previous pK studies and studies within this work (Chapter VI).[13, 76] The pK of an ionizable group is the pH at which the group is half ionized. Below the pK, the ionizable group is protonated and above the pK the group is deprotonated. Asp is charged when deprotonated and Lys is charged when protonated. Asp has a pK of 3.9 when fully solvated in an Ala-Ala-X-Ala-Ala pentapeptide.[13, 76] In 7S mutants, Asp70, Asp71, and Asp92 have pK's of 8.4, 3.9, and 7.2. In 8S the same mutations have pKs of 8.5, 7.2, and 3.9. In 7S, the pKs of K71 and K92 mutants are 7.7 and 10.4, respectively. The I70K mutant was unfolded at the temperature limits of the CD and pK was not obtained. In 8S, K70, K71, and K92 mutations have pKs of 7.4, 8.4, and 10.4. The change in pK between 7S and 8S ionizable groups must be a consequence of the D79F mutation, and the magnitude of

coulombic interactions is calculated by assigning charge values based both on the respective pKs and in the ionized state (Table 12, 13).

Generally, stability contributions due to electrostatic interactions between buried mutations and Asp79 in 7S were small, ranging between -0.5 and 0.5 kcal/mol (Table 12). As would be expected, all Asp mutations were calculated as repulsive and destabilizing and all Lys mutants were stabilizing and attractive when measuring their interaction with Asp79. Interestingly, the groups had the opposite effect on the total stability of the mutant proteins based on coulombic interactions alone. All of the Asp mutants decreased overall free energy and all of the Lys mutants increased the overall free energy. This is most likely a consequence decreasing the net charge of RNase Sa 7S, though the effect due to a change in dielectric constant cannot be ruled out. Lowering the net charge of proteins can increase stability without altering the native topology.[10, 35] The net charge is zero at the isolectric point (pI), positive below the pI, and negative above the pI. The pI of 7S is 4.83 and the pH value at which the protein is charge neutral. At pH 7, the net charge on 7S is -2. The Asp mutations increase the net negative charge when they are above their pK values. Lys mutations decrease the net charge when they are below their pK values. Consequently, this may explain why the buried ionized groups of Asp are more destabilizing than the ionized amine of the Lys groups when measuring the stability by following thermal unfolding using CD (Figure 14).

In Chapter VI, the stability contributions of buried ionizable groups in 7S and 8S were measured and compared. The difference between 7S and 8S indicated that there

were additional stability contributions in 7S that were missing in 8S calculations (Table 10). A comparison between the estimated coulombic contributions (Table 12, 13) and the background free energy measured in Chapter VI indicate that the free energy from non-covalent electrostatic interactions is smaller than the measured additional free energy when the groups are ionized. There are three possible explanations, 1) the dielectric constant value used in calculations may not be correct, resulting in calculated differences in ΔG values, 2) there may be structural rearrangements, and/or 3) groups in 7S are involved in ion pairs, salt bridges, or hydrogen bonds resulting in unaccounted for contribution to stability.

To test for localized dielectric effects, the difference in the change in stability between 7S and 8S was used to estimate the free energy change (ΔG) in Coulomb's law. Using structural data from Chapter IV, the distance between ions is assumed to be equal for 7S and 8S variants. Consequently, native interactions are subtracted out, leaving only the effect of the buried native Asp and its interaction with buried ionizable mutants. Operating under the premise that the interaction between Asp79 and buried mutants will be electrostatic alone, the dielectric constant was calculated. Intuitively, we find that all Asp mutants increase the dielectric constant and all Lys mutations decrease the dielectric constant. The introduction of an ionizable side chain of opposite sign therefore mitigates the polarizing effect of the native buried Asp79, whereas two of the same charges increase the polarizability of the protein interior.

Recent studies in SNase indicate that the induced apparent dielectric constant of buried ionizable groups is in the range of 14-16.[180] The authors calculated the dielectric

constant for the whole protein and an apparent local dielectric constant using the difference in pK observed. Using the 7S/8S model system, we are able to calculate the local dielectric for buried ionizable groups, as background interactions are negated. We find the local dielectric is over a range of 1 – 63. The dielectric for RNase Sa 7S Asp79 is 29, which is close to 27, the calculated average of all variants.

Burying ionizable groups increases the dielectric, but we suggest that the dielectric can be decreased by burying a mutant of opposite charge to that of a native buried ionizable group. Furthermore, the dielectric constant of the interior of 8S should necessarily be lower than the dielectric constant of the interior of 7S when Asp 79 is mutated to Phe 79, resulting in the larger measured $\Delta(\Delta G)$ values (Table 13). Further analysis of the crystal structures of 7S and 8S would allow for the determination of the possible access of solvent to the protein interior and/or buried ionizable groups, side-chain geometry that may indicate non-covalent interactions between buried ionizable mutants and 7S Asp79, and any difference in the measurement of the distances between ions. Structural analyses of obtained mutant structures, as determined by X-ray crystallography are discussed in Chapter V. At this time, 7S I71A is the only mutant for which crystal structures have been resolved to an appreciable degree (1.8Å). All structures were determined in the lab of Dr. Kazufumi Takano (Graduate School of Life and Environmental Sciences, Kyoto Prefectural University, Kyoto, Japan)

CHAPTER VIII

SUMMARY

The aim of this work was to determine the effects that buried ionizable groups have on protein stability. As there is a large desolvation penalty for burying ionizable groups in the protein interior, two stabilized variants of the *Streptomyces aureofaciens* guanylic-specific endonuclease, RNase Sa, were prepared. One of the variants was stabilized by 7 mutations that optimized the geometry of β-turns and is named RNase Sa 7S. The second model has an additional stabilizing mutation, D79F, which replaces a native buried Asp with Phe, and is named 8S for its 8 stabilizing mutations. Candidate buried positions were chosen based on the solvent-accessible surface area (ASA) of their side chains. The in-house computer program *pfis* measures the ASA by using a single solvent sphere with a diameter of 1.4Å to determine the fraction of solvent-surface area contacts between the sphere and protein residues. Ten residues were identified with 0% ASA, three of which were isoleucines at position 70, 71, and 92. Position 70 and 92 are in close proximity to the native buried Asp79 and position 71 is further away on the opposite side of the RNase Sa β-sheet. Taken together, the 7S/8S system provides a unique opportunity to study the stability effects of both burying ionizable groups in the protein interior and the interaction between buried ionizable groups.

The pK = 7.4 for the 90% buried Asp at position 79. There are no other residues in 7S that have a pK within 1 pH unit of pH 7. The conformational stability was measured by thermal denaturation at pH 6, 7, and 9. Thus, a change in stability due to the buried anion was determined. The side chain of Asp79 is protonated and non-

ionized at pH 6 and deprotonated and ionized at pH 9. The change in stability ($\Delta(\Delta G)$) due to ionization of Asp79 is destabilizing and has a magnitude of -1.8 kcal/mol.

The conformational stability of 20 RNase Sa variant proteins has been determined by thermal denaturation using circular dichroism spectrometry in order to measure the stability effects of buried ionizable groups. The two parental proteins are 7S and 8S, and the buried mutant variants of 7S and 8S are Ala, Asp, and Lys mutations at buried positions Ile70, Ile71, and Ile92. Ala mutations were used as both a structural and charge control. Asp mutations were used to study stability effects of buried negative charges. Lys mutations were used to measure stability effects of buried positive charge groups. All of the mutations were destabilizing, and the magnitude of the change in stability was context dependent. The results for Ile → Ala mutants in 7S and 8S were comparable, with destabilizing $\Delta(\Delta G)$ values of +3.7 – +4.9 kcal/mol. Individual hydrophobic carbons have been measured to contribute ≈1 kcal/mol to stability. Ile to Ala mutations remove three such groups. Therefore, the magnitude of the stability change for 7S and 8S Ile→Ala variants is in good agreement with classical determinations of buried hydrophobic group removal.

The change in stability for buried Asp mutants at positions 70, 71, and 92 in 7S are destabilizing and the $\Delta(\Delta G)$ is -10.2, -4.6, and -9.9 kcal/mol, respectively. For 8S, the magnitude of the change in stability for Asp mutants at the same positions was -10.7, -8.4, and -7.4 kcal/mol, respectively. The Lys mutations also show a context dependency. In 7S, the $\Delta(\Delta G)$ for mutants at position 70, 71, and 92 is -11.1, -9.8, and -

8.1 kcal/mol, respectively. For 8S, these values are -8.0, -6.7, and -5.7 kcal/mol for the same positions.

To determine if the context dependency observed was due to differences in the ionization state of mutant groups, the pK of the side chain of each mutant was determined. The pK of buried groups is estimated by fitting the difference in the change in stability ($\Delta\Delta(\Delta G)$) at each pH between the mutant and the parent. Previous studies have determined that ionizable groups can have shifted pK values upon burial into the protein interior in an attempt to mitigate the high cost of having a polar group in a hydrophobic environment. The shift in pK for buried ionizable groups in 7S and 8S was also context dependent and a strong positive correlation was observed between the magnitude of the pK shift and the total change in stability. For instance, there is no observable change in pK for the carboxyl of I71D in 7S, and the $\Delta(\Delta G)$ is -4.6 kcal/mol. In 8S, the pK of the carboxyl of I71D is shifted from 3.9 to 7.2 and the $\Delta(\Delta G)$ is calculated as -8.4 kcal/mol. The conformational stability of each mutant was measured at pH 6, 7, 9, a range in which Asp79 ionizes. All mutants were less stable when charged than when uncharged. Interestingly, the difference in the change in stability between 7S and 8S variants and the parental proteins showed that changes in stability could be different for each mutation type at each location. The only difference between 7S and 8S is that 7S has an Asp and 8S has a Phe at position 79. Therefore, the free energy of the electrostatic interactions between Asp79 and buried ionizable mutants was of interest.

Coulomb's law was used to estimate the stability contribution of electrostatic interactions. The charge of each side group at pH 7 was determined using the measured pK values. Calculated stability contributions due to electrostatic interactions between buried mutations and Asp79 in 7S were smaller than those measured by thermal denaturation, and ranged from -0.5 to 0.5 kcal/mol. The difference may actually be larger and more similar to that reported, since the dielectric constant used in calculations for 8S is necessarily lower than that of 7S because of the removal of the buried Asp79. As expected, Asp79→Asp mutant interactions were destabilizing when both residues were charged, and Asp79→ Lys interactions were stabilizing when both residues are charged. This is possibly due to opposite charges interacting to neutralize the other's effect in the hydrophobic environment of the protein core. The groups had the opposite effect on the stability of the mutant proteins based on whole protein cumulative stability calculations. Based on coulombic calculations, all of the Asp mutants should be stabilizing and all of the Lys mutants should be destabilizing. The observation of stabilizing Asp groups and destabilizing Lys groups may be a consequence of decreasing the net charge of RNase Sa 7S. In general, lowering the net charge of proteins will increase stability. The pI of 7S is 4.83. Asp mutations increase the negative charge when they are above their pK values. Lys mutations decrease the net charge when they are below their pK values, possibly explaining the increased stability of buried ionized Asp compared to the destabilizing contribution of the Lys groups. The differences may also be explained by the localized effect of buried charges on the dielectric constant. The protein core becomes more similar to solvent as the dielectric constant of the protein

interior increases, which could decrease the effect of van der Waal's interactions and the hydrophobic effect. The dielectric constant for 7S was calculated to be 29. As expected, we find that increasing the number of like charges in the protein interior by making buried Asp substitutions increases the dielectric constant. We also find that buried Lys mutations decrease the dielectric value from 2 to 20 fold when made in the Asp79 containing 7S (Table 14).

To address the possibility that structural changes or solvent access to the protein interior may be responsible for the stability differences measured between mutants, the three dimensional structures of two mutant proteins were studied. To date, only the structures 7S I71A and 8S I71D have been resolved by X-ray crystallography. The structures have been solved at 1.8 Å and 2.5 Å resolutions, respectively. The overall structural topology of RNase Sa 7S I71A and 8S I71D are comparable to RNase Sa WT based on structural alignment data from the molecular modelling software PyMol. Additionally, using a solvent sphere interaction radius (fixed van der Waal radius) of 1.4 Å, the buried side-chains of 70, 71, and 92 of both 7S I71A and 8S I71D are completely buried. These results agree with other studies that indicate buried ionizable group mutations have minor structural effect. Structural analysis of all mutants still needs to be performed to make discreet calculations of coulombic interactions, as well as give insight into the solvation state of residue side groups for each mutant. Crystal structure determination for all remaining variants is currently underway.

REFERENCES

[1] Anfinsen, C. B. (1973) Principles that govern the folding of protein chains, *Science 181*, 223-230.

[2] Pace, C. N., Trevino, S., Prabhakaran, E., and Scholtz, J. M. (2004) Protein structure, stability and solubility in water and other solvents, *Philos Trans R Soc Lond B Biol Sci 359*, 1225-1234; discussion 1234-1225.

[3] Nolting, B., Golbik, R., Soler-Gonzalez, A. S., and Fersht, A. R. (1997) Circular dichroism of denatured barstar suggests residual structure, *Biochemistry 36*, 9899-9905.

[4] Dill, K. A. (1990) Dominant forces in protein folding, *Biochemistry 29*, 7133-7155.

[5] Jaenicke, R. (2000) Stability and stabilization of globular proteins in solution, *J Biotechnol 79*, 193-203.

[6] Matthews, B. W. (1987) Genetic and structural analysis of the protein stability problem, *Biochemistry 26*, 6885-6888.

[7] Pace, C. N. (1975) The stability of globular proteins, *CRC Crit Rev Biochem 3*, 1-43.

[8] Pace, C. N. (1990) Measuring and increasing protein stability, *Trends Biotechnol 8*, 93-98.

[9] Pace, C. N. (1990) Conformational stability of globular proteins, *Trends Biochem Sci 15*, 14-17.

[10] Pace, C. N., Grimsley, G. R., and Scholtz, J. M. (2009) Protein ionizable groups: pK values and their contribution to protein stability and solubility, *J Biol Chem 284*, 13285-13289.

[11] Zhang, X. J., Baase, W. A., Shoichet, B. K., Wilson, K. P., and Matthews, B. W. (1995) Enhancement of protein stability by the combination of point mutations in T4 lysozyme is additive, *Protein Engineering 8*, 1017-1022.

[12] Scholtz, J. M., Grimsley, G. R., and Pace, C. N. (2009) Solvent denaturation of proteins and interpretations of the m value, *Methods Enzymol 466*, 549-565.

[13] Grimsley, G. R., Scholtz, J. M., and Pace, C. N. (2009) A summary of the measured pK values of the ionizable groups in folded proteins, *Protein Sci 18*, 247-251.

[14] Wei, Y. (2009) Experimental and Computational Studies on Protein Folding, Misfolding and Stability, In *Department of Biochemistry and Biophysics*, Texas A&M University, College Station.

[15] Parsell, D. A., and Sauer, R. T. (1989) The structural stability of a protein is an important determinant of its proteolytic susceptibility in Escherichia coli, *J Biol Chem 264*, 7590-7595.

[16] Shoichet, B. K., Baase, W. A., Kuroki, R., and Matthews, B. W. (1995) A relationship between protein stability and protein function, *Proc Natl Acad Sci U S A 92*, 452-456.

[17] Matthews, B. W., Nicholson, H., and Becktel, W. J. (1987) Enhanced protein thermostability from site-directed mutations that decrease the entropy of unfolding, *Proc Natl Acad Sci U S A 84*, 6663-6667.

[18] Pace, C. N., Fisher, L. M., and Cupo, J. F. (1981) Globular protein stability: aspects of interest in protein turnover, *Acta Biologica et Medica Germanica 40*, 1385-1392.

[19] Kajander, T., Kahn, P. C., Passila, S. H., Cohen, D. C., Lehtio, L., Adolfsen, W., Warwicker, J., Schell, U., and Goldman, A. (2000) Buried charged surface in proteins, *Structure 8*, 1203-1214.

[20] Trevino, S. R., Gokulan, K., Newsom, S., Thurlkill, R. L., Shaw, K. L., Mitkevich, V. A., Makarov, A. A., Sacchettini, J. C., Scholtz, J. M., and Pace, C. N. (2005) Asp79 makes a large, unfavorable contribution to the stability of RNase Sa, *J Mol Biol 354*, 967-978.

[21] Uversky, V. N., Radivojac, P., Iakoucheva, L. M., Obradovic, Z., and Dunker, A. K. (2007) Prediction of intrinsic disorder and its use in functional proteomics, *Methods Mol Biol 408*, 69-92.

[22] Radivojac, P., Iakoucheva, L. M., Oldfield, C. J., Obradovic, Z., Uversky, V. N., and Dunker, A. K. (2007) Intrinsic disorder and functional proteomics, *Biophys J 92*, 1439-1456.

[23] Wright, P. E., and Dyson, H. J. (2009) Linking folding and binding, *Curr Opin Struct Biol 19*, 31-38.

[24] Pace, C. N., Shirley, B. A., McNutt, M., and Gajiwala, K. (1996) Forces contributing to the conformational stability of proteins, *FASEB J 10*, 75-83.

[25] Marshall, S. A., Morgan, C. S., and Mayo, S. L. (2002) Electrostatics significantly affect the stability of designed homeodomain variants, *J Mol Biol 316*, 189-199.

[26] Razvi, A., and Scholtz, J. M. (2006) Lessons in stability from thermophilic proteins, *Protein Sci 15*, 1569-1578.

[27] Pace, C. N., and Creighton, T. E. (1986) The disulphide folding pathway of ribonuclease T1, *J Mol Biol 188*, 477-486.

[28] Pace, C. N., Grimsley, G. R., Thomson, J. A., and Barnett, B. J. (1988) Conformational stability and activity of ribonuclease T1 with zero, one, and two intact disulfide bonds, *J Biol Chem 263*, 11820-11825.

[29] Thomson, J. A., Shirley, B. A., Grimsley, G. R., and Pace, C. N. (1989) Conformational stability and mechanism of folding of ribonuclease T1, *J Biol Chem 264*, 11614-11620.

[30] Horovitz, A., and Fersht, A. R. (1992) Co-operative interactions during protein folding, *J Mol Biol 224*, 733-740.

[31] Myers, J. K., Pace, C. N., and Scholtz, J. M. (1995) Denaturant m values and heat capacity changes: relation to changes in accessible surface areas of protein unfolding, *Protein Sci 4*, 2138-2148.

[32] Pace, C. N. (1995) Evaluating contribution of hydrogen bonding and hydrophobic bonding to protein folding, *Methods Enzymol 259*, 538-554.

[33] Grimsley, G. R., Shaw, K. L., Fee, L. R., Alston, R. W., Huyghues-Despointes, B. M., Thurlkill, R. L., Scholtz, J. M., and Pace, C. N. (1999) Increasing protein stability by altering long-range coulombic interactions, *Protein Sci 8*, 1843-1849.

[34] Pace, C. N., Alston, R. W., and Shaw, K. L. (2000) Charge-charge interactions influence the denatured state ensemble and contribute to protein stability, *Protein Sci 9*, 1395-1398.

[35] Shaw, K. L., Grimsley, G. R., Yakovlev, G. I., Makarov, A. A., and Pace, C. N. (2001) The effect of net charge on the solubility, activity, and stability of ribonuclease Sa, *Protein Sci 10*, 1206-1215.

[36] Fu, H., Grimsley, G. R., Razvi, A., Scholtz, J. M., and Pace, C. N. (2009) Increasing protein stability by improving beta-turns, *Proteins 77*, 491-498.

[37] Pace, C. N., Hebert, E. J., Shaw, K. L., Schell, D., Both, V., Krajcikova, D., Sevcik, J., Wilson, K. S., Dauter, Z., Hartley, R. W., and Grimsley, G. R. (1998) Conformational stability and thermodynamics of folding of ribonucleases Sa, Sa2 and Sa3, *J Mol Biol 279*, 271-286.

[38] Makhatadze, G. I., and Privalov, P. L. (1994) Hydration effects in protein unfolding, *Biophys Chem 51*, 291-304; discussion 304-299.

[39] Pace, C. N., Fu, H., Fryar, K. L., Landua, J., Trevino, S. R., Shirley, B. A., Hendricks, M. M., Iimura, S., Gajiwala, K., Scholtz, J. M., and Grimsley, G. R. (2011) Contribution of hydrophobic interactions to protein stability, *J Mol Biol 408*, 514-528.

[40] Sturtevant, J. M. (1977) Heat capacity and entropy changes in processes involving proteins, *Proc Natl Acad Sci U S A 74*, 2236-2240.

[41] Becktel, W. J., and Schellman, J. A. (1987) Protein stability curves, *Biopolymers 26*, 1859-1877.

[42] Shortle, D., Meeker, A. K., and Freire, E. (1988) Stability mutants of staphylococcal nuclease: large compensating enthalpy-entropy changes for the reversible denaturation reaction, *Biochemistry 27*, 4761-4768.

[43] Makhatadze, G. I., and Privalov, P. L. (1995) Energetics of protein structure, *Advances in protein chemistry 47*, 307-425.

[44] Fu, H., Grimsley, G., Scholtz, J. M., and Pace, C. N. (2010) Increasing protein stability: importance of DeltaC(p) and the denatured state, *Protein Sci 19*, 1044-1052.

[45] Tanford, C. (1997) How protein chemists learned about the hydrophobic factor, *Protein Sci 6*, 1358-1366.

[46] Bernal, J. D. (1939) *The social function of science*, G. Routledge & sons ltd., London.

[47] Kauzmann, W. (1959) Some factors in the interpretation of protein denaturation, *Advances in protein chemistry 14*, 1-63.

[48] Nozaki, Y., and Tanford, C. (1971) The solubility of amino acids and two glycine peptides in aqueous ethanol and dioxane solutions. Establishment of a hydrophobicity scale, *J Biol Chem 246*, 2211-2217.

[49] Wimley, W. C., Creamer, T. P., and White, S. H. (1996) Solvation energies of amino acid side chains and backbone in a family of host-guest pentapeptides, *Biochemistry 35*, 5109-5124.

[50] Kellis, J. T., Jr., Nyberg, K., and Fersht, A. R. (1989) Energetics of complementary side-chain packing in a protein hydrophobic core, *Biochemistry 28*, 4914-4922.

[51] Pace, C. N. (1992) Contribution of the hydrophobic effect to globular protein stability, *J Mol Biol 226*, 29-35.

[52] Serrano, L., Kellis, J. T., Jr., Cann, P., Matouschek, A., and Fersht, A. R. (1992) The folding of an enzyme. II. Substructure of barnase and the contribution of different interactions to protein stability, *J Mol Biol 224*, 783-804.

[53] Kyte, J., and Doolittle, R. F. (1982) A simple method for displaying the hydropathic character of a protein, *J Mol Biol 157*, 105-132.

[54] Radzicka, A., Young, G. B., and Wolfenden, R. (1993) Lack of water transport by amino acid side chains or peptides entering a nonpolar environment, *Biochemistry 32*, 6807-6809.

[55] Rose, G. D., and Wolfenden, R. (1993) Hydrogen bonding, hydrophobicity, packing, and protein folding, *Annual review of biophysics and biomolecular structure 22*, 381-415.

[56] Wimley, W. C., and White, S. H. (1996) Experimentally determined hydrophobicity scale for proteins at membrane interfaces, *Nat Struct Biol 3*, 842-848.

[57] Lesser, G. J., and Rose, G. D. (1990) Hydrophobicity of amino acid subgroups in proteins, *Proteins 8*, 6-13.

[58] Pace, C. N., Grimsley, G. R., Scholtz, J. M., Shaw, K. L. (2014) Protein Stability, In *eLs* February 17, 2014 ed., pp 1-7.

[59] Takano, K., Scholtz, J. M., Sacchettini, J. C., and Pace, C. N. (2003) The contribution of polar group burial to protein stability is strongly context-dependent, *J Biol Chem 278*, 31790-31795.

[60] Trevino, S. R., Scholtz, J. M., and Pace, C. N. (2007) Amino acid contribution to protein solubility: Asp, Glu, and Ser contribute more favorably than the other hydrophilic amino acids in RNase Sa, *J Mol Biol 366*, 449-460.

[61] Alber, T. (1989) Mutational effects on protein stability, *Annu Rev Biochem 58*, 765-798.

[62] Zhou, H., and Zhou, Y. (2004) Quantifying the effect of burial of amino acid residues on protein stability, *Proteins 54*, 315-322.

[63] Fersht, A., and Winter, G. (1992) Protein engineering, *Trends Biochem Sci 17*, 292-295.

[64] Anfinsen, C. B., and Haber, E. (1961) Studies on the reduction and re-formation of protein disulfide bonds, *J Biol Chem 236*, 1361-1363.

[65] Anfinsen, C. B., Haber, E., Sela, M., and White, F. H., Jr. (1961) The kinetics of formation of native ribonuclease during oxidation of the reduced polypeptide chain, *Proc Natl Acad Sci U S A 47*, 1309-1314.

[66] Flory, P. J. (1956) Role of Crystallization in Polymers and Proteins, *Science 124*, 53-60.

[67] Cupo, J. F., and Pace, C. N. (1983) Conformational stability of mixed disulfide derivatives of beta-lactoglobulin B, *Biochemistry 22*, 2654-2658.

[68] Clarke, J., and Fersht, A. R. (1993) Engineered disulfide bonds as probes of the folding pathway of barnase: increasing the stability of proteins against the rate of denaturation, *Biochemistry 32*, 4322-4329.

[69] Katz, B. A., and Kossiakoff, A. (1986) The crystallographically determined structures of atypical strained disulfides engineered into subtilisin, *J Biol Chem 261*, 15480-15485.

[70] Matsumura, M., Becktel, W. J., Levitt, M., and Matthews, B. W. (1989) Stabilization of phage T4 lysozyme by engineered disulfide bonds, *Proc Natl Acad Sci U S A 86*, 6562-6566.

[71] Betz, S. F. (1993) Disulfide bonds and the stability of globular proteins, *Protein Sci 2*, 1551-1558.

[72] Mitchinson, C., and Wells, J. A. (1989) Protein engineering of disulfide bonds in subtilisin BPN', *Biochemistry 28*, 4807-4815.

[73] Tu, B. P., and Weissman, J. S. (2004) Oxidative protein folding in eukaryotes: mechanisms and consequences, *The Journal of cell biology 164*, 341-346.

[74] Nozaki, Y., and Tanford, C. (1967) Intrinsic dissociation constants of aspartyl and glutamyl carboxyl groups, *J Biol Chem 242*, 4731-4735.

[75] Dawson, R. M. C. (1959) *Data for biochemical research*, Clarendon Press, Oxford.

[76] Thurlkill, R. L., Grimsley, G. R., Scholtz, J. M., and Pace, C. N. (2006) pK values of the ionizable groups of proteins, *Protein Sci 15*, 1214-1218.

[77] Harms, M. J., Schlessman, J. L., Sue, G. R., and Garcia-Moreno, B. (2011) Arginine residues at internal positions in a protein are always charged, *Proc Natl Acad Sci U S A 108*, 18954-18959.

[78] Damjanovic, A., Garcia-Moreno, B., Lattman, E. E., and Garcia, A. E. (2005) Molecular dynamics study of water penetration in staphylococcal nuclease, *Proteins 60*, 433-449.

[79] Laurents, D. V., Huyghues-Despointes, B. M., Bruix, M., Thurlkill, R. L., Schell, D., Newsom, S., Grimsley, G. R., Shaw, K. L., Trevino, S., Rico, M., Briggs, J. M., Antosiewicz, J. M., Scholtz, J. M., and Pace, C. N. (2003) Charge-Charge interactions are key determinants of the pK values of ionizable groups in ribonuclease Sa (pI=3.5) and a basic variant (pI=10.2), *J Mol Biol 325*, 1077-1092.

[80] Rees, D. C. (1980) Experimental evaluation of the effective dielectric constant of proteins, *J Mol Biol 141*, 323-326.

[81] Stigter, D., and Dill, K. A. (1990) Charge effects on folded and unfolded proteins, *Biochemistry 29*, 1262-1271.

[82] Roca, M., Messer, B., and Warshel, A. (2007) Electrostatic contributions to protein stability and folding energy, *FEBS Lett 581*, 2065-2071.

[83] Tanford, C. (1961) *Physical chemistry of macromolecules*, Wiley, New York, New York.

[84] Dzingeleski, G. D., and Wolfenden, R. (1993) Hypersensitivity of an enzyme reaction to solvent water, *Biochemistry 32*, 9143-9147.

[85] Li, L., Li, C., Zhang, Z., and Alexov, E. (2013) On the Dielectric "Constant" of Proteins: Smooth Dielectric Function for Macromolecular Modeling and Its Implementation in DelPhi, *Journal of chemical theory and computation 9*, 2126-2136.

[86] Garcia-Moreno, B., Dwyer, J. J., Gittis, A. G., Lattman, E. E., Spencer, D. S., and Stites, W. E. (1997) Experimental measurement of the effective dielectric in the hydrophobic core of a protein, *Biophys Chem 64*, 211-224.

[87] Barlow, D. J., and Thornton, J. M. (1983) Ion-pairs in proteins, *J Mol Biol 168*, 867-885.

[88] Creighton, T. E. (1991) Stability of folded conformations, *Current Opinion in Structural Biology 1*, 5-16.

[89] Waldburger, C. D., Schildbach, J. F., and Sauer, R. T. (1995) Are buried salt bridges important for protein stability and conformational specificity?, *Nat Struct Biol 2*, 122-128.

[90] Dong, F., and Zhou, H. X. (2002) Electrostatic contributions to T4 lysozyme stability: solvent-exposed charges versus semi-buried salt bridges, *Biophys J 83*, 1341-1347.

[91] Kumar, S., and Nussinov, R. (2001) Fluctuations in ion pairs and their stabilities in proteins, *Proteins 43*, 433-454.

[92] Makhatadze, G. I., Loladze, V. V., Ermolenko, D. N., Chen, X., and Thomas, S. T. (2003) Contribution of surface salt bridges to protein stability: guidelines for protein engineering, *J Mol Biol 327*, 1135-1148.

[93] Spassov, V. Z., Karshikoff, A. D., and Ladenstein, R. (1994) Optimization of the electrostatic interactions in proteins of different functional and folding type, *Protein Sci 3*, 1556-1569.

[94] Wimley, W. C., Gawrisch, K., Creamer, T. P., and White, S. H. (1996) Direct measurement of salt-bridge solvation energies using a peptide model system: implications for protein stability, *Proc Natl Acad Sci U S A 93*, 2985-2990.

[95] Anderson, D. E., Becktel, W. J., and Dahlquist, F. W. (1990) pH-induced denaturation of proteins: a single salt bridge contributes 3-5 kcal/mol to the free energy of folding of T4 lysozyme, *Biochemistry 29*, 2403-2408.

[96] Sun, D. P., Sauer, U., Nicholson, H., and Matthews, B. W. (1991) Contributions of engineered surface salt bridges to the stability of T4 lysozyme determined by directed mutagenesis, *Biochemistry 30*, 7142-7153.

[97] Lee, C. F., Makhatadze, G. I., and Wong, K. B. (2005) Effects of charge-to-alanine substitutions on the stability of ribosomal protein L30e from Thermococcus celer, *Biochemistry 44*, 16817-16825.

[98] Thurlkill, R. L., Grimsley, G. R., Scholtz, J. M., and Pace, C. N. (2006) Hydrogen bonding markedly reduces the pK of buried carboxyl groups in proteins, *J Mol Biol 362*, 594-604.

[99] Giletto, A., and Pace, C. N. (1999) Buried, charged, non-ion-paired aspartic acid 76 contributes favorably to the conformational stability of ribonuclease T1, *Biochemistry 38*, 13379-13384.

[100] Bush, J., and Makhatadze, G. I. (2011) Statistical analysis of protein structures suggests that buried ionizable residues in proteins are hydrogen bonded or form salt bridges, *Proteins 79*, 2027-2032.

[101] Pace, C. N., Fu, H., Fryar, K. L., Landua, J., Trevino, S. R., Schell, D., Thurlkill, R. L., Imura, S., Scholtz, J. M., Gajiwala, K., Sevcik, J., Urbanikova, L., Myers, J. K., Takano, K., Hebert, E. J., Shirley, B. A., and Grimsley, G. R. (2014) Contribution of hydrogen bonds to protein stability, *Protein Sci*.

[102] Myers, J. K., and Pace, C. N. (1996) Hydrogen bonding stabilizes globular proteins, *Biophys J 71*, 2033-2039.

[103] Trevino, S. R., Scholtz, J. M., and Pace, C. N. (2008) Measuring and increasing protein solubility, *J Pharm Sci 97*, 4155-4166.

[104] Bowie, J. U. (2011) Membrane protein folding: how important are hydrogen bonds?, *Curr Opin Struct Biol 21*, 42-49.

[105] Gao, J., Bosco, D. A., Powers, E. T., and Kelly, J. W. (2009) Localized thermodynamic coupling between hydrogen bonding and microenvironment polarity substantially stabilizes proteins, *Nature structural & molecular biology 16*, 684-690.

[106] Mirsky, A. E., and Pauling, L. (1936) On the Structure of Native, Denatured, and Coagulated Proteins, *Proc Natl Acad Sci U S A 22*, 439-447.

[107] Mitchell, J. B., Nandi, C. L., McDonald, I. K., Thornton, J. M., and Price, S. L. (1994) Amino/aromatic interactions in proteins: is the evidence stacked against hydrogen bonding?, *J Mol Biol 239*, 315-331.

[108] McDonald, I. K., and Thornton, J. M. (1994) Satisfying hydrogen bonding potential in proteins, *J Mol Biol 238*, 777-793.

[109] Panasik, N., Jr., Fleming, P. J., and Rose, G. D. (2005) Hydrogen-bonded turns in proteins: the case for a recount, *Protein Sci 14*, 2910-2914.

[110] Fleming, P. J., and Rose, G. D. (2005) Do all backbone polar groups in proteins form hydrogen bonds?, *Protein Sci 14*, 1911-1917.

[111] Pace, C. N. (2009) Energetics of protein hydrogen bonds, *Nature structural & molecular biology 16*, 681-682.

[112] Fersht, A. R., Shi, J. P., Knill-Jones, J., Lowe, D. M., Wilkinson, A. J., Blow, D. M., Brick, P., Carter, P., Waye, M. M., and Winter, G. (1985) Hydrogen bonding and biological specificity analysed by protein engineering, *Nature 314*, 235-238.

[113] Shirley, B. A., Stanssens, P., Hahn, U., and Pace, C. N. (1992) Contribution of hydrogen bonding to the conformational stability of ribonuclease T1, *Biochemistry 31*, 725-732.

[114] Hebert, E. J., Giletto, A., Sevcik, J., Urbanikova, L., Wilson, K. S., Dauter, Z., and Pace, C. N. (1998) Contribution of a conserved asparagine to the conformational stability of ribonucleases Sa, Ba, and T1, *Biochemistry 37*, 16192-16200.

[115] Pace, C. N., Horn, G., Hebert, E. J., Bechert, J., Shaw, K., Urbanikova, L., Scholtz, J. M., and Sevcik, J. (2001) Tyrosine hydrogen bonds make a large contribution to protein stability, *J Mol Biol 312*, 393-404.

[116] Loladze, V. V., Ermolenko, D. N., and Makhatadze, G. I. (2002) Thermodynamic consequences of burial of polar and non-polar amino acid residues in the protein interior, *J Mol Biol 320*, 343-357.

[117] Xu, J., Baase, W. A., Baldwin, E., and Matthews, B. W. (1998) The response of T4 lysozyme to large-to-small substitutions within the core and its relation to the hydrophobic effect, *Protein Sci 7*, 158-177.

[118] Baase, W. A., Liu, L., Tronrud, D. E., and Matthews, B. W. (2010) Lessons from the lysozyme of phage T4, *Protein Sci 19*, 631-641.

[119] Makhatadze, G. I., and Privalov, P. L. (1993) Contribution of hydration to protein folding thermodynamics. I. The enthalpy of hydration, *J Mol Biol 232*, 639-659.

[120] Privalov, P. L. (1979) Stability of proteins: small globular proteins, *Advances in protein chemistry 33*, 167-241.

[121] D'Aquino, J. A., Gomez, J., Hilser, V. J., Lee, K. H., Amzel, L. M., and Freire, E. (1996) The magnitude of the backbone conformational entropy change in protein folding, *Proteins 25*, 143-156.

[122] Schellman, J. A. (1955) The stability of hydrogen-bonded peptide structures in aqueous solution, *Comptes rendus des travaux du Laboratoire Carlsberg. Serie chimique 29*, 230-259.

[123] Laurents, D., Perez-Canadillas, J. M., Santoro, J., Rico, M., Schell, D., Pace, C. N., and Bruix, M. (2001) Solution structure and dynamics of ribonuclease Sa, *Proteins 44*, 200-211.

[124] Spolar, R. S., and Record, M. T., Jr. (1994) Coupling of local folding to site-specific binding of proteins to DNA, *Science 263*, 777-784.

[125] Tanford, C. (1978) The hydrophobic effect and the organization of living matter, *Science 200*, 1012-1018.

[126] Lee, B., and Richards, F. M. (1971) The interpretation of protein structures: estimation of static accessibility, *J Mol Biol 55*, 379-400.

[127] Trinquier, G., and Sanejouand, Y. H. (1998) Which effective property of amino acids is best preserved by the genetic code?, *Protein engineering 11*, 153-169.

[128] Deckert, G., Warren, P. V., Gaasterland, T., Young, W. G., Lenox, A. L., Graham, D. E., Overbeek, R., Snead, M. A., Keller, M., Aujay, M., Huber, R., Feldman, R. A., Short, J. M., Olsen, G. J., and Swanson, R. V. (1998) The complete genome of the hyperthermophilic bacterium Aquifex aeolicus, *Nature 392*, 353-358.

[129] Brokx, R. D., Lopez, M. M., Vogel, H. J., and Makhatadze, G. I. (2001) Energetics of target peptide binding by calmodulin reveals different modes of binding, *J Biol Chem 276*, 14083-14091.

[130] Sgourakis, N. G., Patel, M. M., Garcia, A. E., Makhatadze, G. I., and McCallum, S. A. (2010) Conformational dynamics and structural plasticity play critical roles in the ubiquitin recognition of a UIM domain, *J Mol Biol 396*, 1128-1144.

[131] Vallone, B., Miele, A. E., Vecchini, P., Chiancone, E., and Brunori, M. (1998) Free energy of burying hydrophobic residues in the interface between protein subunits, *Proc Natl Acad Sci U S A 95*, 6103-6107.

[132] Kim, J., Mao, J., and Gunner, M. R. (2005) Are acidic and basic groups in buried proteins predicted to be ionized?, *J Mol Biol 348*, 1283-1298.

[133] Bartlett, G. J., Porter, C. T., Borkakoti, N., and Thornton, J. M. (2002) Analysis of catalytic residues in enzyme active sites, *J Mol Biol 324*, 105-121.

[134] Huyghues-Despointes, B. M., Thurlkill, R. L., Daily, M. D., Schell, D., Briggs, J. M., Antosiewicz, J. M., Pace, C. N., and Scholtz, J. M. (2003) pK values of

histidine residues in ribonuclease Sa: effect of salt and net charge, *J Mol Biol 325*, 1093-1105.

[135] Sevcik, J., Zegers, I., Wyns, L., Dauter, Z., and Wilson, K. S. (1993) Complex of ribonuclease Sa with a cyclic nucleotide and a proposed model for the reaction intermediate, *Eur J Biochem 216*, 301-305.

[136] Kery, V., Both, V., Sevcik, J., and Zelinka, J. (1986) The number and role of histidine residues in the active site of guanyloribonuclease Sa, *General physiology and biophysics 5*, 405-414.

[137] Blaber, M., Lindstrom, J. D., Gassner, N., Xu, J., Heinz, D. W., and Matthews, B. W. (1993) Energetic cost and structural consequences of burying a hydroxyl group within the core of a protein determined from Ala-->Ser and Val-->Thr substitutions in T4 lysozyme, *Biochemistry 32*, 11363-11373.

[138] Pace, C. N. (2001) Polar group burial contributes more to protein stability than nonpolar group burial, *Biochemistry 40*, 310-313.

[139] Sandberg, W. S., and Terwilliger, T. C. (1989) Influence of interior packing and hydrophobicity on the stability of a protein, *Science 245*, 54-57.

[140] Chen, J., and Stites, W. E. (2001) Packing is a key selection factor in the evolution of protein hydrophobic cores, *Biochemistry 40*, 15280-15289.

[141] Chen, J., and Stites, W. E. (2001) Energetics of side chain packing in staphylococcal nuclease assessed by systematic double mutant cycles, *Biochemistry 40*, 14004-14011.

[142] Kramer, R. M., Shende, V. R., Motl, N., Pace, C. N., and Scholtz, J. M. (2012) Toward a molecular understanding of protein solubility: increased negative surface charge correlates with increased solubility, *Biophys J 102*, 1907-1915.

[143] Dao-pin, S., Anderson, D. E., Baase, W. A., Dahlquist, F. W., and Matthews, B. W. (1991) Structural and thermodynamic consequences of burying a charged residue within the hydrophobic core of T4 lysozyme, *Biochemistry 30*, 11521-11529.

[144] Akke, M., and Forsen, S. (1990) Protein stability and electrostatic interactions between solvent exposed charged side chains, *Proteins 8*, 23-29.

[145] Honig, B. H., Hubbell, W. L., and Flewelling, R. F. (1986) Electrostatic interactions in membranes and proteins, *Annu Rev Biophys Biophys Chem 15*, 163-193.

[146] Honig, B. H., and Hubbell, W. L. (1984) Stability of "salt bridges" in membrane proteins, *Proc Natl Acad Sci U S A 81*, 5412-5416.

[147] Sharp, K. A., and Honig, B. (1990) Electrostatic interactions in macromolecules: theory and applications, *Annu Rev Biophys Biophys Chem 19*, 301-332.

[148] Harms, M. J., Castaneda, C. A., Schlessman, J. L., Sue, G. R., Isom, D. G., Cannon, B. R., and Garcia-Moreno, E. B. (2009) The pK(a) values of acidic and basic residues buried at the same internal location in a protein are governed by different factors, *J Mol Biol 389*, 34-47.

[149] Fitch, C. A., Karp, D. A., Lee, K. K., Stites, W. E., Lattman, E. E., and Garcia-Moreno, E. B. (2002) Experimental pK(a) values of buried residues: analysis with continuum methods and role of water penetration, *Biophys J 82*, 3289-3304.

[150] Isom, D. G., Castaneda, C. A., Cannon, B. R., and Garcia-Moreno, B. (2011) Large shifts in pKa values of lysine residues buried inside a protein, *Proc Natl Acad Sci U S A 108*, 5260-5265.

[151] Isom, D. G., Castaneda, C. A., Cannon, B. R., Velu, P. D., and Garcia-Moreno, E. B. (2010) Charges in the hydrophobic interior of proteins, *Proc Natl Acad Sci U S A 107*, 16096-16100.

[152] Isom, D. G., Cannon, B. R., Castaneda, C. A., Robinson, A., and Garcia-Moreno, B. (2008) High tolerance for ionizable residues in the hydrophobic interior of proteins, *Proc Natl Acad Sci U S A 105*, 17784-17788.

[153] Sevcik, J., Lamzin, V. S., Dauter, Z., and Wilson, K. S. (2002) Atomic resolution data reveal flexibility in the structure of RNase Sa, *Acta Crystallogr D Biol Crystallogr 58*, 1307-1313.

[154] PyMOL. (2010) The PyMOL Molecular Graphics System, Version 1.3, Schrödinger, LLC., (Pymol, Ed.).

[155] Dwyer, J. J., Gittis, A. G., Karp, D. A., Lattman, E. E., Spencer, D. S., Stites, W. E., and Garcia-Moreno, E. B. (2000) High apparent dielectric constants in the interior of a protein reflect water penetration, *Biophys J 79*, 1610-1620.

[156] Karp, D. A., Gittis, A. G., Stahley, M. R., Fitch, C. A., Stites, W. E., and Garcia-Moreno, E. B. (2007) High apparent dielectric constant inside a protein reflects structural reorganization coupled to the ionization of an internal Asp, *Biophys J 92*, 2041-2053.

[157] Uversky, V. N., Karnoup, A. S., Segel, D. J., Seshadri, S., Doniach, S., and Fink, A. L. (1998) Anion-induced folding of Staphylococcal nuclease: characterization of multiple equilibrium partially folded intermediates, *J Mol Biol 278*, 879-894.

[158] Uversky, V. N., Segel, D. J., Doniach, S., and Fink, A. L. (1998) Association-induced folding of globular proteins, *Proc Natl Acad Sci U S A 95*, 5480-5483.

[159] Bacova, M., Zelinkova, E., and Zelinka, J. (1971) Exocellular ribonuclease from Streptomyces aureofaciens. I. Isolation and purification, *Biochim Biophys Acta 235*, 335-342.

[160] Shlyapnikov, S. V., Both, V., Kulikov, V. A., Dementiev, A. A., Sevcik, J., and Zelinka, J. (1986) Amino acid sequence determination of guanyl-specific ribonuclease Sa from Streptomyces aureofaciens, *FEBS Lett 209*, 335-339.

[161] Zelinkova, E., Bacova, M., and Zelinka, J. (1971) Exocellular ribonuclease from Streptomyces aureofaciens. II. Properties and specificity, *Biochim Biophys Acta 235*, 343-352.

[162] Yakovlev, G. I., Mitkevich, V. A., Shaw, K. L., Trevino, S., Newsom, S., Pace, C. N., and Makarov, A. A. (2003) Contribution of active site residues to the activity and thermal stability of ribonuclease Sa, *Protein Sci 12*, 2367-2373.

[163] Hebert, E. J., Grimsley, G. R., Hartley, R. W., Horn, G., Schell, D., Garcia, S., Both, V., Sevcik, J., and Pace, C. N. (1997) Purification of ribonucleases Sa, Sa2, and Sa3 after expression in Escherichia coli, *Protein Expr Purif 11*, 162-168.

[164] Fu, H., Pace, C. N., and Scholtz, J. M. (2010) Understanding forces that contribute to protein stability Application for increasing protein stability, p 1 online resource., Texas A&M University,, College Station, Tex.

[165] Woody, R. W. (1994) Contributions of tryptophan side chains to the far-ultraviolet circular dichroism of proteins, *Eur Biophys J 23*, 253-262.

[166] Sambrook, J., and Russell, D. W. (2001) *Molecular cloning : a laboratory manual*, 3rd ed., Cold Spring Harbor Laboratory Press, Cold Spring Harbor, N.Y.

[167] Creighton, T. E. (1997) *Protein structure : a practical approach*, 2nd ed., IRL Press at Oxford University Press, Oxford ; New York.

[168] Berisio, R., Lamzin, V. S., Sica, F., Wilson, K. S., Zagari, A., and Mazzarella, L. (1999) Protein titration in the crystal state, *J Mol Biol 292*, 845-854.

[169] Karpusas, M., Baase, W. A., Matsumura, M., and Matthews, B. W. (1989) Hydrophobic packing in T4 lysozyme probed by cavity-filling mutants, *Proc Natl Acad Sci U S A 86*, 8237-8241.

[170] Jackson, S. E., Moracci, M., elMasry, N., Johnson, C. M., and Fersht, A. R. (1993) Effect of cavity-creating mutations in the hydrophobic core of chymotrypsin inhibitor 2, *Biochemistry 32*, 11259-11269.

[171] Chen, J., and Stites, W. E. (2001) Higher-order packing interactions in triple and quadruple mutants of staphylococcal nuclease, *Biochemistry 40*, 14012-14019.

[172] Buckle, A. M., Henrick, K., and Fersht, A. R. (1993) Crystal structural analysis of mutations in the hydrophobic cores of barnase, *J Mol Biol 234*, 847-860.

[173] Holder, J. B., Bennett, A. F., Chen, J., Spencer, D. S., Byrne, M. P., and Stites, W. E. (2001) Energetics of side chain packing in staphylococcal nuclease assessed by exchange of valines, isoleucines, and leucines, *Biochemistry 40*, 13998-14003.

[174] Khechinashvili, N. N. (1990) Thermodynamic properties of globular proteins and the principle of stabilization of their native structure, *Biochim Biophys Acta 1040*, 346-354.

[175] Schwarz, H., Hinz, H. J., Mehlich, A., Tschesche, H., and Wenzel, H. R. (1987) Stability studies on derivatives of the bovine pancreatic trypsin inhibitor, *Biochemistry 26*, 3544-3551.

[176] Sevcik, J., Hill, C. P., Dauter, Z., and Wilson, K. S. (1993) Complex of ribonuclease from Streptomyces aureofaciens with 2'-GMP at 1.7 A resolution, *Acta Crystallogr D Biol Crystallogr 49*, 257-271.

[177] Trevino, S. R., Schaefer, S., Scholtz, J. M., and Pace, C. N. (2007) Increasing protein conformational stability by optimizing beta-turn sequence, *J Mol Biol 373*, 211-218.

[178] Bosshard, H. R., Marti, D. N., and Jelesarov, I. (2004) Protein stabilization by salt bridges: concepts, experimental approaches and clarification of some misunderstandings, *Journal of molecular recognition : JMR 17*, 1-16.

[179] Marti, D. N., and Bosshard, H. R. (2004) Inverse electrostatic effect: electrostatic repulsion in the unfolded state stabilizes a leucine zipper, *Biochemistry 43*, 12436-12447.

[180] Bossa, G. V., Fahr, A., and Pereira de Souza, T. (2014) Study of pK Values and Effective Dielectric Constants of Ionizable Residues in Pentapeptides and in Staphylococcal Nuclease (SNase) Using a Mean-Field Approach, *J Phys Chem B 118*, 4053-4061.